人類遺傳疾病。第一部份：法布瑞氏症之分子生物學研究。第二部份：以瓦氏效應為標靶，經由 DNA 甲基化的改變，活化沉默的抑癌基因。

Human Genetic Diseases. Part I: Molecular Studies of Fabry Disease. Part II: Reactivation of Silenced Tumor Suppressor Genes via Changes in DNA Methylation by Targeting the Warburg Effect.

研究生：林翔宇 (Hsiang-Yu Lin)

指導教授：牛道明教授 (Dau-Ming Niu, M.D., Ph.D.)

國立陽明大學

臨床醫學研究所

博士論文

Institute of Clinical Medicine

National Yang-Ming University

Doctoral Dissertation

中華民國一〇一年五月

May, 2012

誌 謝

今天能有博士畢業論文的完成，回顧這一路走來，需要感謝的人很多。首先要感謝我的指導老師牛道明教授，牛老師帶領我進入了轉譯醫學，也就是臨床與基礎醫學整合研究的殿堂，從研究計畫的撰寫、實驗上的指導、乃至於未來學術生涯的規畫，處處提供我最溫暖的扶持。此外，我要感謝在我赴美進修一年中的指導老師陳慶士教授，他不但給予我實驗的構想與信心、為人處世的教誨、亦在我最艱困的階段給了我無微不至的關懷。林炫沛醫師是我在馬偕紀念醫院小兒遺傳科的臨床啟蒙恩師，也是我努力學習的標竿與典範；在林醫師的諄諄指導下，啟發了我對人類遺傳疾病的高度研究興趣，並以「罕見疾病」為主題，撰寫了多篇原著論文刊登於國際醫學期刊；馬偕紀念醫院兒科部陳銘仁主任與李宏昌主任，以及醫研部陳持平主任平日亦對我十分關照，他們在這段日子中，均大力支持我在臨床醫療工作之餘，能兼職攻讀博士學位，本人在此一併表達心中的誠摯謝忱。

「得之於人者太多，出之於己者太少」；在漫長的研究過程中，要感謝許多實驗室老師以及同學的支持與協助，包括翁于一博士、Dr. Tim HM Huang、Dr. Samuel Kulp、Dr. Dasheng Wang、朱伯振博士、李崑豪博士、賴奕如博士、劉美瑛博士、俊翰、憶萩、筱菁、士霖、志謙、瑋凌、恩旗、会凌、曉琪、家維、如慧、鈺琇，均是我實驗與臨床工作的良師兼益友。因為有他們的幫助，此篇論文才得以順利完成。此外也要特別感謝馬偕紀念醫院給予我在職攻讀學位的機會和實質的支持與鼓勵，以及罕見疾病基金會、國家科學委員會與臺灣兒科醫學會在這段期間對此研究論文的各項重要獎助。

在此誠心感謝參與學位考的陳燕彰老師、呂佩融老師、顧記華老師與林炫沛老師給予我論文上的指導以及研究心得的分享，使我的博士論文能更臻完善。

在我四年的博士學程中，經歷了人生的高低潮起伏；忙碌的臨床與實驗工作，雖常使人疲憊不堪，但偶有進展，則令人振奮不已。2010年獲得國科會「補助博士生赴國外研究」獎助學金至美國俄亥俄州立大學醫學中心進修一年，由於賢內助彩鳳無怨無悔地照顧兩個聰明調皮的小孩，並在我失意時給我鼓勵，使我無後顧之憂，得以繼續朝著理想大步邁進，在此由衷地感謝她。也要感謝一路上辛苦栽培我的父母，沒有他們無私的付出與奉獻就不會有今天的我。而兩個孩子倢彤與姮彤，在我的忙碌生活中所帶來的體貼與歡笑，成為我最大的鼓舞力量。

最後，謹將此論文獻給我最深愛的家人，以及勇敢的法布瑞氏症病友們。

2012.5.17 於 台北北投

本研究榮獲財團法人罕見疾病基金會
第 11 屆博碩士論文獎助學金獎助

本研究榮獲行政院國家科學委員會
98 年度「補助博士生赴國外研究」
獎助學金獎助
(NSC98-2917-I-010-103)

本研究榮獲 2012 臺灣兒科醫學會

第 210 屆學術演講會「年輕研究者獎」

Table of Contents

ABSTRACT

Part I: Molecular Studies of Fabry Disease.

BACKGROUND. Fabry disease is an X-linked lysosomal storage disease, affecting an estimated 1 in ~50,000 males, results from deficient α-galactosidase A (α-Gal A) activity. A cardiac variant of Fabry disease mimicking hypertrophic cardiomyopathy (HCM) is defined as the presence of otherwise unexplained myocardial hypertrophy. Fabry disease was first thought to affect males only, and females were generally considered to be asymptomatic carriers. However, recent research suggests that female carriers of Fabry disease may still develop vital organ damage causing severe morbidity and mortality. Besides, information regarding the clinical outcome of enzyme replacement therapy (ERT) for Fabry disease in Asian patients is limited. **METHODS.** To determine the disease incidence in the Taiwan population, a Fabry disease newborn screening study was initiated by assaying the α-Gal A activity using dried blood spots. Through the pedigree studies of the identified newborns with IVS4+919G>A mutation, we studied enzyme assay and clinical assessment for 94 adults with this mutation [22 men, 72 women; mean age: men 57.8±6.0 (range 42-68), women 39.1±14.1 years (range 19-82)]. We identified 121 newborns with 20 different *GLA* gene mutations, and also found that most female carriers were not detected by enzyme assays. A streamlined method for high resolution melting (HRM) analysis was designed to screen for *GLA* gene mutations using a same PCR and melting program. Primer sets were designed to cover the 7 exons and the Chinese common intronic mutation, IVS4+919G>A of *GLA* gene. We also reviewed 38 Taiwanese patients with Fabry disease (21 males and 17 females; age range, 14.4 to 79.1 years; 15 with classical type, 2 with renal type, and 21 with cardiac type) treated with biweekly intravenous infusions of agalsidase beta (1 mg/kg) or agalsidase alpha (0.2 mg/kg) for 6-36 months. Echocardiography, urine albumin-to-creatinine ratio, and estimated glomerular filtration rate (eGFR) were evaluated at baseline and after ERT. **RESULTS.** Low plasma α-Gal A activity and presence of a Fabry mutation was demonstrated in 45 neonates (3 females). Eight different mutations were

identified, including 3 known missense mutations (R112H, A143T, R356W), 4 novel missense mutations (G104V, M296L, G360C, K391T), and one known intronic mutation (IVS4+919G>A). The IVS4+919G>A mutation was most common (82% of patients). A total of 20 maternal grandparents of infants harboring this intronic mutation were evaluated by echocardiography, mutation analysis and α-Gal A activity assay. The intronic mutation was found in 9 grandfathers and 11 grandmothers. Of these grandparents, 3 grandfathers (33%) but none of the grandmothers had HCM. Additionally, 16 males who had been diagnosed with idiopathic HCM were screened by mutation analysis and α-Gal A activity; 4 (25%) showed deficient plasma α-Gal A activity in combination with the intronic mutation. Plasma α-Gal A activity assay was 10.4±11.2% of normal in the men and 48.6±19.5% of normal in the women. Echocardiography in 90 of the adults revealed left ventricular hypertrophy (LVH) in 19 (21%), including 14 of 21 men (67%) and 5 of 69 women (7%). Microalbuminuria, based on the urine albumin-to-creatinine ratio measured on at least two occasions, was present in 17 of 86 subjects (20%) (men: 5/20, 25%; women: 12/66, 18%). At least one ocular manifestation consistent with Fabry disease was present in 41 of 52 subjects (79%) who underwent ophthalmologic examination, including 8 (15%) with conjunctival vessel tortuosity, 15 (29%) with cornea verticillata, 10 (19%) with Fabry cataract, and 34 (65%) with retinal vessel tortuosity. Among subjects over 40 years of age, men were more likely than women to have LVH [14/21 (67%) vs 5/25 (20%), $p<0.001$]. The HRM analysis was successful in identifying heterozygous and hemizygous patients with the 20 surveyed mutations. We were also successful in using this method to test dried blood spots of newborns afflicted with Fabry mutations without having to determine DNA concentration before PCR amplification. After 6-36 months of ERT, echocardiography revealed reductions of left ventricular mass, the thicknesses of intraventricular septum, and left posterior wall in 19 (19/31, 61%), 25 (25/32, 78%), and 20 (20/33, 61%) patients, respectively. For 17 patients with microalbuminuria (based on urine albumin-to-creatinine ratio) at baseline, 16 patients (94%) showed some degree of improvement after ERT. For 16 patients with abnormal eGFR (based

on plasma creatinine) at baseline, 10 patients (63%) revealed improvement of renal function after ERT. No severe clinical events were reported during the treatment. **CONCLUSION.** Our newborn screening study in the Taiwan population revealed an incidence of Fabry mutations of ~1 in 1,400 males. We found an unexpected high prevalence of the cardiac variant mutation IVS4+919G>A among both newborns (~1 in 1,600 males) and idiopathic HCM patients. The early identification of undiagnosed patients allows timely therapeutic intervention providing a better clinical outcome. Cardiovascular, renal and ocular abnormalities are highly prevalent in adult Taiwan Chinese subjects with the Fabry mutation IVS4+919G>A. Our findings contribute to the limited understanding of the course of this late-onset disease variant and underscore the need for close follow up in such patients. HRM could be a reliable and sensitive method for use in the rapid screening of females for *GLA* mutations. ERT was well tolerated by all patients. This treatment is thus beneficial and appears to be safe for treatment of Fabry disease in Taiwanese patients.

Part II: Reactivation of Silenced Tumor Suppressor Genes via Changes in DNA Methylation by Targeting the Warburg Effect.

BACKGROUND. Targeting tumor metabolism by energy restriction-mimetic agents (ERMAs) has emerged as a strategy for cancer therapy/prevention. Evidence suggests a mechanistic link between ERMA-mediated antitumor effects and epigenetic gene regulation. **METHODS.** Microarray analysis showed that a novel thiazolidinedione-derived ERMA, CG-12, and glucose deprivation could suppress DNA methyltransferase (DNMT)1 expression and reactivate DNA methylation-silenced tumor suppressor genes in LNCaP prostate cancer cells. Thus, we investigated the effects of a potent CG-12 derivative, CG-5, vis-à-vis 2-deoxyglucose, glucose deprivation and/or 5-aza-deoxycytidine, on DNMT isoform expression (Western blotting, RT-PCR), DNMT1 transcriptional activation (luciferase reporter assay), and expression of genes frequently hypermethylated in prostate cancer (quantitative real-time PCR). Promoter methylation in these genes was

assessed by pyrosequencing analysis. SiRNA-mediated knockdown and ectopic expression of DNMT1 were used to validate DNMT1 as a target of CG-5. **RESULTS.** CG-5 and glucose deprivation upregulated the expression of DNA methylation-silenced tumor suppressor genes, including *GADD45a*, *GADD45b*, *IGFBP3*, *LAMB3*, *BASP1*, *GPX3*, and *GSTP1*, but also downregulated methylated tumor/invasion-promoting genes, including *CD44*, *S100A4*, and *TACSTD2*. In contrast, 5-aza-deoxycytidine induced global reactivation of these genes. CG-5 mediated these epigenetic effects through transcriptional repression of DNMT1, which was associated with reduced expression of Sp1 and E2F1. SiRNA-mediated knockdown and ectopic expression of DNMT1 corroborated DNMT1's role in CG-5-mediated modulation of gene expression. Pyrosequencing revealed differential effects of CG-5 versus 5-aza-deoxycytidine on promoter methylation in the genes examined. **CONCLUSION.** These findings reveal a previously uncharacterized epigenetic effect of ERMAs on DNA methylation-silenced tumor suppressor genes, which may foster novel strategies for prostate cancer therapy.

中文摘要

第一部份：法布瑞氏症之分子生物學研究。

背景。法布瑞氏症是一種性聯遺傳的溶酶體儲積症，在男性的發生率約為1/50,000，起因為缺乏α-半乳糖苷酶A（α-Gal A）的活性。心臟變異型法布瑞氏症類似肥厚型心肌病變，被定義為存在著其他不明原因的心肌肥厚。法布瑞氏症起初被認為只影響男性，女性通常被認為是無症狀的帶原者。然而，最近的研究顯示，法布瑞氏症的女性帶原者仍可能造成重要的器官傷害，導致嚴重的發病率與死亡率。此外，有關於以酵素替代療法治療亞洲的法布瑞氏症患者臨床療效的資訊十分有限。**方法**。為了確定法布瑞氏症在台灣人口中的發生率，我們使用乾燥血片進行α-Gal A酵素活性的新生兒篩檢。並經由帶有法布瑞氏症基因(*GLA*)突變點IVS4+919G>A家族成員的追溯，進行帶有此突變點的94位成人 [22位男性與72位女性；平均年齡：男性57.8±6.0歲（年齡範圍42-68歲），女性39.1±14.1歲（年齡範圍19-82歲）] 的酵素分析與臨床評估。另外確認了121名新生兒帶有20種不同的*GLA*基因突變點，同時也發現大多數的女性帶原者無法以酵素檢測來確認。因此，我們設計出一個利用高解析溶解分析法的簡化方法篩檢*GLA*基因突變，使用同一組聚合酶連鎖反應與溶解程序。引子的設計為覆蓋7個外顯子以及華人常見的內含子突變，即*GLA*基因的IVS4+919G>A。我們並回溯分析38位台灣的法布瑞氏症病患（包括21位男性與17位女性，年齡範圍為14.4至79.1歲，其中15位屬典型病患，2位屬腎臟型病患，21位屬心臟型病患）接受每兩週一次的靜脈注射 agalsidase beta （1毫克/公斤）或 agalsidase alpha （0.2毫克/公斤），為期6-36個月。在酵素替代療法開始前與治療後，以心臟超音波，尿液白蛋白與肌酐酸比值，以及預估的腎小球濾過率（eGFR）進行病患的追蹤評估。**結果**。在110,027名新生兒中，低的血漿α-Gal A活性與同時存在法布瑞氏症突變點在45名新生兒（包含3名女性新生兒）中獲得證明。我們總共確定了8個不同的基因突變，包括3個已知的錯意突變（R112H、A143T、R356W），4個新的錯意突變（G104V、M296L、G360C、K391T），以及一個已知的內含子突變（IVS4+919 G>A）。IVS4+919G>A突變是其中最常見者（占了全部基因突變

的82%）。共有20位具有此內含子突變的嬰兒的外祖父母以心臟超音波、基因突變分析以及α-Gal A的活性檢測進行評估。此內含子突變被發現存在於9位外祖父與11位外祖母。在這些外祖父母中，3位外祖父（占33%）有肥厚型心肌病變，但是外祖母均無肥厚型心肌病變。此外，16位先前診斷為不明原因的肥厚型心肌病變的男性進行了基因突變分析以及α-Gal A酵素活性的篩檢，結果顯示4位男性（占25%）缺乏血漿α-Gal A酵素活性並合併此內含子突變。此外，94位成人的血漿α-Gal A活性測定值為正常男性的10.4±11.2%，以及正常女性的48.6±19.5%。90位成人的心電圖顯示有19位左心室肥厚（LVH）（占21%），其中包括21位男性中的14位（占67%）與69位女性中的5位（占7%）。根據至少兩次測量尿液中的白蛋白與肌酸酐的比值，顯微白蛋白尿存在於86例中的17例（占20%）（男性：5/20，占25%；女性：12/66，占18%）。至少有一項與法布瑞氏症的眼部表現一致，存在於52例接受眼科檢查中的41例（占79%），包括8例（占15%）為結膜血管彎曲，15例（占29%）為渦狀角膜，10例（占19%）為法布瑞氏症白內障，34例（占65%）為視網膜血管彎曲。在超過40歲的受試者中，男性比女性更可能發生左心室肥大 [男性：14/21（占67%）；女性：5/25（占20%），p <0.001]。高解析溶解分析法成功地確認了帶有這20個*GLA*基因突變點的異型合子與半合子的患者。我們同時成功地使用此方法測試帶有*GLA*基因突變點的新生兒的乾燥血片，而無需在聚合酶連鎖反應放大之前即決定DNA的濃度。在經過6至36個月的酵素替代治療後，心臟超音波顯示19位患者 (19/31，61%) 的左心室質量減少，25位患者 (25/32，78%) 的心室間隔厚度減少，以及20位患者 (20/33，61%) 的左心室後壁厚度減少。對於17位在治療前即出現顯微白蛋白尿（根據尿液的白蛋白與肌酸酐的比值）的患者，其中16位 (94%) 在酵素替代治療後有改善。對於16位在治療前即出現異常 eGFR（根據血漿的肌酸酐）的患者，其中10位 (63%) 在酵素替代治療後的腎功能有改善。全部患者在治療期間並無嚴重臨床事件的報告。**結論**。我們在台灣族群的新生兒篩檢研究顯示，法布瑞氏症在男性的發生率約為1/1,400。我們發現了一個出乎意料的心臟變異型突變點IVS4+919G>A在男性新生兒 (發生率約為1/1,600) 與不明原因的肥厚型心肌病變患者間的高盛行率。對於尚未診斷的患者若能早期確診，可以提供及時的治療，並同時具有更好的臨床效果。就帶有*GLA*基因突變點

IVS4+919G>A 的台灣華人成人而言，心血管、腎臟與眼部異常的盛行率是很高的。我們的研究結果有助於增進目前對於這種晚發性變異疾病病程的有限了解，並顯示出密切追蹤這些病人的重要性。此外，使用高解析溶解分析法快速篩檢帶有法布瑞氏症突變點的女性是一個可靠與具敏感性的方法。酵素替代療法對於所有患者的耐受性良好，治療結果顯示出對於台灣的法布瑞氏症患者有著安全而有助益的療效。

第二部份：以瓦氏效應為標靶，經由 DNA 甲基化的改變活化沉默的抑癌基因。 **背景**。以能量限制模仿劑（ERMAs）作為腫瘤代謝的標靶治療已經成為癌症的治療以及預防的策略。證據顯示ERMA參與的抗腫瘤作用與表觀遺傳基因的調控之間有著機轉上的相關性。**方法**。微陣列分析顯示，一個新的thiazolidinediones衍生的ERMA，CG-12，以及葡萄糖剝奪能抑制DNA甲基轉移酶（DNMT）1的表現並活化在LNCaP前列腺癌細胞中受到DNA甲基化而沉默的抑癌基因。因此，我們研究一個強力的CG-12衍生物，CG-5，連同2-deoxyglucose，葡萄糖剝奪以及5-aza-deoxycytidine 在DNMT異構酶的表現（西方墨點法，反轉錄聚合酶連鎖反應）、DNMT1的轉錄活化（螢光素酶報導基因分析），以及經常在前列腺癌中高度甲基化基因的表現的影響（定量即時聚合酶連鎖反應）。以焦磷酸測序分析來評估這些基因中啟動子的甲基化程度。SiRNA參與的基因減弱與DNMT1的異位表現被用來驗證DNMT1為CG-5的標靶。**結果**。CG-5與葡萄糖剝奪可上調DNA甲基化沉默的抑癌基因的表現，包括GADD45a，GADD45b，IGFBP3，LAMB3，BASP1，GPX3，以及GSTP1，但也下調甲基化的腫瘤/入侵促進基因，包括CD44，S100A4，以及TACSTD2。相反地，5-aza-deoxycytidine會導致這些基因的全面再活化。CG-5經由DNMT1的轉錄抑制，參與這些表觀遺傳效應，其與Sp1與E2F1的降低表現有關。SiRNA參與的基因減弱以及DNMT1的異位表現，證實了DNMT1在CG-5參與調節的基因表現中所扮演的角色。焦磷酸測序顯示CG-5與5-aza-deoxycytidine在測試基因的啟動子甲基化有著不同的效應。**結論**。這些發現顯示一個先前所未知的ERMAs對於DNA甲基化沉默的抑癌基因的表觀遺傳效應，這可能開啟治療前列腺癌的新策略。

Part I: Molecular Studies of Fabry Disease

LIST OF ABBREVIATIONS

α-Gal A: *α*-galactosidase A

Gb-3: globotriaosylceramide

HCM: hypertrophic cardiomyopathy

LVH: left ventricular hypertrophy

ERT: enzyme replacement therapy

DBS: dried blood spot

HRM: high resolution melting

PCR: polymerase chain reaction

EDTA: ethylene diamine tetraacetic acid

LVM: left ventricular mass

IVS: intraventricular septum

LPW: left posterior wall

INTRODUCTION

1.1. Newborn screening for Fabry disease

Fabry disease (MIM 301500) is an X-linked lysosomal storage disorder resulting from deficient α-galactosidase A (α-Gal A) activity. It has been estimated that this disease affects 1 in ~50,000 males in the general population (1,2). α-Gal A is an enzyme involved in the metabolic breakdown of globotriaosylceramide (Gb-3) and deficient activity of this enzyme results in Gb-3 accumulation in the walls of small blood vessels, nerves, dorsal root ganglia, renal glomerular and tubular epithelial cells, and cardiomyocytes. It is a complex multisystemic disorder characterized clinically by peripheral neuropathic pains (chronic burning and acute episodes of severe pain), gastrointestinal disturbances, characteristic skin lesions (angiokeratomata), progressive renal impairment, cardiomyopathy, and early stroke (1).

In the past decades, two variant types of Fabry disease with manifestations primarily involving the heart (3-8) or kidneys (9,10) have been reported, and several studies found that the Fabry cardiac variants usually mimic idiopathic hypertrophic cardiomyopathy (HCM). Patients with the cardiac variant lack the classical symptoms of Fabry disease and present in the 5^{th}-8^{th} decades of life with left ventricular hypertrophy (LVH), arrhythmias, and/or cardiomyopathy (3-8). Previous studies have shown that 1-4% of male patients with LVH or HCM had undiagnosed Fabry disease (6-8).

Enzyme replacement therapies (ERT) are available and experiences to date indicate that early therapeutic intervention results in a better outcome (11-15). Therefore, early detection of Fabry disease, especially of the variant types, is important. In the past decade, a new fluorimetric α-Gal A activity assay using dried blood spots (DBS) has been successfully developed and is a useful tool for Fabry disease screening initiatives (16-18). Spada et al were the first to report the use of this assay in their Italian newborn screening program. This group found a higher than expected incidence of α-Gal A deficiency (1 in ~3,100 newborns) with a late-onset to classic type ratio of 11 to 1 (19).

Our newborn screening study aimed at assessing the incidence of Fabry disease in the Taiwan Chinese population and is the largest Fabry screening

study performed to date. In addition, our study aimed at identifying unrecognized Fabry patients among family members of diagnosed newborns and among individuals with idiopathic HCM.

1.2. Enzyme assay and clinical assessment in subjects with a Chinese hotspot late-onset Fabry mutation (IVS4+919G>A)

There is increasing recognition that manifestations in heterozygous females can range from no symptoms at all to abnormalities as severe as those in affected males (20-22). Patients with the renal variant develop proteinuria and may progress to end-stage renal disease, typically after 50 years of age. Screening by plasma α-Gal A activity has shown that 0.25% to 1% of men undergoing hemodialysis were identified with previously undiagnosed Fabry disease (9,10,23). Patients with neurologic variant also lack the classic symptoms, but develop cerebrovascular disease at around 40 years of age. The prevalence of Fabry disease in young patients (18-55 years old) with cryptogenic stroke was reported to be as high as 4.9% in men and 2.4% in women (24). Ocular findings may suggest the diagnosis in some individuals, where progressive deposition of Gb-3 in ocular structures may result in abnormalities at the level of the conjunctival vessels, cornea, lens, or retinal vessels (25-28).

In Japan, an IVS4+919G>A splicing mutation has been reported in patients with the late-onset cardiac phenotype (29). Lin et al (30) screened ~57,000 newborn boys and found various Fabry mutations in ~1 in 1,400, 83% of whom had the cardiac variant mutation IVS4+919G>A, for an incidence of ~1 in 1,600. Hwu et al (31) screened ~90,000 baby boys and found Fabry mutations in ~1 in 1,250, 86% with IVS4+919G>A, an incidence of 1 in 1,500. This suggests a substantial incidence of the mutation in the Taiwanese population as a whole, but little is known about its phenotype in adult men and women. We previously looked for LVH in 20 maternal grandparents of babies carrying this mutation (30). The aim of the present study was to perform enzyme assays and assess clinical manifestations in a larger group of Taiwanese adults who carry the

IVS4+919G>A mutation in order to help to delineate the natural history of late-onset Fabry disease associated with this genotype.

1.3. The use of high resolution melting (HRM) analysis to detect Fabry mutations in heterozygous females via DBS

Recently, we conducted a study that revealed a surprisingly high incidence of the cardiac variant *GLA* mutation IVS4+919G>A (~1 in 1,500-1,600 males) in the Taiwan Chinese population (30). Via family studies of newborns with the IVS4+919G>A mutation, we evaluated the clinical manifestations in the adults older than 40 years with this mutation. We found that 47 out of 93 subjects (51%) had LVH, including 28 males (28/39; 72%) and 19 females (19/54; 35%). We also found a positive correlation between disease-onset rate and age of the patient (Fig. 1). In addition, none of the 19 female subjects had α-Gal A enzyme activity less than 3.1 μmol/h/L (25% of the normal mean; 25% is our cutoff value of newborn screening). Very similar finding was observed for our female patients who have classic type mutations and significant systemic involvement. Only 2 out of these 12 females had α-Gal A enzyme activity less than 3.1 μmol/h/L. We also analyzed the enzyme activity of 35 young females (age > 40 years old) with IVS4+919G/A mutation, who did not suffer from LVH and found that around 89% of these females had enzyme activity greater than 25% of the normal mean (Fig. 2). These findings showed that current newborn screening techniques are insufficient in identifying female carriers of Fabry mutations. Considering that most female carriers even with sufficient residual enzymatic activity could still suffer from significant systematic disease, we aimed to develop a new method of newborn screening for Fabry mutations that would be able to detect female carriers.

1.3.1. HRM analysis

It has long been noted that HRM analysis provides a simple, reliable and cost-effective method to identify sequence variants (32-35). The procedure is conducted firstly by a polymerase chain reaction (PCR) amplification in the presence of an appropriate DNA binding dye, followed by the formation of heteroduplex molecules, and a final melting and analysis step. Through this

study, we aimed to develop a streamlined method for HRM analysis of the 7 exons (including the flanking intronic sequences) and the Chinese common intronic mutation, IVS4+919G>A of *GLA* gene using the same PCR and melting program. We also successfully used this method with DBS extracts of the newborns with Fabry mutations without the necessary step of determining DNA concentration before PCR amplification.

1.4. ERT for Fabry disease---experience in Taiwan

Before 2001, treatment of patients with Fabry disease was exclusively supportive. Advancement of molecular genetic techniques led to the development of ERT. There are two forms of ERT: agalsidase α (AGALA) (Replagal®; Shire Human Genetic Therapies Inc, Cambridge, MA) and agalsidase β (AGALB) (Fabrazyme®; Genzyme Corporation, Cambridge, MA). Previous studies showed that ERT was an effective treatment for neuropathic pain (36) and can stabilize renal function or at least slow the decline of renal function in many patients with Fabry nephropathy (11,13,14,37-41) and stabilize or improve surrogate parameters like cardiac size in those with cardiomyopathy (37,42-44). However, information regarding the clinical outcome of ERT for Asian Fabry disease is limited. We evaluated the effects of ERT for 38 Taiwanese patients with Fabry disease in this study.

MATERIALS AND METHODS

2.1. Newborn screening for Fabry disease

2.1.1. Participants

The large-scale newborn screening program for Fabry disease was based on assessment of the α-Gal A enzyme activity using DBS on filter paper, and was conducted at two newborn screening centers, the Chinese Foundation of Health, and the Taipei Institute of Pathology, Taipei, Taiwan. The centers screen ~55% of all newborns in Taiwan. Routine newborn screening DBS samples collected by the age of 3 days in 110,027 newborns between January 2008 and January 2009 were analyzed. Parental informed written consent was obtained for each sample collected. The study was approved by the ethics committee of the Taipei Veterans General Hospital, Taipei, Taiwan.

2.1.2. DBS test

α-Gal A activity in DBS on filter paper was determined using a fluorescence-based high-throughput method with modifications of a reported procedure (16). To establish a normal population mean, α-Gal A activity was measured in 10,000 anonymous newborn samples. Newborns with α-Gal A activity <3 μmol/hr/L (i.e. <20% of the normal mean) were considered “screen positive”, and for these individuals a second blood spot was requested and assayed. Re-tested newborns with blood spot α-Gal A activities <2 μmol/hr/L (i.e. <10% of the normal mean) were considered “double DBS screen positive”, and were recalled to Taipei Veterans General Hospital for confirmatory testing, including genetic analysis of the *GLA* gene (Fig. 3).

2.1.3. Plasma α-Gal A enzyme activity assay

Plasma α-Gal A activity was determined using the substrate 4-methyl-umbelliferyl α-D-galactopyranoside (5 mM) freshly prepared in 117 mM N-acetyl-D-galactosamine/50 mM citric-phosphate buffer, pH 4.6, before every assay. In brief, 50 μL of plasma was mixed with 300μL of the substrate solution, incubated at 37 ^{o}C for 2 hours, and 0.2N glycine-NaOH was added to stop the reaction. Fluorescence intensity was measured with the excitation and emission wavelengths of 365 μm and 450 μm, respectively (45,46).

2.1.4. *GLA* gene mutation analysis

Patients with low α-Gal A enzyme activities (normal range: 7.9-16.9 nmol/hr/mL plasma) (45,46) were subject to genetic analysis. Blood samples were obtained from these patients in blood collecting tubes containing ethylene diamine tetraacetic acid (EDTA) and samples were stored at 4°C. DNA was isolated from whole blood using the GFX genomic Blood DNA Purification Kit (Amersham Biosciences, UK) following the manufacturer's instructions. The human *GLA* gene consists of 7 exons. Each exon of *GLA* gene was amplified by PCR using appropriate primers (47). The PCR products were analyzed by 1.5% agarose I (Amresco) gel electrophoresis and then eluted in the PCR Advanced PCR Clean Up System (Viogene, U.S.A.). Direct sequencing of the *GLA* gene was processed using the BigDye Terminator v3.1 Cycle Sequencing Kit (Applied Biosystems) and ABI Prism® 3730 Sequencer.

2.1.5. Pedigree studies

For each patient, a complete pedigree was drawn and genetic counseling and pedigree analysis were provided to family members. Parents and grandparents of these patients were offered the combination of α-Gal A activity assay, mutation analysis and related medical evaluations.

2.1.6. Screening of patients with idiopathic HCM in cardiac clinics

Twenty-three patients (16 males, 7 females; mean age 50.6 ± 14.3 years; age range 18-67 years), who had been diagnosed with idiopathic HCM, were subject to analyses of plasma α-Gal A activity and the IVS4+919G>A mutation.

2.2. Enzyme assay and clinical assessment in subjects with a Chinese hotspot late-onset Fabry mutation (IVS4+919G>A)

2.2.1. Study design and subjects

Pedigree analysis was offered to the parents of the newborns with the IVS4+919G>A mutation who had been identified via the Fabry disease newborn screening program in Taiwan (30). Once families had consented to participate, parents, grandparents and other blood relatives underwent mutation analysis. Ninety-four adult subjects who were found to have the IVS4+919G>A mutation were enrolled in the current study. Informed written

consent was obtained from each of the subjects. The study was approved by the ethics committee of Taipei Veterans General Hospital, Taipei, Taiwan.

2.2.2. Molecular, biochemical and clinical assessments

The *GLA* exons and adjacent intronic and promoter regions were sequenced using standard techniques as described elsewhere (48,49). Plasma α-Gal A enzyme activity was measured according to the method described by Desnick et al (46) and expressed as numerical value and as the percentage of the mean in normals (i.e. 12.4 nmol/h/mL plasma) (45,46).

A total of 94 subjects carried the mutation and were asked to undergo screening for cardiac, renal, and ocular abnormalities. However, it was up to the subjects to follow through with all instructions. All had at least one of the examinations.

Spot urine samples for measurement of albumin and creatinine levels were collected on at least two occasions to rule out confounding factors unrelated to Fabry disease. The ratio of concentrations of urinary albumin and creatinine expressed as mg/mmol was used to estimate the total daily albumin excretion. Microalbuminuria was defined as urinary albumin-to-creatinine ratio ≥2.0 mg/mmol for men and ≥2.8 mg/mmol for women on at least two occasions, based on the National Kidney Foundation's Kidney Disease Outcome Quality Initiative working group definition (50).

Cardiac evaluation included electrocardiography and standard echocardiography. LVH was defined as left ventricular mass >259 g in men and >166 g in women (51).

Ophthalmological evaluation included slit lamp examination of the bulbar conjunctiva, cornea, lens and fundus.

2.2.3. Statistical analysis

The Statistical Package for Social Sciences (SPSS®) version 11.5 (SPSS Inc, Chicago, IL) was used to analyze the plasma α-Gal A activity, as well as clinical manifestations and gender differences. Relationships between clinical findings and age, as well as clinical findings and plasma α-Gal A activity were tested using Pearson correlation, and significance was tested using Fisher r-z

transformations. Differences were considered to be statistically significant if the *p* value was less than 0.05.

2.3. The use of HRM analysis to detect Fabry mutations in heterozygous females via DBS

2.3.1. Subjects

From Jan 2008 to Dec 2010, a total of 299,007 (156,179 males) newborns were screened for Fabry disease at our cooperative newborn screening centers (Taipei Institute of Pathology and Chinese Foundation of Health). From this screening, we identified 121 (106 males) newborns carrying Fabry mutations. Thereafter, we identified 218 family members (including males and females) carrying Fabry mutations via family studies. A total of 20 different mutations were identified in these patients (Fig. 4). Aside from the c.274G>T mutation, which was only identified in one female heterozygous patient, all other mutations were identified in both male and female patients enrolled in the HRM analysis study. Thirteen unaffected individuals were analyzed as normal controls in this study.

2.3.2. Methods

Genomic DNA samples were extracted from whole blood or DBS using MagCore HF16 Automatic DNA/RNA Purification system (RBC Bioscience Corp., Taiwan) with MagCore Tissue Genomic DNA Extraction Kit (RBC Bioscience Corp., Taiwan). DNA concentrations were determined using a Nanodrop spectrophotometer (Infinigen, USA). The sequences of primer sets, annealing temperatures and fragments sizes of each amplicon used in PCR and HRM analysis are listed in Table 2. Primer sets were designed using GenBank accession number NM_000169.2 as a reference sequence. The primer sets were used to amplify the sequences of seven *GLA* exons and the region including IVS4+919G>A. The PCR mixture used contained 1 × Roche LighCycler High Resolution Melting Master, 2 pmol of each primer and 6 ng of genomic DNA for a total volume of 20 μL. For the dry blood sample tests, 2 μL of out of 30 μL extracts, which were extracted from 3 punched (5 mm in diameter) DBS, were substituted for the 6 ng of genomic DNA. The PCR and

HRM analyses were performed using a Roche LightCycler® 480 system. The amplification was performed with an initial denaturation at 95°C for 10 min, followed by 45 cycles of denaturation at 95°C for 10 s, annealing at 60°C for 15 s and extension at 72°C for 12 s. To facilitate heteroduplex formation, all the PCR products were heated to 95°C for 1 min and cooled down to 40°C. Melting curves were generated by heating the samples from 65 to 95°C at a ramp rate of 1°C/s. The melting curves were normalized by selecting linear regions of pre- and post-melting transition, and defined as 100% and 0%. The melting curves were displayed as melting peaks. Mutations were identified through a change in melting curve position, shape or deviated melting curve shape.

All the sequence variations are described according to the guidelines for mutation nomenclature recommended by Human Genome Variation Society (http://www.hgvs.org/mutnomen/) using the cDNA sequence NM_000169.2 as the reference. PCR products of normal genotype are described as “c.[=]+[=]”, while hemizygous PCR products are described as “c.[variation]” and heterozygous PCR products are denoted as “c.[variation]+[=]”.

2.4. ERT for Fabry disease---experience in Taiwan

We reviewed 38 Taiwanese patients with Fabry disease (21 males and 17 females; age range, 14.4 to 79.1 years; 15 with classic type, 2 with renal type, and 21 with cardiac type) treated with biweekly intravenous infusions of agalsidase β (1 mg/kg) or agalsidase α (0.2 mg/kg) for at least 6 months. Left ventricular mass (LVM), the thicknesses of intraventricular septum (IVS) and left posterior wall (LPW) by echocardiographic assessments (52, 53), urine albumin-to-creatinine ratio, and estimated glomerular filtration rate (eGFR) (54) were evaluated at baseline and after ERT.

RESULTS

3.1. Newborn screening for Fabry disease

3.1.1. Fabry screening in newborns

Of the 110,027 newborns screened, 57,451 (52.2%) were males and 52,576 (47.8%) females. There were 67 “double DBS screen positive” newborns (9 females) recalled to our hospital for confirmatory testing, of whom 45 newborns (3 females) were identified to have low plasma α-Gal A activity and a *GLA* mutation (Table 3). Eight mutations were detected, including 3 known missense mutations (R112H [55,56], A143T [57,58], R356W [55,59]), 4 novel missense mutations (G104V, M296L, G360C, K391T), and one known intronic splicing mutation (IVS4+919G>A) (29) (Table 4). None of these mutations were found in 50 unrelated healthy females. The IVS4+919G>A mutation was noted to be the most common mutation among these newborns (82% of patients). Although this splicing mutation has been found in Japanese Fabry patients with a cardiac variant (29), its incidence in Japan is still unknown. In our study, the incidence of Fabry mutations was 1 in 1,368 for males. If the 4 novel missense mutations were excluded, the incidence of the known disease-causing mutations would be 1 in 1,512 males.

3.1.2. Pedigree studies

Data on enzyme activity levels and genetic analyses from the maternal grandparents was limited due to the unavailability of data, personal concerns or death. Among the 35 male neonates with the IVS4+919G>A mutation, 20 maternal grandparents were ascertained to have the same mutation, including 9 grandfathers and 11 grandmothers (Table 5). Because of the high prevalence of the Fabry cardiac variant mutation IVS4+919G>A among the Taiwan Chinese population, we paid attention to the cardiac conditions of family members with the IVS4+919G>A mutation. Among 9 maternal grandfathers with the IVS4+919G>A mutation, 3 (33%) had HCM, compared with none of the 11 grandmothers with this disease (Table 5). The plasma α-Gal A activities of the 9 grandfathers ranged from 0.56 to 2.40 nmol/hr/mL, while those of the 11 grandmothers ranged from 3.87 to 10.72 nmol/hr/mL (Table 5).

3.1.3. Screening of patients with idiopathic HCM in cardiac clinics

To explore the occurrence of the cardiac variant mutation IVS4+919G>A in Taiwan Chinese idiopathic HCM patients, we analyzed the plasma α-Gal A activities and presence of this mutation in 23 patients diagnosed with HCM in the outpatient clinics. Four out of 16 male patients (25%) had both deficient plasma α-Gal A activities (ranging from 0.65 to 0.98 nmol/hr/mL) and the IVS4+919G>A mutation (Table 6). In contrast, the plasma α-Gal A activities in male patients without the IVS4+919G>A mutation ranged from 9.39 to 14.53 nmol/hr/mL. It is noteworthy that none of the female patients was detected to have the IVS4+919G/A mutation and that their plasma α-Gal A activities ranged from 6.59 to 16.12 nmol/hr/mL.

Histological examination of endomyocardial tissue of Patient 4 in Table 6, a 67-year-old male patient with HCM, showed disorderly arranged myocytes with marked hypertrophy and large perinuclear and sarcoplasmic vacuoles, accompanied by focal interstitial fibrosis, which is consistent with the diagnosis of Fabry disease (Fig. 5).

3.2. Enzyme assay and clinical assessment in subjects with a Chinese hotspot late-onset Fabry mutation (IVS4+919G>A)

Among the 94 adult subjects with the IVS4+919G>A mutation, there were 22 men and 72 women. Their mean age (± SD, range) was 57.8 (6.0, 42-68) and 39.1 (14.1, 19-82) years, respectively (Fig. 6). Half of the subjects were women under 40 years of age, and 22 men (23% of all subjects) and 25 women (27%) were older than 40.

The plasma α-Gal A activity was analyzed in all subjects; the mean (± SD, % of normal) values were 1.29 (1.39, 10.4 ± 11.2) nmol/h/mL plasma for men and 6.03 (2.42, 48.6 ± 19.5) nmol/h/mL plasma for women (Fig. 7). There were no correlations ($p > 0.05$) between clinical findings and plasma α-Gal A activity in both men and women.

Echocardiographic examinations (n = 90) revealed LVH in 67% of 21 men assessed and in 7% of 69 women (Table 7). Men over 40 years were more likely to have LVH than women over 40 (67% and 20%, respectively; $p <$

0.001). LVH was more likely to occur in women over 40 than in women under 40 years of age ($p < 0.005$) and developed progressively ($r = 0.588$, $p < 0.01$).

Microalbuminuria or higher levels of proteinuria were found in 17 subjects (20% of 86), including 5 men (25%) and 12 women (18%, Table 7). There was no significant difference between its presence in men (25%) and women (30%) older than 40 ($p = 0.700$), and between women older and younger than 40 ($p = 0.06$). However, (micro)albuminuria or proteinuria developed progressively in women ($r = 0.281$, $p < 0.05$).

At least one Fabry-related ocular manifestation was present in 41 subjects (79% of subjects examined); in 43% of men and 84% of women. Ocular abnormalities included retinal vessel tortuosity (29%, 71%, respectively), cornea verticillata (14%, 31%), Fabry cataract (0%, 22%) and conjunctival vessel tortuosity (14%, 16%) (Table 7, Fig. 8). There were no statistically significant differences between genders or age categories. The examinations were mostly performed by one ophthalmologist, PKL (79%), whereas 21% of the subjects were examined by other ophthalmologists at the ophthalmology outpatient clinic.

3.3. The use of HRM analysis to detect Fabry mutations in heterozygous females via DBS

Initially we used the original sequence primers (total 8 primer sets, Table 2) which had been used for sequencing in previous studies (30), (47), (60), (61), (62), (63), and (64), to cover all seven exons of the *GLA* gene and the intronic IVS4+919G>A mutation. However, two mutations, c.1172A>C and c.1194delA, both located at the 3′ region of exon 7, were not identified in heterozygous or hemizygous patients (Fig. 9B). The IVS4+919G>A mutation was not identified in hemizygous patients.

The amplicons of exon 7 and IVS4+919G>A mutation were the two largest amplicons (352 and 446 bp) in these 8 original sequence primer sets (241-446 bp, Table 2). Because the ideal amplicon length is less than 250 bp for HRM analysis, we designed two new primer sets (exon 7-1 and 7-2, Table 2 and Fig. 9) to cover exon 7 and a new IVS4 primer set (IVS4-1) to cover the

IVS4+919G>A mutation (Table 2). All new designed primer sets created smaller amplicons (220, 233 and 121 bp, respectively). Thereafter, both the heterozygous and hemizygous patients of these mutations could be identified by HRM analysis (Fig. 9C, 10). The HRM curves of the identified mutations (excluding IVS4+919G>A) are shown in Fig. 11.

The MagCore HF16 Automatic DNA/RNA Purification system was then used to extract DNA samples from DBS. We found that the DNA concentration extracted from blood spots via this DNA extraction system were usually within the acceptable concentrations (around 6 ng/μL) for HRM analysis. Therefore, this method was successful in identifying the mutations from the DBS of the newborns without determining DNA concentration before the PCR amplification. In order to examine the discrimination ability, we performed HRM analysis with 30 samples of different genotypes. The results of 30 DBS samples, including 13 normal, 7 hemizygous and 10 heterozygous individuals with IVS+919G>A mutation, in one HMR analysis are shown in Fig. 10.

3.4. ERT for Fabry disease---experience in Taiwan

After 6-36 months of ERT, echocardiography revealed reductions of LVM (Table 8, Fig. 12, 13), the thicknesses of IVS (Table 9), and LPW (Table 10) in 19 (19/31, 61%), 25 (25/32, 78%), and 20 (20/33, 61%) patients, respectively. For 17 patients with microalbuminuria (based on urine albumin-to-creatinine ratio) at baseline, 16 patients (94%) showed some degree of improvement after ERT (Table 11). For 16 patients with abnormal eGFR (based on plasma creatinine) at baseline, 10 patients (63%) revealed improvement of renal function after ERT (Table 12). No severe clinical events were reported during the treatment.

DISCUSSION

4.1. Newborn screening for Fabry disease

One of the important findings of our large-scale newborn screening study in the Taiwan Chinese population is the high incidence of Fabry mutations. The incidence of Fabry mutations was 1 in 1,368 for males. This incidence is about 30 times higher than previous estimates (1,2) and 2 times higher as compared to the incidence found in an Italian newborn screening study (19).

Eight different mutations were identified, including 3 known missense mutations (R112H [55,56], A143T [57,58], R356W [55,59]), 4 novel missense mutations (G104V, M296L, G360C, K391T), and one known intronic mutation (IVS4+919G>A) (29). The IVS4+919G>A mutation was most common (82% of patients). The 3 known mutations which have been reported to be associated with mild classic (R356W [55,59]) or late-onset renal or cardiac (R112H [55,56], A143T [57,58]) forms. The intronic mutation (IVS4+919G>A) was reported to be a cardiac variant Fabry mutation (29).

None of the 4 novel mutations were found in 50 unrelated healthy females, which makes the possibility of polymorphisms unlikely. However, whether these mutations will eventually cause Fabry disease remains unknown. Further comprehensive family studies and long-term follow up for identified individuals with these mutations are warranted. If the 4 novel missense mutations are excluded, the incidence of the known disease-causing mutations would be 1 in 1,512 males.

In our study, only one newborn was noted to have a previously reported mutation (R356W) causing a classic phenotype (Table 4). Therefore, the calculated incidence of classic Fabry disease in the Taiwan Chinese population is ~1 in 57,000 males which is equivalent to previous estimates (1,2).

There was a surprisingly high incidence of the IVS4+919G>A mutation among newborns with α-Gal A deficiency. This intronic mutation was detected in 83.3% of the 42 male newborns found with Fabry mutations which translates in an incidence of ~1 in 1,600 male newborns. This IVS4+919G>A mutation has been reported to be associated with cardiac variant Fabry disease by Ishii

et al (29). It can activate an alternative splicing in intron 4 causing insertion of a 57-nucleotide sequence between exons 4 and 5 of the α-Gal A cDNA and subsequent premature termination after 7 altered amino acid residues downstream from exon 4. In general, the alternatively spliced transcript was present in a small amount (<5 % of normal transcript) in most normal human tissues. However, in Fabry patients with the IVS4+919G>A mutation, the alternatively spliced transcript will be largely increased (>70 % in lymphoblasts) and the enzyme activity will be decreased to <10% of normal activity (lymphoblast).

Another interesting finding of our study is that the mild-form pathogenic mutation IVS4+919G>A apparently does not consistently cause Fabry-related HCM in all affected individuals. Out of the 9 maternal grandfathers with the IVS4+919G>A mutation, only 3 had HCM (Table 5). It remains to be elucidated why some patients with this mutation suffer from cardiomyopathy as early as in their forties, while others with this same mutation do not have any symptoms or signs of cardiomyopathy even in their seventies. In this study, no correlation between the plasma α-Gal A activity and the existence of HCM was found. However, the sample size is too small to make definite conclusions regarding the likelihood of the IVS4+919G>A mutation leading to the cardiac variant of Fabry disease. Because the newborn screening is still ongoing, we hope that we will be able to eventually expand the database and get a clearer picture of this. Further investigations are required to identify genes or other factors involved in the modification of clinical expression of Fabry disease and to elucidate if there are other pathogenic mutations related to mild phenotypes.

Fabry disease has historically been described as an X-linked recessive disease, however, a substantial proportion of heterozygous females will develop disease manifestations. In some, the disease presentation may be as severe as seen in young males and others may remain relatively asymptomatic until late adulthood (21,22). This phenomenon is, in part, caused by skewed X chromosome inactivation. If most of the mutation-harboring X chromosomes are inactive in females, then the clinical presentation will be rather mild. On the other hand, the clinical presentation

can be severe when most of the normal X chromosomes are inactive. With regard to cardiac involvement in female Fabry patients, Fabry disease may account for up to 12% of females with late-onset HCM (65). Kampmann et al evaluated 55 affected females and reported echocardiographic evidence of cardiac involvement in 56% of females aged <38 years, in 86% of females aged >38 years, and in all female patients >45 years of age (66). Schiffmann et al reported natural history data on 168 ERT-naive female Fabry patients of whom 35% had developed a cardiac event (e.g. arrhythmia, angina, myocardial infarction, cardiac surgery) by a mean age of ~44 years (67). X-inactivation patterns vary widely between female Fabry patients and different tissues, and the enzyme activity measured in lymphocytes can be very different from other tissues, such as heart or kidney. Therefore, in females, the result of the lymphocyte enzyme activity assay is not predictive of disease severity in a particular organ, and the result may fall within the normal range although the female can be clinically affected (68). Thus, the lymphocyte enzyme activity assay is not suitable as a screening tool in female populations and, it is not surprising that only a very few females were detected via the enzyme activity screening in this study. Screening for hot spot mutations may be an alternative method to detect unidentified female Fabry patients in high risk populations.

Although only 1/3 of the grandfathers with the IVS4+919G>A mutation had significant HCM, the high prevalence of this mutation in the Taiwan Chinese population points at an important presence of the cardiac variant of Fabry disease among patients with HCM in this particular population. Although the studied sample size of HCM is small and the Fabry screening in patients with HCM is still ongoing, we strongly recommend that Fabry disease must be ruled out before the diagnosis of idiopathic HCM is made in the Taiwan Chinese population, both in males and females.

There are few debates that early detection, genetic counseling, regular follow-up and timely early therapeutic intervention for the classic Fabry disease is beneficial. However, for the individuals who have atypical Fabry mutations, particularly, for those whose residual enzyme activities are more than 10-20%

of normal, the strategy for regular follow up and therapeutic intervention should be different from those with the classic type, because our study showed that a significant proportion of the individuals over fifty years of age with IVS4+919G>A mutation still have not developed any symptoms or signs of this disease. Therefore, the early detection of babies with atypical Fabry mutations results in several clinical impacts: When is the best time to start evaluating the cardiac conditions of these individuals with IVS4+919G>A mutation? When is the best time to start ERT? Do we need to start ERT early, when there are only controversial or minimal manifestations of heart problems? Or do we need to wait until the cardiac manifestations become marked? Several reports indicate that ERT for the advanced form of Fabry cardiomyopathy is not very effective (12). Therefore, further investigations are needed to find out the best way for early detection of meaningful cardiac manifestations in patients with atypical Fabry mutations, and to identify the most appropriate time for them to start ERT.

4.2. Enzyme assay and clinical assessment in subjects with a Chinese hotspot late-onset Fabry mutation (IVS4+919G>A)

The natural history of early-onset “classic” Fabry disease is well documented in the literature (1,69). Cases of late-onset forms of Fabry disease have been reported but, to date, there are no reports of clinical findings in sizeable cohorts of patients. This is the first report describing the clinical features in both male and female patients carrying the IVS4+919G>A mutation in the *GLA* gene. We confirm a high prevalence of cardiovascular, renal, and ocular manifestations associated with Fabry disease in these Taiwan Chinese adult subjects, including women. Similar to the findings of Ishii et al (29) of ~10% residual α-Gal A activity in lymphocytes from patients hemizygous for the IVS4+919G>A mutation, the mean enzyme activity in the 22 men in our study was 10.4% of normal. Our study is the first to report α-Gal A activities in heterozygous women with the IVS4+919G/A mutation, i.e. 48.6% of the normal mean (n=72), and 14 women (19.4%) had normal α-Gal A enzyme activity [normal range: 7.9-16.9 nmol/h/mL plasma (45,46)].

Among subjects over 40 years of age, 67% (14/21) of men and 20% (5/25) of women had LVH. The high incidence in men is consistent both with the study from Japan and our earlier investigation (29,30). However, the present study also revealed a substantial number of women over 40 with the mutation who also had LVH. Our study was not designed to rule out other causes of LVH, so we cannot conclusively state that these individuals in fact had late-onset Fabry disease as a cause of their cardiac abnormality. However, as we previously found some cases of HCM in which the patients carried this mutation (30). In a population with a relatively high incidence of this genotype, perhaps gene testing should be considered in patients who appear to have idiopathic HCM.

Microalbuminuria was also relatively common in our subjects who were tested, one quarter of the men and nearly a third of the women over 40 years of age. As with LVH, it's possible that they may have had latent renal disease from other causes. But our study suggests that late-onset Fabry disease belongs in the differential diagnosis for these individuals.

Ocular findings are also among the early hallmarks of Fabry disease (25-28) and readily detectable by slit lamp examination. Progressive deposition of Gb-3 in ocular structures often leads to cornea verticillata (vortex keratopathy), changes of conjunctival and retinal vessels (dilatation, tortuosity, aneurysms) or lenticular changes (a "spoke-like" pattern at the level of the posterior capsule, usually referred to as "Fabry cataract"). Most women (84%) and less than half (43%) of men had at least one of these ocular manifestations. The prevalences of Fabry cataract (22%) and retinal vessel tortuosity (71%) among females were surprisingly high as compared to previous reports (Table 13). It remains to be elucidated if there is an ethnic predilection for these types of ocular abnormalities in the Taiwan Chinese Fabry patient population, or specifically in subjects with the IVS4+919G>A mutation. The prevalence of cornea verticillata was considerably lower (14% of men, 31% of women) as compared with the overall gender-specific prevalences of ~75% reported by other groups (Table 13). This may support the belief that the IVS4+919G>A mutation is a rather mild pathogenic mutation.

Our findings demonstrate that the phenotype associated with this mutation cannot be accurately predicted from the genotype alone. As expected, men who were hemizygous for IVS4+919G>A had lower enzyme activity than did women who were heterozygous. Further investigations are needed to identify genes or other factors that modify the clinical expression of late-onset Fabry disease related to this mutation.

ERT has been used to treat Fabry disease and experience reveals that early medical intervention provides a better clinical outcome (12,14,70). This leaves little doubt that early detection and timely therapy are important for patients with classic Fabry disease. These paradigms are also applicable for patients with the late-onset mutation IVS4+919G>A as cardiovascular, renal and ocular manifestations are highly prevalent among these individuals. Our data contribute to the understanding of the clinical course of this late-onset variant and provide a rational for modification of current follow up and therapeutic intervention strategies.

Limitations

Fabry disease is an X-linked lysosomal storage disorder, but we had relatively few men in our sample (Fig. 6). As subjects were selected based on the family pedigree of neonates found to have the IVS4+919G>A mutation, most were young mothers or maternal grandparents. Half were women younger than 40. It would be good to study larger groups of men, especially those younger than 40. Another limitation is the lack of complete data for all of our subjects, as they were not uniformly able to follow through on all the examinations.

4.3. The use of HRM analysis to detect Fabry mutations in heterozygous females via DBS

The results of our study have demonstrated that HRM is a reliable and sensitive method for use in rapid screening of females or even males carrying known *GLA* mutations in Taiwan. Recently, HRM analysis for detection of known and unknown mutations has grown in popularity, as HRM analysis does not require post-PCR manipulation of samples, unlike DNA sequencing

technologies and conventional gel-based or HPLC-based scanning methods (35). The cost of the reagents used in this study was less than $1 (U.S.) per sample per amplicon, making HRM a cost-effective gene variation analysis technique. In addition to PCR, HRM analysis takes only 15 min, amplifying as high as 384 wells at one time for melting analysis. Therefore, HRM has the potential to be an effective alternative method for Fabry newborn screening, especially when considering the fact that current screening methods are not reliable in females.

Although, in our study, all the hemizygous mutations could be easily identified in our study, the detection rates of hemizygous mutations were only around 75% in several studies (71,72). In a situation like this, it has been suggested that mixing the normal male DNA with the hemizygous male DNA could produce artificial heterozygotes, which would in turn increase the detection rate of hemizygous mutations. However, the increased time required to add the same amount and concentration of DNA to each male PCR tube and the fact that the current high-throughput enzymatic method for identifying male Fabry patients is highly reliable, make the HRM method to be the preferable choice only in identifying female Fabry patients this time.

The interpretation of mutation analysis via HRM is a challenge owing to the sensitivity of HRM profiles to variable concentrations of nucleic acids or salts (73,74). It is therefore recommended that DNA samples that have been prepared using a common extraction procedure be used for HRM. In our study, DNA was extracted from DBS via a steady automatic DNA extraction system, which ensured the consistency of the DNA concentration (around 6 ng/μL). In addition, the isolation reagents used to prepare DNA contain little salt, making the determination of DNA concentration unnecessary for DBS analysis. Hence, the unique advantages of HRM analysis in blood spot analysis may make HRM a possible choice for disease screening in the near future.

Another important factor to consider in the usage of HRM screening is the efficiency of any such screening operation. Each year, around 100,000 female newborns are born in Taiwan. There are 3 newborn screening centers in Taiwan, based respectively in the National Taiwan University Hospital, Taipei

Institute of Pathology, and Chinese Foundation of Health. If we divide these 100,000 female babies by 200 working days and three newborn screening centers, there are around 167 female babies to be screened for Fabry disease per center each day. Therefore, with the use of an appropriate automated nucleic acid extraction system and high throughput melting analyzer, each center could screen all 167 daily female newborns for the IVS4 mutation within 2 h (including PCR) with one analyzer. Within 8 h, each center (with two melting analyzers) could easily screen for all exons of the *GLA* gene and the Chinese common intronic IVS4 mutation. Therefore, we propose that, with an appropriately designed system, HRM analysis could be used as a simple, rapid and reliable method in female newborn screening for Fabry mutations. This method may also be viable in the detection of heterozygous Fabry patients within female patient populations suffering from HCM, renal impairment, or stroke.

A possible concern regarding HRM analysis, however, may still be its sensitivity. Two mutations were missed in the initial screening using the original primer sets, raising concerns that the method established so far is not sensitive enough to identify all Fabry mutations, especially those located at exons 2 and 6 with their amplicons are greater than 300 bp. Therefore, it will be necessary to enlarge the sample size of Fabry mutations in future studies through cooperation with other Fabry centers.

4.4. ERT for Fabry disease---experience in Taiwan

For most Taiwanese patients with Fabry disease, ERT can stabilize or improve surrogate parameters, like LVM, the thicknesses of IVS and LPW in those with LVH, improve microalbuminuria, and stabilize renal function in those with Fabry nephropathy. Our results were consistent with those of previous studies (11,13,14,37-44).

CONCLUSIONS

5.1. Newborn screening for Fabry disease

This study in the Taiwan Chinese population demonstrates the feasibility of a large-scale neonatal screening program for Fabry disease. The incidence of Fabry mutations among newborns was unexpectedly high (~1 in 1,400 male newborns), as was the prevalence of the cardiac variant mutation IVS4+919G>A. The diagnosis of Fabry disease should be considered in all patients with idiopathic HCM. The early identification of undiagnosed patients allows timely medical intervention providing a better clinical outcome.

5.2. Enzyme assay and clinical assessment in subjects with a Chinese hotspot late-onset Fabry mutation (IVS4+919G>A)

This study documents a high prevalence of cardiovascular, renal, and ocular manifestations in Taiwan-Chinese adult subjects with Fabry mutation IVS4+919G>A. This hotspot mutation has been described as a “cardiac variant” mutation, but our data demonstrate that the clinical manifestations are not confined only to the heart. Although more detailed data on the longitudinal progression of the disease will be required, our findings will be helpful in determining the necessity and timing of therapeutic intervention with ERT.

5.3. The use of HRM analysis to detect Fabry mutations in heterozygous females via DBS

Considering that a large percentage of Fabry female patients could not be identified with the current screening method, HRM analysis may be well-suited for use as a rapid newborn screening technique for Fabry disease, particularly in identifying female Fabry patients.

5.4. ERT for Fabry disease---experience in Taiwan

ERT was well tolerated by all patients. This treatment is thus beneficial and appears to be safe for treatment of Fabry disease in Taiwanese patients.

CLINICAL PERSPECTIVE

This study in the Taiwan Chinese population demonstrates the feasibility of a large-scale neonatal screening program for Fabry disease. The incidence of Fabry mutations among newborns was unexpectedly high (~1 in 1,400 male newborns), as was the prevalence of the cardiac variant mutation IVS4+919G>A. We think this information, the fact that there is a high prevalence of Fabry cardiac variants in Chinese patients with HCM, is important for general cardiovascular physicians. Because, if they have chances to take care of Chinese patients with HCM, they should be alert to the possibilities of cardiac Fabry disease existing in these patients. After all, the general cardiovascular physicians are in the first line of caring for patients with HCM. The early identification of undiagnosed patients allows timely therapeutic intervention, providing a much better clinical outcome. Therefore we think this information is not only important to the cardiovascular geneticists but also to general cardiovascular physicians.

We developed a method for HRM analysis of *GLA* gene using a same PCR/melting program. All Fabry mutations in heterozygous or hemizygous patients can be identified with HRM. We also develop this HRM method in DBS of newborns with Fabry mutations.

REFERENCES

1. Desnick RJ, Ioannou YA, Eng CM. α-galactosidase A deficiency: Fabry disease. In: Scriver CR, Beaudet AL, Sly WS, Valle D, eds. The Metabolic and Molecular Bases of Inherited Disease. New York: McGraw-Hill, 2001; 3733-74.

2. Meikle PJ, Hopwood JJ, Clague AE, Carey WF. Prevalence of lysosomal storage disorders. JAMA 1999; 281: 249-54.

3. von Scheidt W, Eng CM, Fitzmaurice TF, Erdmann E, Hubner G, Olsen EG, et al. An atypical variant of Fabry's disease with manifestations confined to the myocardium. N Engl J Med 1991; 324: 395-9.

4. Chimenti C, Ricci R, Pieroni M, Natale L, Russo MA, Frustaci A. Cardiac variant of Fabry's disease mimicking hypertrophic cardiomyopathy. Cardiologia 1999; 44: 469-73.

5. Ommen SR, Nishimura RA, Edwards WD. Fabry disease: a mimic for obstructive hypertrophic cardiomyopathy? Heart 2003; 89: 929-30.

6. Nakao S, Takenaka T, Maeda M, Kodama C, Tanaka A, Tahara M, et al. An atypical variant of Fabry's disease in men with left ventricular hypertrophy. N Engl J Med 1995; 333: 288-93.

7. Sachdev B, Takenaka T, Teraguchi H, Tei C, Lee P, McKenna WJ, et al. Prevalence of Anderson-Fabry disease in male patients with late onset hypertrophic cardiomyopathy. Circulation 2002; 105: 1407-11.

8. Monserrat L, Gimeno-Blanes JR, Marín F, Hermida-Prieto M, García-Honrubia A, Pérez I, et al. Prevalence of Fabry disease in a cohort of 508 unrelated patients with hypertrophic cardiomyopathy. J Am Coll Cardiol 2007; 50: 2399-403.

9. Nakao S, Kodama C, Takenaka T, Tanaka A, Yasumoto Y, Yoshida A, et al. Fabry disease: detection of undiagnosed hemodialysis patients and identification of a "renal variant" phenotype. Kidney Int 2003; 64: 801-7.

10. Kotanko P, Kramar R, Devrnja D, Paschke E, Voigtlander T, Auinger M, et al. Results of a nationwide screening for Anderson-Fabry disease among dialysis patients. J Am Soc Nephrol 2004; 15: 1323-9.

11. Germain DP, Waldek S, Banikazemi M, Bushinsky DA, Charrow J, Desnick RJ, et al. Sustained, long-term renal stabilization after 54 months of agalsidase

beta therapy in patients with Fabry disease. J Am Soc Nephrol 2007; 18: 1547-57.
12. Weidemann F, Niemann M, Breunig F, Herrmann S, Beer M, Störk S, et al. Long-term effects of enzyme replacement therapy on Fabry cardiomyopathy: evidence for a better outcome with early treatment. Circulation 2009; 119: 524-9.
13. Schiffmann R, Ries M, Timmons M, Flaherty JT, Brady RO. Long-term therapy with agalsidase alfa for Fabry disease: safety and effects on renal function in a home infusion setting. Nephrol Dial Transplant 2006; 21: 345-54.
14. Banikazemi M, Bultas J, Waldek S, Wilcox WR, Whitley CB, McDonald M, et al. Agalsidase-beta therapy for advanced Fabry disease: a randomized trial. Ann Intern Med 2007; 146: 77-86.
15. Pierre-Louis B, Kumar A, Frishman WH. Fabry disease: cardiac manifestations and therapeutic options. Cardiol Rev 2009; 17 :31-5.
16. Chamoles NA, Blanco M, Gaggioli D. Fabry disease: enzymatic diagnosis in dried blood spots on filter paper. Clin Chim Acta 2001; 308: 195-6.
17. Meikle PJ, Ranieri E, Simonsen H, Rozaklis T, Ramsay SL, Whitfield PD, et al. Newborn screening for lysosomal storage disorders: clinical evaluation of a two-tier strategy. Pediatrics 2004; 114: 909-16.
18. Li Y, Scott CR, Chamoles NA, Ghavami A, Pinto BM, Turecek F, et al. Direct multiplex assay of lysosomal enzymes in dried blood spots for newborn screening. Clin Chem 2004; 50: 1785-96.
19. Spada M, Pagliardini S, Yasuda M, Tukel T, Thiagarajan G, Sakuraba H, et al. High incidence of later-onset Fabry disease revealed by newborn screening. Am J Hum Genet 2006; 79: 31-40.
20. Deegan P, Bähner AF, Barba-Romero MA, Hughes D, Kampmann C, Beck M. Natural history of Fabry disease in females in the Fabry Outcome Survey. J Med Genet 2006; 43: 347-52.
21. Wang RY, Lelis A, Mirocha J, Wilcox WR. Heterozygous Fabry women are not just carriers, but have a significant burden of disease and impaired quality of life. Genet Med 2007; 9: 34-45.
22. Wilcox WR, Oliveira JP, Hopkin RJ, Ortiz A, Banikazemi M,

Feldt-Rasmussen U, et al. Females with Fabry disease frequently have major organ involvement: lessons from the Fabry Registry. Mol Genet Metab 2008; 93: 112-28.
23. Tanaka M, Ohashi T, Kobayashi M, Eto Y, Miyamura N, Nishida K, et al. Identification of Fabry's disease by the screening of alpha-galactosidase A activity in male and female hemodialysis patients. Clin Nephrol 2005; 64: 281-7.
24. Rolfs A, Böttcher T, Zschiesche M, Morris P, Winchester B, Bauer P, et al. Prevalence of Fabry disease in patients with cryptogenic stroke: a prospective study. Lancet 2005; 366: 1794-6.
25. Nguyen TT, Gin T, Nicholls K, Low M, Galanos J, Crawford A. Ophthalmological manifestations of Fabry disease: a survey of patients at the Royal Melbourne Fabry Disease Treatment Centre. Clin Experiment Ophthalmol 2005; 33: 164-8.
26. Orssaud C, Dufier J, Germain D. Ocular manifestations in Fabry disease: a survey of 32 hemizygous male patients. Ophthalmic Genet 2003; 24: 129-39.
27. Sher NA, Letson RD, Desnick RJ. The ocular manifestations in Fabry's disease. Arch Ophthalmol 1979; 97: 671-6.
28. Sodi A, Ioannidis AS, Mehta A, Davey C, Beck M, Pitz S. Ocular manifestations of Fabry's disease: data from the Fabry Outcome Survey. Br J Ophthalmol 2007; 91: 210-4.
29. Ishii S, Nakao S, Minamikawa-Tachino R, Desnick RJ, Fan JQ. Alternative splicing in the alpha-galactosidase A gene: increased exon inclusion results in the Fabry cardiac phenotype. Am J Hum Genet 2002; 70: 994-1002.
30. Lin HY, Chong KW, Hsu JH, Yu HC, Shih CC, Huang CH, et al. High incidence of the cardiac variant of Fabry disease revealed by newborn screening in the Taiwan Chinese population. Circ Cardiovasc Genet 2009; 2: 450-6.
31. Hwu WL, Chien YH, Lee NC, Chiang SC, Dobrovolny R, Huang AC, et al. Newborn screening for Fabry disease in Taiwan reveals a high incidence of the later-onset GLA mutation c.936+919G>A (IVS4+919G>A). Hum Mutat 2009; 30: 1397-405.

32. Cho MH, Ciulla D, Klanderman BJ, Raby BA, Silverman EK. High-resolution melting curve analysis of genomic and whole-genome amplified DNA. Clin Chem 2008; 54: 2055-8.
33. Erali M, Voelkerding KV, Wittwer CT. High resolution melting applications for clinical laboratory medicine. Exp Mol Pathol 2008; 85: 50-8.
34. Reed GH, Kent JO, Wittwer CT. High-resolution DNA melting analysis for simple and efficient molecular diagnostics. Pharmacogenomics 2007; 8: 597-608.
35. Vossen RH, Aten E, Roos A, den Dunnen JT. High-resolution melting analysis (HRMA): more than just sequence variant screening. Hum Mutat 2009; 30: 860-6.
36. Schiffmann R, Kopp JB, Austin HA 3rd, Sabnis S, Moore DF, Weibel T, et al. Enzyme replacement therapy in Fabry disease: a randomized controlled trial. JAMA 2001; 285: 2743-9.
37. Beck M, Ricci R, Widmer U, Dehout F, de Lorenzo AG, Kampmann C, et al. Fabry disease: overall effects of agalsidase alfa treatment. Eur J Clin Invest 2004; 34: 838-44.
38. Thofehrn S, Netto C, Cecchin C, Burin M, Matte U, Brustolin S, et al. Kidney function and 24-hour proteinuria in patients with Fabry disease during 36 months of agalsidase alfa enzyme replacement therapy: a Brazilian experience. Ren Fail 2009; 31: 773-8.
39. Schwarting A, Dehout F, Feriozzi S, Beck M, Mehta A, Sunder-Plassmann G, et al. Enzyme replacement therapy and renal function in 201 patients with Fabry disease. Clin Nephrol 2006; 66: 77-84.
40. Hoffmann B, Beck M, Sunder-Plassmann G, Borsini W, Ricci R, Mehta A, et al. Nature and prevalence of pain in Fabry disease and its response to enzyme replacement therapy-a retrospective analysis from the Fabry Outcome Survey. Clin J Pain 2007; 23: 535-42.
41. West M, Nicholls K, Mehta A, Clarke JT, Steiner R, Beck M, et al. Agalsidase alfa and kidney dysfunction in Fabry disease. J Am Soc Nephrol 2009; 20: 1132-9.
42. Weidemann F, Breunig F, Beer M, Sandstede J, Turschner O, Voelker W, et

al. Improvement of cardiac function during enzyme replacement therapy in patients with Fabry disease: a prospective strain rate imaging study. Circulation 2003; 108: 1299-1301.
43. Imbriaco M, Pisani A, Spinelli L, Cuocolo A, Messalli G, Capuano E, et al. Effects of enzyme-replacement therapy in patients with Anderson-Fabry disease: a prospective long-term cardiac magnetic resonance imaging study. Heart 2009; 95: 1103-7.
44. Hughes DA, Elliott PM, Shah J, Zuckerman J, Coghlan G, Brookes J, et al. Effects of enzyme replacement therapy on the cardiomyopathy of Anderson-Fabry disease: a randomised, double-blind, placebo-controlled clinical trial of agalsidase alfa. Heart 2008; 94: 153-8.
45. Sheu SS, Chan LP, Liao SC, Hsiao KJ, Shu KH, Lu YS, et al. Fabry's disease: clinical, pathologic and biochemical manifestations in two Chinese males. Zhonghua Yi Xue Za Zhi 1994; 54: 368-72.
46. Desnick RJ, Allen KY, Desnick SJ, Raman MK, Bernlohr RW, Krivit W. Fabry's disease: enzymatic diagnosis of hemizygotes and heterozygotes. Alpha-galactosidase activities in plasma, serum, urine, and leukocytes. J Lab Clin Med 1973; 81: 157-71.
47. Chen CH, Shyu PW, Wu SJ, Sheu SS, Desnick RJ, Hsiao KJ. Identification of a novel point mutation (S65T) in alpha-galactosidase A gene in Chinese patients with Fabry disease. Mutations in brief no. 169. Hum Mutat 1998; 11 :328-30.
48. Shabbeer J, Robinson M, Desnick RJ. Detection of alpha-galactosidase a mutations causing Fabry disease by denaturing high performance liquid chromatography. Hum Mutat 2005; 25: 299-305.
49. Shabbeer J, Yasuda M, Benson SD, Desnick RJ. Fabry disease: identification of 50 novel alpha-galactosidase A mutations causing the classic phenotype and three-dimensional structural analysis of 29 missense mutations. Hum Genomics 2006; 2: 297-309.
50. National Kidney Foundation. K/DOQI clinical practice guidelines for chronic kidney disease: evaluation, classification, and stratification. Am J Kidney Dis 2002; 39: S1-266.

51. Levy D, Savage DD, Garrison RJ, Anderson KM, Kannel WB, Castelli WP. Echocardiographic criteria for left ventricular hypertrophy: the Framingham Heart Study. Am J Cardiol 1987; 59: 956-60.
52. Devereux RB, Alonso DR, Lutas EM, Gottlieb GJ, Campo E, Sachs I, et al. Echocardiographic assessment of left ventricular hypertrophy: comparison to necropsy findings. Am J Cardiol 1986; 57: 450-8.
53. Lang RM, Bierig M, Devereux RB, Flachskampf FA, Foster E, Pellikka PA, et al. Recommendations for chamber quantification: a report from the American Society of Echocardiography's Guidelines and Standards Committee and the Chamber Quantification Writing Group, developed in conjunction with the European Association of Echocardiography, a branch of the European Society of Cardiology. J Am Soc Echocardiogr 2005; 18: 1440-63.
54. Levey AS, Stevens LA, Schmid CH, Zhang YL, Castro AF 3rd, Feldman HI, et al. A New Equation to Estimate Glomerular Filtration Rate. Ann Intern Med. 2009; 150: 604-12.
55. Ishii S, Chang HH, Kawasaki K, Yasuda K, Wu HL, Garman SC, et al. Mutant alpha-galactosidase A enzymes identified in Fabry disease patients with residual enzyme activity: biochemical characterization and restoration of normal intracellular processing by 1-deoxygalactonojirimycin. Biochem J 2007; 406: 285-95.
56. Eng CM, Niehaus DJ, Enriquez AL, Burgert TS, Ludman MD, Desnick RJ. Fabry disease: twenty-three mutations including sense and antisense CpG alterations and identification of a deletional hot-spot in the alpha-galactosidase A gene. Hum Mol Genet 1994; 3: 1795-9.
57. Spada M, Marongiu A, Voglino G, Merlino S, Alluto A, La Dolcetta M, et al. Molecular study in 20 unrelated male patients with Fabry disease: the A143T genotype correlates with the late-onset end-stage nephropathy. J Inherit Metab Dis 2003; 26: 171.
58. Eng CM, Ashley GA, Burgert TS, Enriquez AL, D'Souza M, Desnick RJ. Fabry disease: thirty-five mutations in the alpha-galactosidase A gene in patients with classic and variant phenotypes. Mol Med 1997; 3: 174-82.
59. Bernstein HS, Bishop DF, Astrin KH, Kornreich R, Eng CM, Sakuraba H, et

al. Fabry disease: six gene rearrangements and an exonic point mutation in the alpha-galactosidase gene. J Clin Invest 1989; 83: 1390-9.
60. Lin HY, Chong KW, Hsu JH, Yu HC, Huang CH, Niu DM. Novel human pathological mutations. Gene symbol: GLA. Disease: Fabry disease. Hum Genet 2010; 127: 124.
61. Lin HY, Huang CH, Yu HC, Chong KW, Hsu JH, Lee PC, et al. Enzyme assay and clinical assessment in subjects with a Chinese hotspot late-onset Fabry mutation (IVS4+919G→A). J Inherit Metab Dis 2010; 33: 619-24.
62. Lin HY, Niu DM, Chong KW, Hsu JH, Yu HC, Huang CH. Novel human pathological mutations. Gene symbol: GLA. Disease: Fabry disease. Hum Genet 2010; 127: 122-3.
63. Niu DM, Lin HY, Chong KW, Hsu JH, Yu HC, Huang CH. Novel human pathological mutations. Gene symbol: GLA. Disease: Fabry disease. Hum Genet 2010; 127: 122.
64. Wu KH, Tzung TY, Ro LS, Hsiao KJ. A novel mutation (c. 1072_1074delGAG) in the alpha-galactosidase gene of a Taiwanese family with Fabry disease. Acta Derm Venereol 2004; 84: 310-1.
65. Chimenti C, Pieroni M, Morgante E, Antuzzi D, Russo A, Russo MA, et al. Prevalence of Fabry disease in female patients with late-onset hypertrophic cardiomyopathy. Circulation 2004; 110: 1047-53.
66. Kampmann C, Baehner F, Whybra C, Martin C, Wiethoff CM, Ries M, et al. Cardiac manifestations of Anderson-Fabry disease in heterozygous females. J Am Coll Cardiol 2002; 40: 1668-74.
67. Schiffmann R, Warnock DG, Banikazemi M, Bultas J, Linthorst GE, Packman S, et al. Fabry disease: progression of nephropathy, and prevalence of cardiac and cerebrovascular events before enzyme replacement therapy. Nephrol Dial Transplant 2009; 24: 2102-11.
68. Linthorst GE, Vedder AC, Aerts JM, Hollak CE. Screening for Fabry disease using whole blood spots fails to identify one-third of female carriers. Clin Chim Acta 2005; 353: 201-3.
69. Zarate YA, Hopkin RJ. Fabry's disease. Lancet 2008; 372: 1427-35.
70. Wraith JE, Tylki-Szymanska A, Guffon N, Lien YH, Tsimaratos M, Vellodi A,

et al. Safety and efficacy of enzyme replacement therapy with agalsidase beta: an international, open-label study in pediatric patients with Fabry disease. J Pediatr 2008; 152: 563-70.
71. Wittwer CT. High-resolution DNA melting analysis: advancements and limitations. Hum Mutat 2009; 30: 857-9.
72. Farrar JS, Reed GH, Wittwer CT. High resolution melting curve analysis for molecular diagnostics. G.P. Patrinos, W.J. Ansorge (Eds.), Molecular diagnostics, Academic Press, Burlington, MA, USA 2009; 229-45.
73. Gundry CN, Vandersteen JG, Reed GH, Pryor RJ, Chen J, Wittwer CT. Amplicon melting analysis with labeled primers: a closed-tube method for differentiating homozygotes and heterozygotes. Clin Chem 2003; 49: 396-406.
74. Seipp MT, Durtschi JD, Liew MA, Williams J, Damjanovich K, Pont-Kingdon G, et al. Unlabeled oligonucleotides as internal temperature controls for genotyping by amplicon melting. J Mol Diagn 2007; 9: 284-9.

FIGURES AND TABLES

A

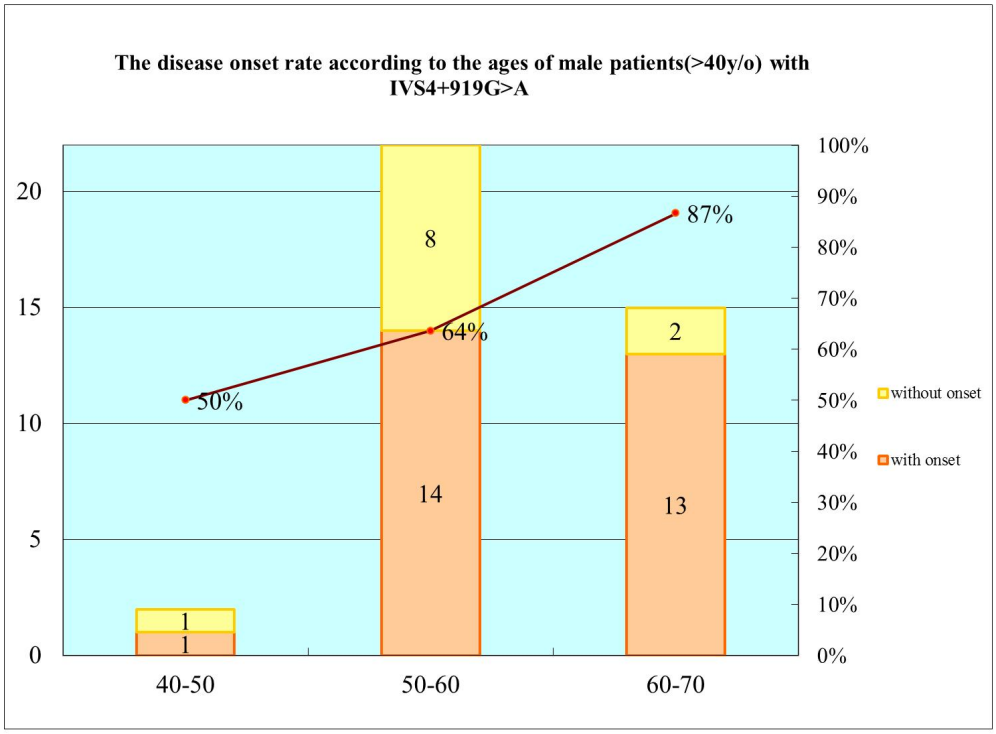

B

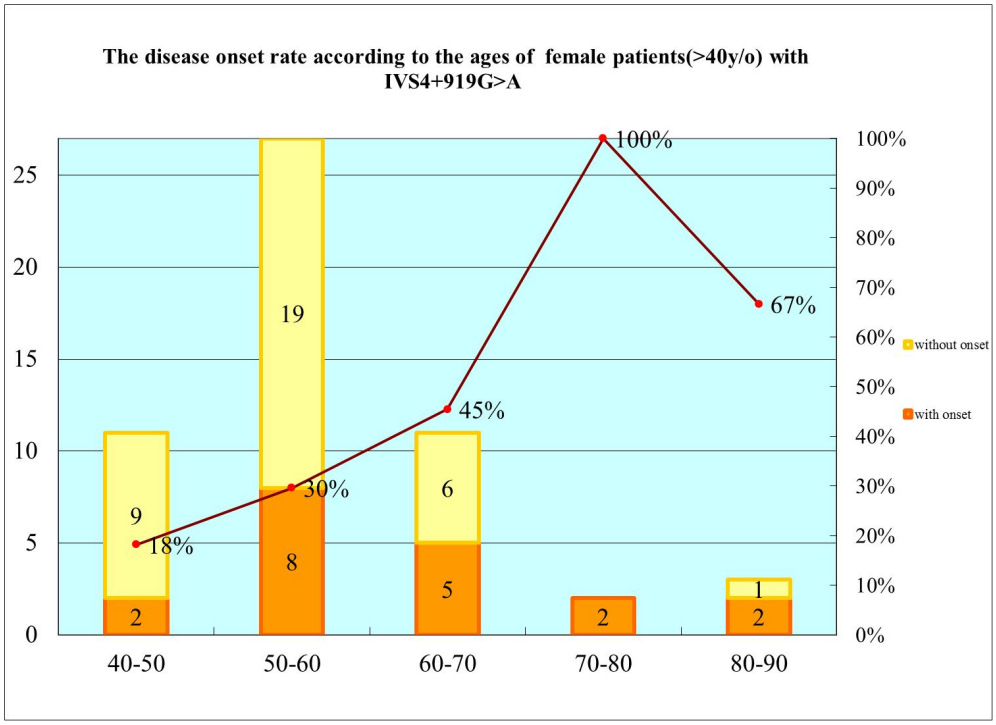

Fig. 1. Age-onset of patients with the IVS4+919G>A mutation. The age-onset of male and female patients with the IVS4+919G>A mutation were showed in panels A and B, respectively. Seventy-two percent of male adults with IVS4+919G>A mutation, who were older than 40 years of age, had developed hypertrophic cardiomyopathy. The disease onset rate is positively correlated with the age of the patient. The disease onset rate of male Fabry patients increased from 50% to 64%, and then to 87%, as the age progressed from forties to fifties and then to sixties (A). The disease onset rate of female Fabry patients increased from 18% to 100%, as age progressed from forties to seventies. One woman at the age group of 80 did not show any sign of hypertrophic cardiomyopathy (B).

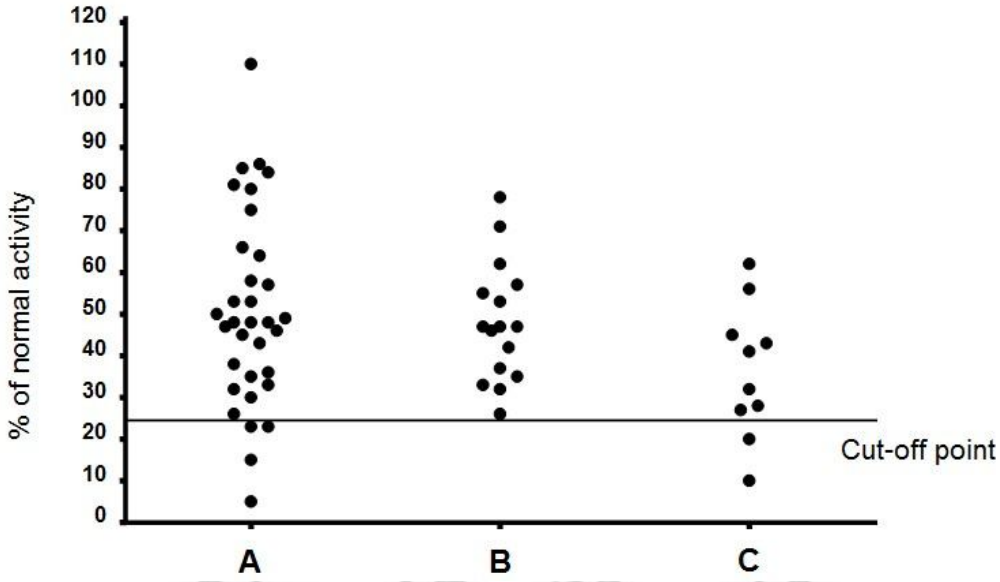

Fig. 2. Residual α-galactosidase A activity of female adults carrying IVS4+919G>A or classic mutations identified in Taiwan. A: females with IVS4+919G>A mutation, but without HCM (n = 31); B: females with IVS4+919G>A mutation and HCM (n = 16); C: females with classic mutations and major organ involvement (n = 10). Activity is expressed as percentage of the mean of normal activity (12.4 ± 2.25 nmol/h/mL plasma). The line indicates 25% of the mean enzymatic activity of the normal control.

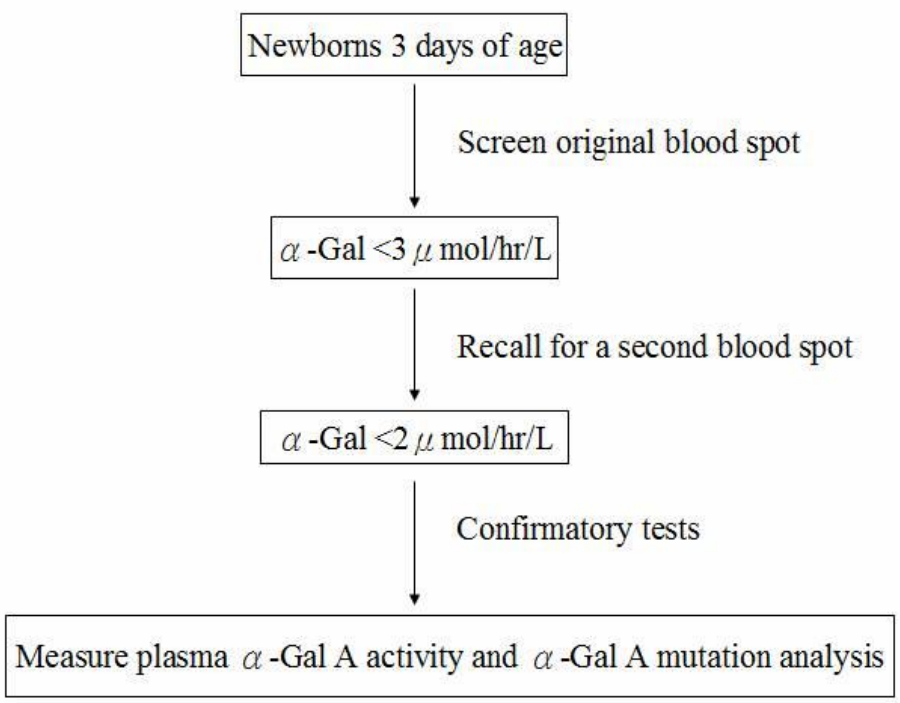

Fig. 3. Algorithm used in the newborn screening program for Fabry disease in Taiwan.

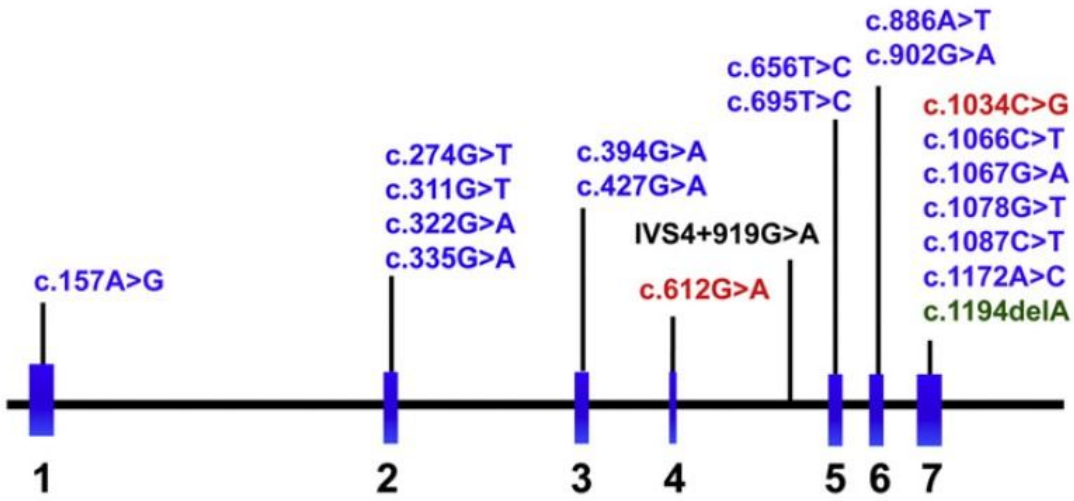

Fig. 4. Schematic representation of the exon/intron organization of the *GLA* gene with indication of positions of mutations identified in the Taiwan Chinese population. A total of 20 *GLA* mutations, identified in Taiwanese patients, including missense (blue); nonsense (red), deletion (green) and splicing site mutations (black) were examined in this study.

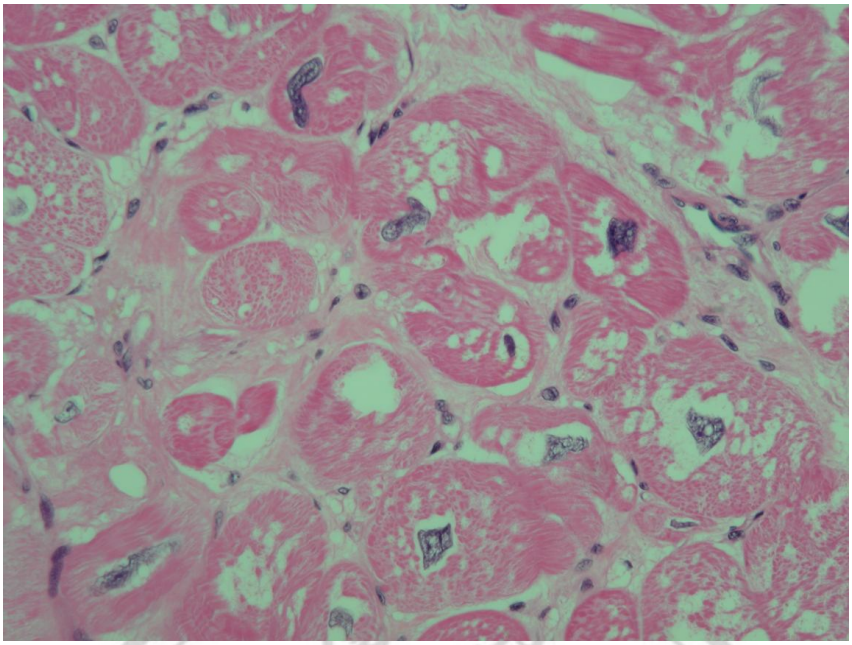

Fig. 5. Histological examination of endomyocardial tissue (Patient 4 in Table 6) showed markedly hypertrophic and disarrayed myocytes with large perinuclear and sarcoplasmic vacuoles (hematoxylin and eosin; x400).

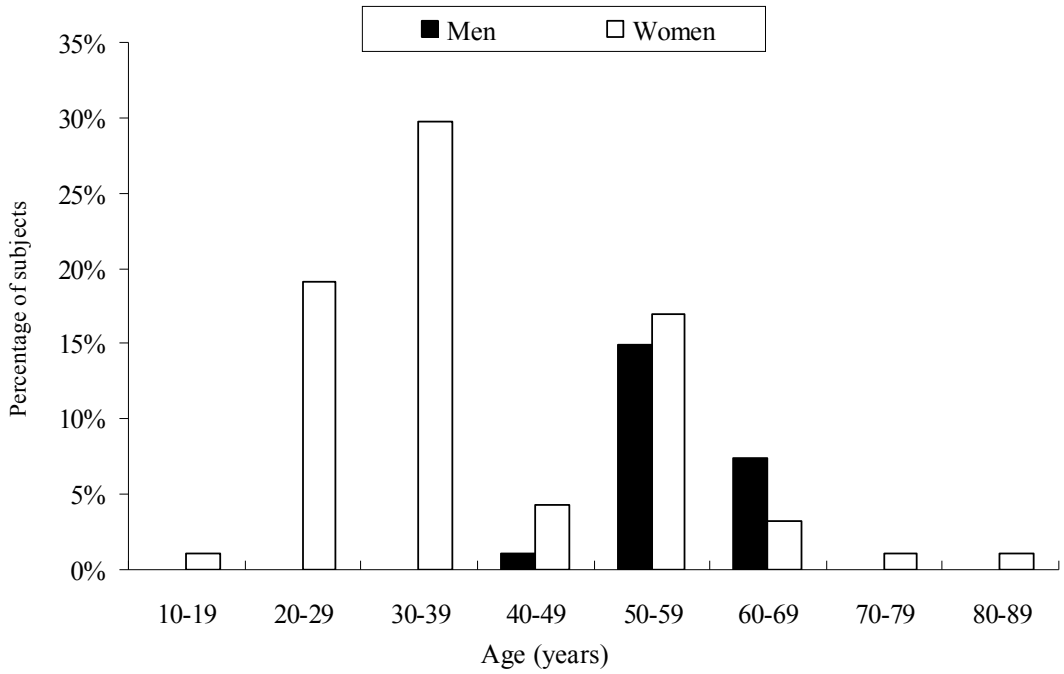

Fig. 6. Age distribution of adult subjects with late-onset Fabry mutation IVS4+919G>A (n = 94; 72 women, 22 men).

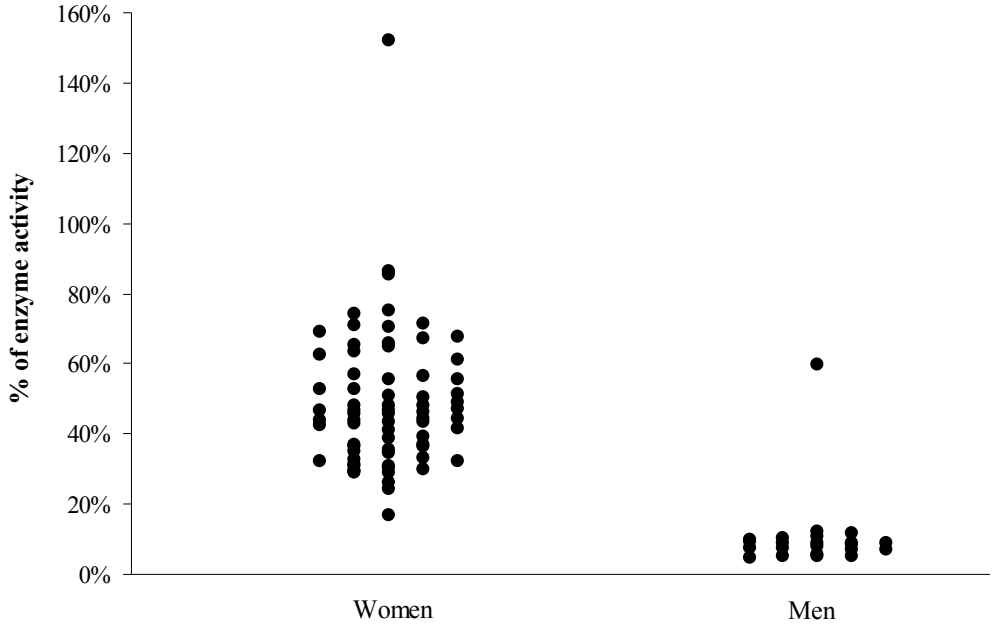

Fig. 7. Residual α-galactosidase activity in women (n=72) and men (n=22) with late-onset Fabry mutation IVS4+919G>A. Activity is expressed as percentage of the normal mean (12.4 ± 2.25 nmol/h/mL plasma).

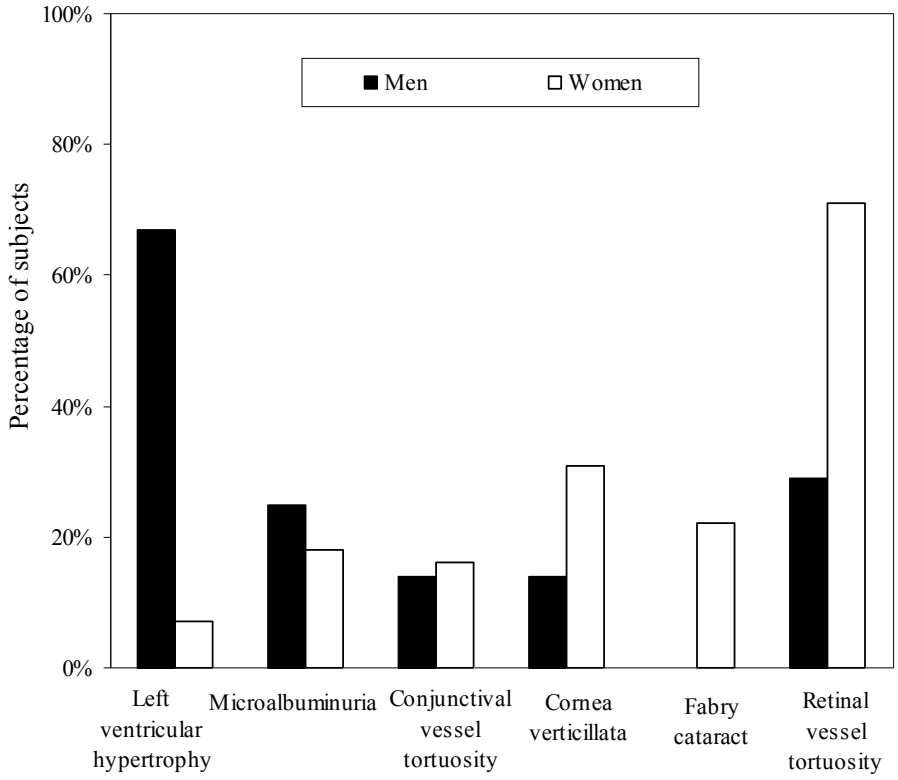

Fig. 8. Prevalence of individual abnormalities in men (n=22) and women (n=72) with late-onset Fabry mutation IVS4+919G>A.

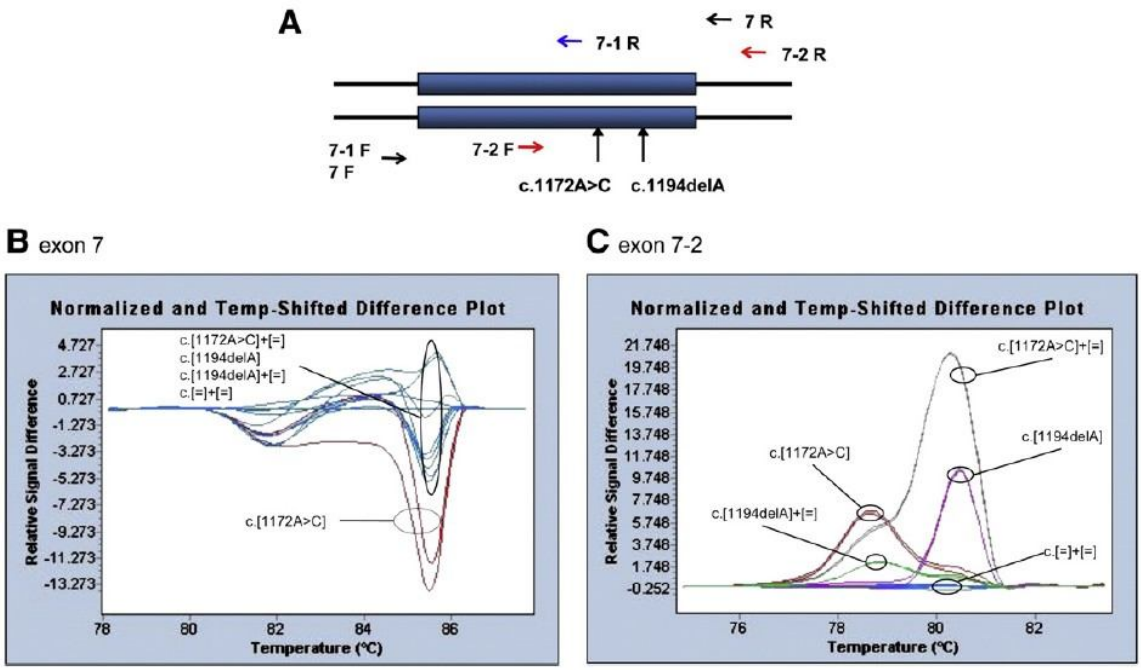

Fig. 9. HRM analysis of exon 7 of the *GLA* gene. The primer set 7 was first used in this HRM analysis. With this primer set, however, two mutations, c.1172A>C and c.1194delA, both of which are located at the 3′ terminal of exon 7, were not identified in heterozygous or hemizygous patients (Fig. 9B). The amplicon of this primer set (352 bp) was larger than the ideal amplicon length for HRM analysis (less than 250 bp). Therefore two primer sets (exon 7-1 and 7-2) covering the entire exon 7 coding region sequence (Table 2 and Fig. 9A) were designed to replace primer set 7. The primer set “exon 7-1” covered the 5′ region of exon 7 and was designed to amplify a fragment of 220 bp. The primer set, exon 7-2, covered the 3′ region of exon 7 and was designed to amplify a fragment of 233 bp. Using this new primer set 7-2 for HRM analysis, the samples with c.1172A>C and c.1194delA mutations were easily identified.

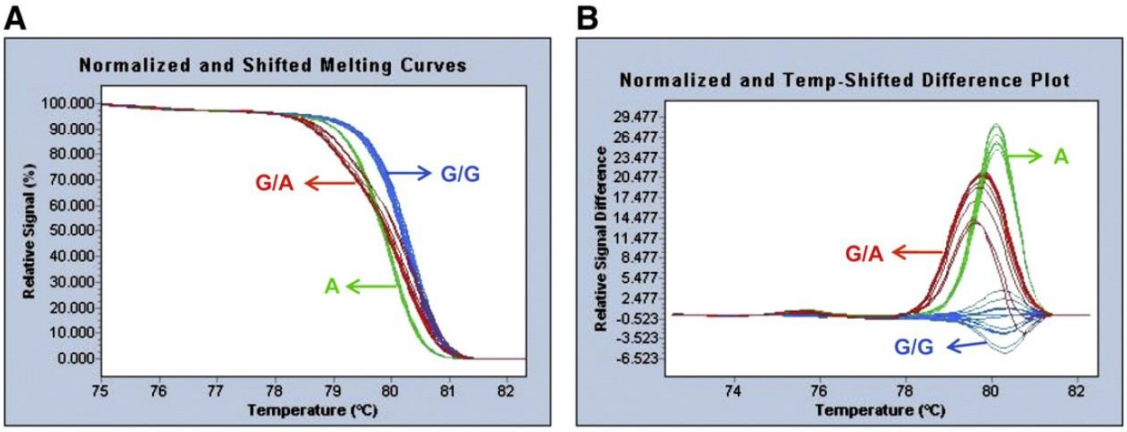

Fig. 10. An example of simultaneous screening for the IVS4+919G>A mutation in 30 samples. In order to examine the sensitivity of HRM for the Chinese common mutation, IVS4+919G>A, in larger sample amount at the same run, 30 samples with the wild type (n = 13), heterozygous (n = 10) and hemizygous (n = 7). IVS4+919G>A mutation were simultaneously screened by HRM analysis. The hemizygous IVS4+919G>A samples (genotype: A) could be distinguished from wild type sample (genotype: G/G) by their T_m variations, while heterozygous samples (genotype: G/A) have a different melting curve shape (A). Thus, individuals with the different genotypes of IVS4+919G>A were clearly distinguishable from the wild type. Samples with the IVS4+919G>A hemizygous genotype are marked in green, heterozygous are in red and wild-type samples are in blue. (A): Normalized melting curve. (B): Difference plot.

A exon 1

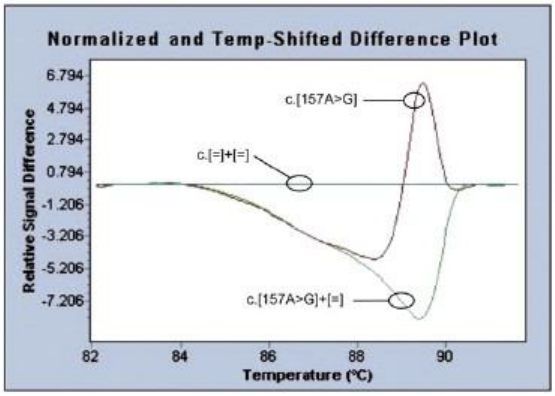

B exon 2

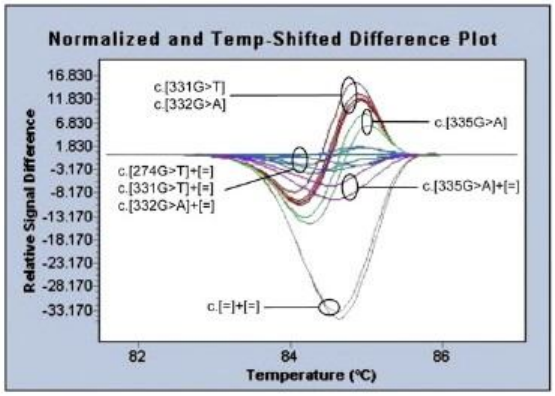

C exon 3

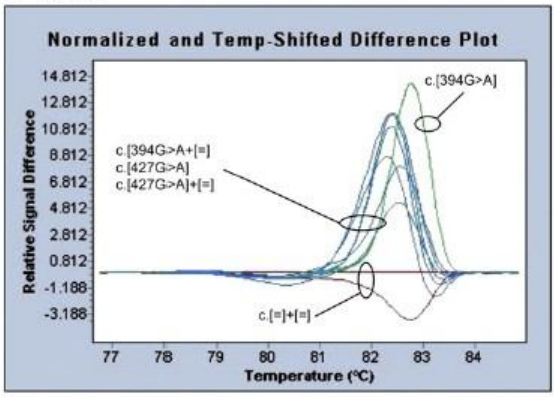

D exon 4

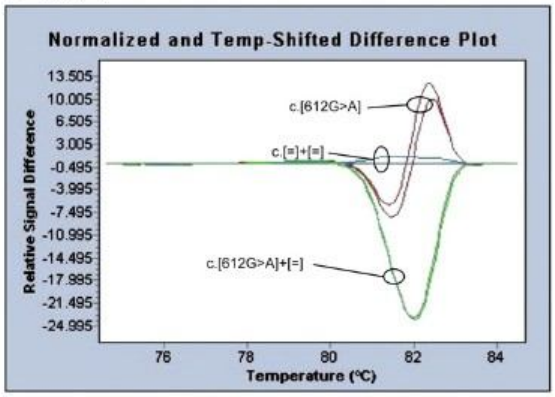

E exon 5

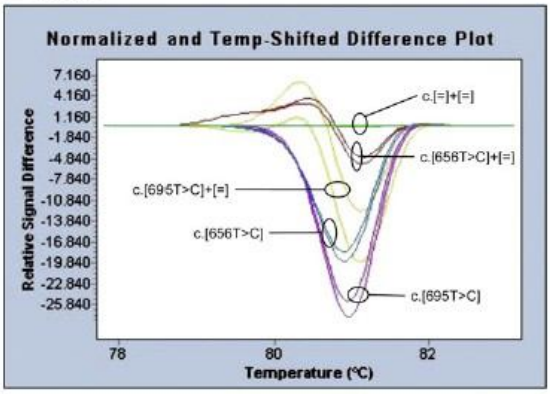

F exon 6

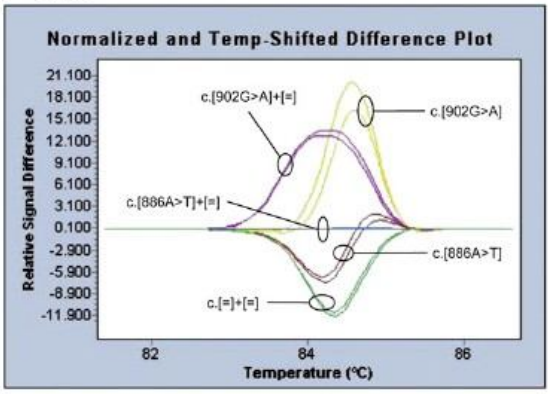

G exon 7-1

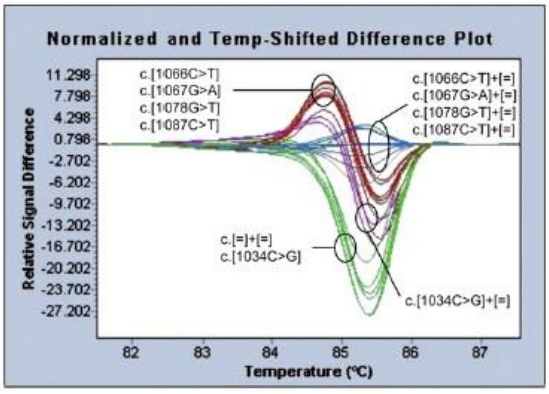

H c.1034C>G

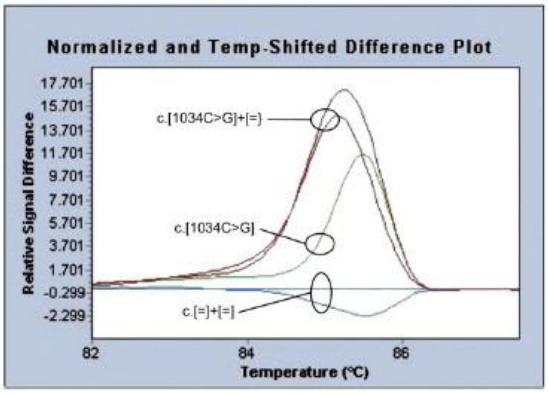

Fig. 11. HRM curves of the mutations which were identified at exons in this study. Panels A through F show the normalized difference plots for each amplicon. (A) exon 1, containing the wild type and mutant c.157A>G; (B): exon 2, containing the wild type and mutants c.274G>A, c.331G>T, c.332G>A and c.335G>A; (C) exon 3, containing the wild type and mutants c.394G>A and c.427G>A; (D) exon 4, containing the wild type and mutant c.612G>A; (E) exon 5, containing the wild type and mutants c.656T>C and c.695T>C; (F) exon 6, containing the wild type and mutants c.886A>T and c.902G>A. (G) exon 7-1, containing the wild type and mutants c.1034C>G, c.1066C>T, c.1067G>A, c.1078G>T and c.1087C>T. Notably, the hemizygous c.1034C>G mutation could be distinguished from the wild-type sequence when analyzed alone (panel H); however, this discrimination disappeared when the samples were analyzed with all other mutations. The HRM curves of exon 7-2 are shown in Fig. 9C.

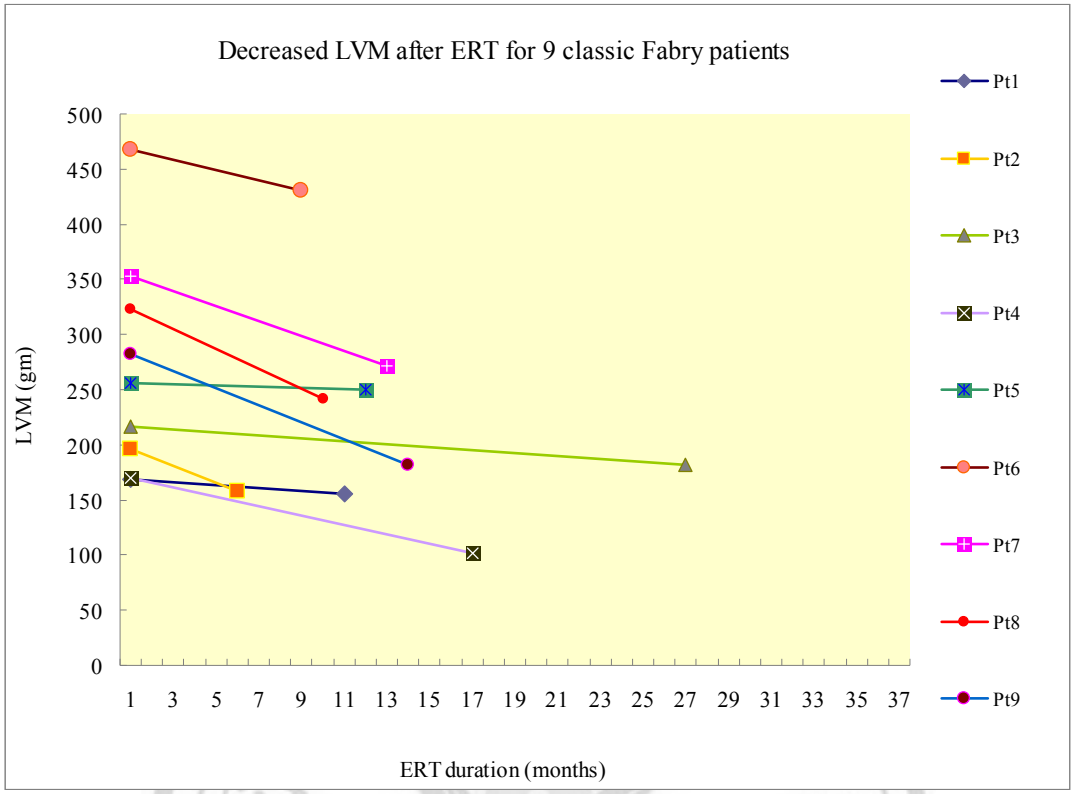

Fig. 12. Decreased left ventricular mass after ERT for 9 classic Fabry patients.

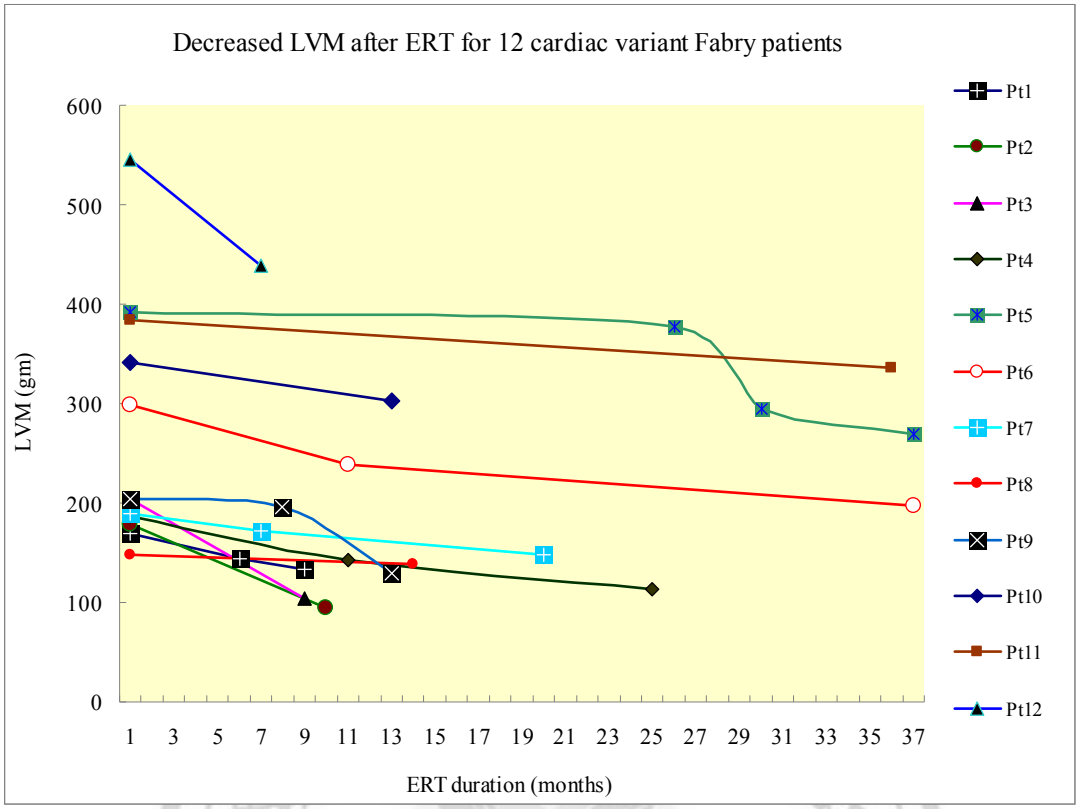

Fig. 13. Decreased left ventricular mass after ERT for 12 cardiac variant Fabry patients.

Table 1. Subjects with Fabry mutations identified from newborn screening, family studies of the newborns, and clinics. (Jan. 2008-Jan. 2012)

Mutation type	N (newborn	N (family	N	Total	Potential
IVS4+919G>A	**138**	**273**	**34**	**445**	**Cardiac variant**
Classic	**6 (3.5%)**	**12**	**17**	**35 (6.3%)**	
c.274G>T (p.D92Y)	0	0	1	1	
c.319C>T (p.Q107X)	0	0	3	3	
c.394G>A (p.G132R)	1	2	0	3	
c.612G>A (p.W204X)	0	0	6	6	
c.1034C>G (p.S345X)	1	1	0	2	
c.1066C>T (p.R356W)	1	2	0	3	Mild classic
c.1081G>C (p.G361X)	1	2	0	3	
c.1087C>T (p.R363C)	1	1	0	2	Mild classic
c.1194delA	0	0	7	7	
c.1228A>G (p.T410A)	1	4	0	5	
Non-classic	**6 (3.5%)**	**13**	**4**	**23 (4.2%)**	
c.335G>A (p.R112H)	1	2	4	7	Renal variant
c.427G>A (p.A143T)	2	3	0	5	Renal/cardiac
c.902G>A (p.R301Q)	3	8	0	11	Classic/cardiac
Novel	**20 (11.2%)**	**27**	**3**	**50 (9%)**	
c.157A>G (p.N53D)	2	5	0	7	
c.311G>T (p.G104V)	2	2	0	4	
c.322G>A (p.A108T)	2	4	0	6	
c.656T>C (p.I219T)	0	0	3	3	
c.695T>C (p.I232T)	1	1	0	2	
c.886A>T (p.M296L)	1	1	0	2	
c.911G>C (p.S304T)	1	2	0	3	
c.1067G>A (p.R356Q)	2	2	0	4	
c.1078G>T (p.G360C)	6	7	0	13	Cardiac/renal
c.1172A>C (p.K391T)	3	3	0	6	
Total	**170**	**325**	**58**	**553**	

Table 2. Primer sets used for high resolution melting (HRM) analysis.

Amplicon	Forward primer	Position	Reverse primer	Position	Anneal temperature	Size (bp)
Exon 1	TTAAAAGCCCAGGTTACCCG	c.1–32_–51	AAAGCAAAGGGAAGGGAG	c.194 + 16_ + 33	60	280
Exon 2	AATCCCAAGGTGCCTAATAAA	c.195–61_–81	TACAGAAGTGCTTACAGTCCT	c.369 + 34_ + 54	60	310
Exon 3	TCTCTTTCTGCTACCTCACG	c.370–46_–65	TCTTTCCTTTGTGGCTAAATC	c.547 + 20_ + 40	60	282
Exon 4	TATAGCCCCAGCTGGAAATTC	c.548–41_–61	GTTGGACTTTGAAGGAGACCT	c.639 + 68_88	60	241
Exon 5	GAAGGCTACAAGTGCCTCCT	c.640–69_–88	AGCCTACCGCAGGGTCTT	c.801 + 37_ + 54	60	293
Exon 6	AAGAATGTTTCCTCCTCTCT	c.802–30_–49	CAAAGTTGGTATTGGGTATAT	c.999 + 33_53	60	300
Exon 7[a]	GCTAAGCAACCACACTTTCT	c.1000–14_–31	GAAGTAGTAGTTGGCAATA	*12_*30	60	352
Exon 7-1	GCTAAGCAACCACACTTTCT	c.1000–14_–31	GAACCCTAGCTTCCTTTTCACAG	c.1166_1188	60	220
Exon 7-2	GTAATCCTGCCTGCTTCATCA	c.1134_1153	ACCTAGCCTTGAGCTTTTAA	*50–*69	60	233
IVS4[a]	TCTGTCCCTCAACACTGCAA	c.639 + 641_ + 660	TAGGCAGGTGGGATATCAGG	c.639 + 1067_ + 1086	60	446
IVS4-1	TTTTCTTCTCAGAGCTCCACA	c.639 + 854_ + 874	TGCGAGAGATACAGTCAAAGTCA	c.639 + 952_ + 974	60	121

a: Exon 7 and IVS4 were originally used for sequence analysis and were not suitable for HRM analysis.

Table 3. Results of the newborn screening program for Fabry disease in Taiwan (Jan. 2008-Jan. 2009).

Newborns ≤ 3 days of age tested with DBS, n	Males 57,451	Incidence (%) 95% CI[d]	Females 52,576	Incidence (%) 95% CI[d]	Total 110,027	Incidence (%) 95% CI[d]
First DBS test positive[a], n	1,094	1.90 ± 0.11	515	0.98 ± 0.08	1,609	1.46 ± 0.07
Second DBS test positive[b], n	58	0.10 ± 0.03	9	0.02 ± 0.01	67	0.06 ± 0.01
Newborns with Fabry mutations[c], n	42	0.07 ± 0.02	3	0.006 ± 0.007	45	0.04 ± 0.01
Intronic splicing mutation: IVS4+919G>A (male) or IVS4+919G/A (female), n	35	0.06 ± 0.02	2	0.004 ± 0.005	37	0.034 ± 0.01

DBS: dried blood spot; CI: confidence interval.

[a] α-Gal activity <3 μmol/hr/L.

[b] α-Gal <2 μmol/hr/L.

[c] Deficient plasma α-Gal A activity and identification of *GLA* mutation.

[d] Calculated using a normal approximation to the binomial distribution. Some incidences are small and lower confidence intervals have negative values.

Table 4. Results of *GLA* gene mutation analysis and α-Gal A enzyme activity screening in 110,027 newborns.

Patient no.	Gender	Location	*GLA* mutation	DBS α-Gal A activity (μmol/hr/L)	Plasma α-Gal A activity* (nmol/hr/mL)	Potential phenotype
Missense mutation						
1	M	Exon 2	c.311G>T, p.G104V	0.50	0.60	Unknown
2	M	Exon 2	c.334 G>A, p.R112H	0.35	1.70	Renal/cardiac variant
3	M	Exon 3	c.427 G>A, p.A143T	0.94	3.42	Renal/cardiac variant
4	M	Exon 6	c.886 A>T, p.M296L	0.01	1.04	Unknown
5	M	Exon 7	c.1066 C>T, p.R356W	0.01	3.13	Mild classic
6	F	Exon 7	c.1078 G>T, p.G360C	0.97	7.40	Unknown
7	M	Exon 7	c.1078 G>T, p.G360C	0.37	3.60	Unknown
8	M	Exon 7	c.1172 A>C, p.K391T	1.37	1.70	Unknown
Intronic splicing mutation						
Total number of patients	**Gender**	**Location**	***GLA* mutation**	**DBS α-Gal A activity (μmol/hr/L)**	**Plasma α-Gal A activity* (nmol/hr/mL)**	**Potential phenotype**
35	M	Intron 4	IVS4+919G>A	1.00±0.42	2.80±0.71	Cardiac variant
2	F	Intron 4	IVS4+919G/A	1.08±0.21	4.61±2.27	Cardiac variant

DBS: dried blood spot.

*Normal reference range: 7.9-16.9 nmol/hr/mL.

Table 5. Plasma α-Gal A activity and echocardiographic features in maternal grandparents with *GLA* mutations IVS4+919G>A (grandfather) or IVS4+919G/A (grandmother).

Family	Maternal grandparents	Age (y)	Plasma α-Gal A Activity* (nmol/hr/mL)	*GLA* Mutation	Echocardiography
14	Grandfather	67	0.72	IVS4+919G>A	HCM, mild MR, TR
17	Grandfather	57	1.12	IVS4+919G>A	Minimal PR, MR
18	Grandfather	53	1.26	IVS4+919G>A	Mild TR
22	Grandfather	52	1.16	IVS4+919G>A	Minimal PR, mild TR
23	Grandfather	54	0.84	IVS4+919G>A	Minimal MR, mild TR
26	Grandfather	62	2.40	IVS4+919G>A	HCM, mild AR, MR, TR
33	Grandfather	57	0.64	IVS4+919G>A	HCM, mild TR
34	Grandfather	56	0.56	IVS4+919G>A	Minimal PR, mild TR
35	Grandfather	54	0.63	IVS4+919G>A	Minimal TR
10	Grandmother	56	6.51	IVS4+919G/A	Mild TR
12	Grandmother	45	5.53	IVS4+919G/A	Minimal TR
19	Grandmother	51	5.81	IVS4+919G/A	Moderate MR, mild to moderate TR, mild AR
30	Grandmother	49	3.87	IVS4+919G/A	Mild TR
32	Grandmother	62	5.96	IVS4+919G/A	Moderate TR, mild MR, MVP
36	Grandmother	56	10.72	IVS4+919G/A	Minimal TR
37	Grandmother	57	8.13	IVS4+919G/A	Minimal MR, TR
40	Grandmother	51	5.97	IVS4+919G/A	Mild TR
41	Grandmother	54	9.33	IVS4+919G/A	Mild TR
43	Grandmother	55	5.98	IVS4+919G/A	Mild TR
45	Grandmother	54	5.36	IVS4+919G/A	Minimal TR

*Normal reference range: 7.9-16.9 nmol/hr/mL.

HCM, hypertrophic cardiomyopathy; MR, mitral regurgitation; TR, tricuspid regurgitation; PR, pulmonary regurgitation; AR, aortic regurgitation; MVP, mitral valve prolapse.

Table 6. Clinical profiles, plasma α-Gal A activity, and echocardiographic features in 4 patients with both the intronic splicing mutation (IVS4+919G>A) and hypertrophic cardiomyopathy from the outpatient clinics.

Patient no.	Age (y)	Gender	Plasma α-Gal A activity* (nmol/hr/mL)	*GLA* mutation	Echocardiography
1	42	M	0.65	IVS4+919G>A	HCM, mild TR
2	67	M	0.69	IVS4+919G>A	HCM, minimal AR, mild PR, MR
3	53	M	0.88	IVS4+919G>A	HCM
4	67	M	0.98	IVS4+919G>A	HCM, mild AS, MR, TR

*Normal reference range: 7.9-16.9 nmol/hr/mL.

HCM, hypertrophic cardiomyopathy; TR, tricuspid regurgitation; AR, aortic regurgitation; PR, pulmonary regurgitation; MR, mitral regurgitation; AS, aortic stenosis.

Table 7. Clinical findings in subjects with Fabry mutation IVS4+919G>A.

Examinations	Echocardiography (n=90)	Urinary analysis (n=86)	Slit lamp examination (n=52)				
Findings*	Left ventricular hypertrophy	Microalbuminuria	Conjunctival vessel tortuosity	Cornea verticillata	Fabry cataract	Retinal vessel tortuosity	At least one Fabry ocular finding
Men any age	14/21 (67)	5/20 (25)	1/7 (14)	1/7 (14)	0/7 (0)	2/7 (29)	3/7 (43)
Women any age	5/69 (7)	12/66 (18)	7/45 (16)	14/45 (31)	10/45 (22)	32/45 (71)	38/45 (84)
Men aged ≥40 years	14/21 (67)	5/20 (25)	1/7 (14)	1/7 (14)	0/7 (0)	2/7 (29)	3/7 (43)
Women aged ≥40 years	5/25 (20)	7/23 (30)	1/11 (9)	2/11 (18)	2/11 (18)	6/11 (55)	8/11 (73)
p value	<0.001	0.700	0.751	0.841	0.257	0.310	0.229
Women aged <40 years	0/44 (0)	5/43 (12)	6/34 (18)	12/34 (35)	8/34 (24)	26/34 (76)	30/34 (88)
p value difference women aged ≥ and <40 years	<0.005	0.060	0.507	0.297	0.718	0.171	0.227

* n/subjects examined (%)

Table 8. Changes of left ventricular mass for 38 Fabry patients after receiving ERT

Type	Gender	Number	Improvement	Aggravation	Stable	Unknown	Comparable after ERT
Classic	F	11	6	2	2	1	10
Cardiac	F	6	4	0	1	1	5
Classic	M	4	2	1	0	1	3
Renal	M	2	0	0	0	2	0
Cardiac	M	15	7	3	3	2	13
Total		38	19	6	6	7	31

Table 9. Changes of the thickness of intraventricular septum for 38 Fabry patients after receiving ERT

Type	Gender	Number	Improvement	Aggravation	Stable	Unknown	Comparable after ERT
Classic	F	11	8	3	0	0	11
Cardiac	F	6	4	1	0	1	5
Classic	M	4	3	0	0	1	3
Renal	M	2	0	0	0	2	0
Cardiac	M	15	10	2	1	2	13
Total		38	25	6	1	6	32

Table 10. Changes of the thickness of left posterior wall for 38 Fabry patients after receiving ERT.

Type	Gender	Number	Improvement	Aggravation	Stable	Unknown	Comparable after ERT
Classic	F	11	5	5	1	0	11
Cardiac	F	6	5	0	0	1	5
Classic	M	4	3	1	0	0	4
Renal	M	2	0	0	0	2	0
Cardiac	M	15	7	6	0	2	13
Total		38	20	12	1	5	33

Table 11. Changes of urine albumin-to-creatinine ratio (ACR) for 38 Fabry patients after receiving ERT (normal range of ACR: M<2.0, F<2.8).

Type	Gender	Number	ACR normal	ACR abnormal	Improvement	Aggravation	Unknown	Comparable after ERT
Classic	F	11	3	8	7	1	0	8
Cardiac	F	6	3	3	3	0	0	3
Classic	M	4	2	2	1	0	1	1
Renal	M	2	1	1	1	0	0	1
Cardiac	M	15	11	4	4	0	0	4
Total		38	20	18	16	1	1	17

Table 12. Changes of estimated glomerular filtration rate (eGFR) for 38 Fabry patients after receiving ERT (normal range of eGFR: >90mL/min/1.73m^2).

Type	Gender	Number	eGFR normal	No data	eGFR abnormal	Improvement	Aggravation
Classic	F	11	4	1	6	4	2
Cardiac	F	6	4	0	2	1	1
Classic	M	4	2	0	2	1	1
Renal	M	2	1	1	0	0	0
Cardiac	M	15	8	1	6	4	2
Total		38	19	3	16	10	6

Table 13. Prevalence of ocular manifestations of classic Fabry disease in various populations compared with Taiwan Chinese with a late-onset Fabry disease gene.

References	Year	Area	Males, Females	Ocular manifestations			
				Conjunctival vessel tortuosity (%)	Cornea verticillata (%)	Fabry cataract (%)	Retinal vessel tortuosity (%)
Sher et al	1979	USA	37 males	78	94.5	37	70
			25 females	46	88	14	25
Orssaud et al	2003	France	32 males	68.7	43.7	37.5	56.2
Nguyen et al	2005	Australia	34 males	97.1	94.1	11.8	76.5
			32 females	78.1	71.9	0	18.8
Sodi et al	2007	10 European countries*	91 males	NR	73.1	23.1	NR
			82 females	NR	76.9	9.8	NR
Present study	2010	Taiwan	7 males	14	14	0	29
			45 females	16	31	22	71

* The majority of the patients originated from Italy (n=33), the UK (n=28), Spain (n=26) and Norway (n=23).

NR, not reported.

Part II: Reactivation of Silenced Tumor Suppressor Genes via Changes in DNA Methylation by Targeting the Warburg Effect

LIST OF ABBREVIATIONS

ERMA: energy restriction-mimetic agent

2-DG: 2-deoxyglucose

KLF6: Kruppel-like factor 6

DNMT: DNA methyltransferase

FBS: fetal bovine serum

5Aza-dC: 5-aza-2-deoxycytidine

siRNA: short interfering RNA

MTT: 3-(4,5-dimethylthiazol-2-yl)- 2,5-diphenyltetrazolium bromide

RT-PCR: reverse-transcription polymerase chain reaction

qRT: quantitative real time

AR: androgen receptor

INTRODUCTION

Cells undergoing malignant transformation often exhibit a shift in cellular metabolism from oxidative phosphorylation to glycolysis, known as the Warburg effect, to gain growth advantage in the microenvironment (1,2). Recent evidence suggests that this enhanced glycolysis is attributable to the dysregulation of multiple oncogenic signaling pathways (1), including those mediated by hypoxia-inducible factor 1 (3), Akt (4), c-Myc (5), and p53 (6). This glycolytic shift enables cancer cells to adapt to low-oxygen environments, to produce biosynthetic building blocks needed for cell proliferation, to acidify the local environment to facilitate tumor invasion, and to generate NADPH and glutathione through the pentose phosphate shunt to increase resistance to oxidative stress (1,2). Thus, the Warburg effect is considered to be a fundamental property of neoplasia, thereby constituting the basis for tumor imaging by [^{18}F]2-fluoro-2-deoxyglucose positron emission tomography (7). From a therapeutic perspective, targeting glycolysis represents a therapeutically relevant strategy for cancer prevention and treatment (2), of which the proof-of-concept is provided by the *in vivo* efficacy of dietary caloric restriction and natural product-based energy restriction-mimetic agents (ERMAs), such as 2-deoxyglucose (2-DG) and resveratrol, in suppressing carcinogenesis in various animal models.

Previously, based on the scaffold of thiazolidinediones, we developed a novel class of ERMAs, as represented by CG-12, that mimic the ability of 2-DG and glucose deprivation to elicit starvation-like cellular responses with high potency in cancer cells through the inhibition of glucose uptake (8). The suppressive effect of CG-12 on energy metabolism leads to an intricate signaling network mediated by silent information regulator 1, AMP-activated protein kinase, and oxidative stress, the interplay among which culminates in autophagy and apoptosis in cancer cells. More recently, we demonstrated an epigenetic effect of CG-12 in cancer cells involving histone acetylation and H3 lysine 4 methylation, leading to the transcriptional activation of Kruppel-like factor 6 (*KLF6*) and a series of proapoptotic genes (9). In this study, we report the unique ability of CG-5, a structurally optimized CG-12 derivative (structures,

Fig. 1A) to suppress the expression of DNA methyltransferase (DNMT)1 and DNMT3A in prostate cancer cells, resulting in the reactivation of a series of DNA methylation-silenced tumor suppressor genes. Pyrosequencing analysis indicates that this gene reactivation was attributable to hypomethylation in the promoter regions of these tumor suppressor genes. In light of the important role of aberrant DNA methylation in carcinogenesis (10), the present finding underscores the translational potential of this novel class of glucose uptake inhibitors in prostate cancer prevention and therapy.

MATERIALS AND METHODS

Cell culture and reagents

LNCaP, PC-3, and DU-145 prostate cancer cells were obtained from the American Type Culture Collection (Manassas, VA). Cells were maintained in 10% fetal bovine serum (FBS)-supplemented RPMI 1640 medium (Invitrogen, Carlsbad, CA). CG-12 was synthesized in our laboratory according to a published procedure (11), and the synthesis of CG-5 will be described elsewhere. Glucose-free RPMI 1640 medium was purchased from Invitrogen. 2-DG, 5-aza-2-deoxycytidine (5Aza-dC) and MG132 were purchased from Sigma-Aldrich (St. Louis, MO). Short interfering RNA (siRNA) for DNMT1 was obtained from Santa Cruz. The FLAG-tagged DNMT1 plasmid was purchased from Addgene (Cambridge, MA). Antibodies used and their sources are as follows: DNMT1 (New England Biolabs, Ipswich, MA); DNMT3A and DNMT3B (Cell Signaling Technology, Inc., Beverly, MA); β-actin (MP Biomedicals, Irvine, CA); HDAC1 (Millipore, Billerica, MA); Sp1 (Santa Cruz Biotechnology, Santa Cruz, CA); goat anti-rabbit IgG-HRP conjugates and rabbit anti-mouse IgG-HRP conjugates (Jackson ImmunoResearch Laboratories, West Grove, PA). The sequences of all primers used are listed in Supplementary Table 1.

Glucose uptake assay

LNCaP cells were seeded in six-well plates (3×10^5 cells/well) for 24 h. Cells were washed twice with Krebs-Ringer phosphate buffer (126 mM NaCl, 2.5 mM KCl, 25 mM $NaHCO_3$, 1.2 mM NaH_2PO_4, 1.2 mM $MgCl_2$, 2.5 mM $CaCl_2$, pH 7.4) and were then treated with individual agents in Krebs-Ringer phosphate buffer. After 1.5 h, glucose uptake was initiated by adding 1 mL Krebs-Ringer buffer containing 1 mCi/mL [^{3}H]2-DG (PerkinElmer Life Science) and 100 mM non-radioactive 2-DG and was terminated by washing with cold PBS. The cells were lysed in 500 mL lysis buffer (10 mM Tris-HCl pH 8.0, 0.1 % SDS) and aliquots were taken for measurement of radioactivity using a scintillation counter (Beckman LS6500).

Cell viability assay

Cell viability was determined using the 3-(4,5-dimethylthiazol-2-yl)-2,5-diphenyltetrazolium bromide (MTT) assay. LNCaP cells were seeded at 5000 cells/well and normal cells were seeded at 8000 cells/well in 96-well plates and incubated in 10% FBS-supplemented medium for 24 h. Cells were then treated with individual agents for 72 h. Drug-containing medium was replaced with medium containing MTT (0.5 mg/mL), followed by incubation at 37 ^{o}C for 1 h. After removal of medium, the reduced MTT dye in each well was solubilized in 100 μL of DMSO and absorbance at 570 nm was measured.

Transient transfection, RNA interference, and luciferase assay

LNCaP cells were transfected by electroporation using Nucleofector kit R (Lonza, Walkersville, MD) according to the manufacturer's protocol and then cultured in 6-well plates in 10% FBS-supplemented RPMI 1640 medium. For siRNA experiments, cells were nucleofected with scrambled or DNMT1-specific siRNA and seeded into 6-well plates (5 × 10^5 cells/well) for drug treatments and subsequent analyses. For the DNMT1 promoter-luciferase reporter assay, transfected LNCaP cells were cultured in 6-well plates, and treated with CG-5 for 48 h. Luciferase activities were determined with the dual-luciferase system (Promega, Madison, WI), which uses co-transfected herpes simplex virus thymidine kinase promoter-driven *Renilla reniformis* luciferase as an internal control.

Reverse-transcription polymerase chain reaction (RT-PCR)

Total RNA was isolated and reverse-transcribed to cDNA using TRIzol reagent (Invitrogen) and the iScript cDNA synthesis kit (Bio-Rad), respectively, according to the manufacturer's recommended procedures. Briefly, 1 μg of total RNA was reverse-transcribed with 1 μL iScript reverse transcriptase and 4 μL 5× iScript reaction mixture in a 20 μL reaction volume. The reaction was carried out at 25°C for 5 minutes, at 42°C for 30 minutes, and then the reverse transcriptase was deactivated by heating at 85°C for 5 minutes. For semi-quantitative PCR, products were resolved by 1.5% agarose gel electrophoresis and visualized with ethidium bromide. For real-time PCR,

cDNAs were amplified in iQ SYBR Green Supermix kit (Bio-Rad) and detected with the Bio-Rad iCycler system (Bio-Rad), using the following running conditions: 95°C for 3 minutes, 45 cycles at 95°C for 10 seconds, 55°C for 10 seconds, and 72°C for 30 seconds. Relative gene expression was normalized to 18S rRNA and calculated by using the 2(-Delta Delta C(T)) method (12).

The DNMT1 promoter-luciferase reporter plasmid construction

The genomic sequence of DNMT1 (NC_00019.9) was obtained from the National Center for Biotechnology Information. The promoter fragment containing the putative Sp1 binding consensus sequence of DNMT1 (-573 to +85) was PCR-amplified from whole genomic DNA isolated from LNCaP cells. The amplified fragments were cloned into KpnI/BglII sites of the pGL3-Basic vector (Promega) to generate the construct pGL3-DNMT1-Luc.

Western blotting

Western blotting was performed as described previously (8). Densitometric analysis of protein bands was performed by using Gel-Pro Analyzer (V3.1, Media Cybernetics, Bethesda, MD) to determine the relative intensities of drug-treated samples *versus* those of vehicle-treated controls after normalization to the internal reference protein β-actin.

DNA methylation analysis by pyrosequencing

To determine methylation levels of candidate genes in samples, the Pyrosequencing System (Qiagen, Valencia, CA) was used to detect methylated CpG sites in sequencing reactions (13). Genomic DNA (500 ng) was treated with sodium bisulfite using the EZ DNA Methylation kit (Zymo Research, Orange, CA). Bisulfite-treated DNA was amplified with specific primers for each gene of interest. The PyroMark Assay Design program and the Pyro Q-CpG software were used for primer designs and data analysis, respectively. Average methylation levels of individual CpG sites for each DNA sample were calculated.

Statistical analysis

Data from quantitative real time (qRT)-PCR, luciferase reporter assays and pyrosequencing were analyzed using Student's *t* test. Differences between group means were considered significant at $P < 0.05$.

RESULTS

Pursuant to our hypothesis that energy restriction mediates antitumor effects, in part, through epigenetic gene regulation, we examined the effect of 10 μM CG-12 versus glucose depletion on global gene expression in LNCaP cells via cDNA microarray analysis after 48 h of treatment. This microarray analysis showed that both treatments gave rise to a significant reduction in the gene expression of *DNMT1*, accompanied by modest, but statistically significant, decreases in *DNMT3B* expression and no change in *DNMT3A* levels (Table 1).

The ability of CG-12 and glucose starvation to downregulate DNMT expression suggests a mechanistic link between energy restriction and epigenetic regulation of gene expression by targeting DNA methylation. Previously, a global survey of DNA methylation patterns in prostate cancer cell lines identified a number of cancer-related genes that were transcriptionally silenced due to aberrant promoter hypermethylation (14). Based on this report, we examined the microarray data for the effect of CG-12 versus glucose depletion on the expression of 13 reported DNA methylation-silenced genes (Table 2). Among these 13 genes, *BASP1*, *GADD45a*, *GADD45b*, *GPX3*, *GSTP1*, *IGFBP3*, *KRT7*, *LAMB3*, *PDLIM4*, and *THBS1* are tumor-suppressive genes, whereas *CD44*, *S100A4*, and *TACSTD2* have been associated with tumorigenesis or aggressive phenotype of prostate cancer (15-17). It is noteworthy that CG-12 mimicked the ability of glucose starvation to activate the expression of *GADD45a*, *GADD45b*, and *IGFBP3*, while many other genes examined were not affected by either treatment with the exception of *THBS1* gene upregulation by CG-12.

Energy restriction suppresses the expression of DNMT1 and DNMT3A through transcriptional repression and proteasomal degradation, respectively

In the course of our structural modifications of CG-12, we identified a structurally optimized derivative, CG-5, in which the terminal methylcyclohexyl ring was replaced by a 3-pentyl moiety. This simple modification bestowed on CG-5 improved potency relative to CG-12 in suppressing [^{3}H]-2DG uptake

(IC_{50}, 6 μM versus 9 μM) and cell viability (IC_{50}, 4.5 μM versus 6 μM) in LNCaP cells (Fig. 1A). To validate our microarray data, we examined the dose-dependent suppressive effects of CG-5 and 2-DG vis-à-vis glucose starvation on the expression of DNMT1, DNMT3A, and DNMT3B, at both protein and mRNA levels, in LNCaP cells. In addition, the DNMT inhibitor 5-aza-dC was used as a control in light of its reported activity in suppressing DNMT1 expression via proteasomal degradation (29,30), and, to a lesser extent, DNMT3A through a yet unidentified mechanism (31).

Western blot analysis indicated that CG-5, 2-DG, and glucose depletion shared with 5-aza-dC the ability to decrease the expression levels of DNMT1 and, to a lesser extent, DNMT3A in a dose- or time-dependent manner (Fig. 1B, upper panel). Nevertheless, the mechanism underlying energy restriction-facilitated downregulation of DNMT1 was different from that of 5-aza-dC as CG-5, 2-DG, and glucose starvation decreased DNMT1 mRNA levels, while no significant changes were noted in response to 5-aza-dC (Fig. 1B, lower panel). In addition, no changes in the mRNA level of DNMT3A were noted in response to any of these treatments, suggestive of a posttranslational effect on protein levels.

Nevertheless, no changes in the protein or mRNA expression level of DNMT3B were noted by either CG-5 or glucose depletion, which contrasted the microarray data that showed a modest decrease in *DNMT3B* gene expression in response to either treatment (Table 1). This discrepancy might arise from inherent systematic errors associated with microarrays (32).

To examine the mechanism by which CG-5 suppressed the mRNA expression of DNMT1, we assessed its effect on the promoter activity of DNMT1 by using a DNMT1 promoter-luciferase reporter construct. As shown, CG-5 diminished the luciferase activity in a dose-dependent manner (Fig. 2A), which suggested that CG-5 suppressed DNMT1 expression through transitional repression. As the core promoter region of *DNMT1* contains three Sp1 (33) and four E2F (34) binding sites, this finding prompted us to examine the effect of CG-5 on the expression of these two transcription factors and their

target genes, androgen receptor (AR) for Sp1 (35) and cyclins D3 and E for E2F1 (36,37).

In line with our previously finding with CG-12 (8,9), CG-5 facilitated a dose-dependent decrease in the protein level of Sp1 without affecting the mRNA expression, indicative of proteasomal degradation (Fig. 2B). It is noteworthy that CG-5 also downregulated the expression of E2F1, at both protein and mRNA levels, suggesting a different mode of regulation from that of Sp1. Moreover, decreases in the expression of Sp1 and E2F1 were accompanied by parallel decreases in the expression of their respective targets, namely AR and cyclins D3 and E (Fig. 2B).

As for the CG-5-mediated inhibition of DNMT3A protein expression, a role for proteasomal degradation was supported by the ability of the proteasome inhibitor MG-132 to rescue DNMT3A protein expression from drug-induced suppression in LNCaP cells (Fig. 2C).

Similar findings regarding the unique ability of CG-5 to suppress the expression of DNMT1 and DNMT3A without disturbing that of DNMT3B was also noted in PC-3 and DU-145 cells (Fig. 3), indicating that this was not a cell line-specific effect. Moreover, the drug effect on DNMT1 expression correlated with that of E2F1 and Sp1 in a dose-dependent manner, suggestive of a causal relationship.

Differential effects of energy restriction on the activation of DNA methylation-silenced genes

LNCaP cells were exposed to 5 μM CG-5 or 5 μM 5-aza-dC in 10% FBS-supplemented RPMI 1640 medium for 48 or 72 h, or to 10% FBS-supplemented glucose-free medium for 72 h. qRT-PCR analysis indicates that these treatments led to distinct patterns of activation of these epigenetically silenced genes (Fig. 4). Among the 13 genes examined, 5-aza-dC mediated varying degrees of activation of 12 genes relative to the DMSO control (at 72 h: *GSTP1*, 510-fold; *KRT7*, 295-fold; *CD44*, 26-fold; *TACSTD2*, 23-fold; *BASP1*, 12-fold; *LAMB3*, 10-fold; *IGFBP3*, 9-fold; *GPX3*, *S100A4*, and *THBS1*, 8-fold; *PDLIM4* and *GADD45a*, 3-fold), while no

significant change in *GADD45b* mRNA expression was noted (Fig. 4A). In contrast to 5-aza-dC, CG-5 activated 7 of the 13 genes with a distinct preference for the two DNA damage response genes *GADD45a* and *GADD45b* (81- and 31-fold, respectively), followed by *IGFBP3* (12-fold), *LAMB3* (11-fold), *BASP1* (9-fold), *GPX3* (5-fold), and *GSTP1* (2-fold) at 72 h, while only modest increases (<2-fold) in the gene expression of *KRT7* and *THBS1* were noted (Fig. 4B). Moreover, CG-5 downregulated the mRNA levels of *PDLIM4*, *S100A4*, and *TACSTD2* by 97%, 56%, and 95%, respectively, relative to the control. Although CG-5 caused a modest, but statistically insignificant, increase in *CD44* mRNA expression at 48 h (1.16-fold), the treatment led to a 54% decrease ($P < 0.05$) at 72 h. It is noteworthy that two of these downregulated genes, *S100A4* and *TACSTD2*, are associated with the promotion of tumorigenesis, tumor invasion, and metastasis (15,27), and that CD44 represents a putative marker for prostate cancer stem cells (38).

As compared to CG-5-induced energy restriction, glucose deprivation showed a qualitatively similar, but muted effect on gene activation, which, in part, was reflective of smaller decreases in the expression levels of DNMT1 and DNMT3A. Glucose-depleted medium shared the ability of CG-5 to activate *GADD45a* (3.3-fold), *LAMB3* (2.7-fold), *BASP1* (2.4-fold), and *GADD45b* (1.8-fold), as well as to downregulate the expression of *PDLIM4* and *S100A4*, while having no significant impact on the mRNA expression of *CD44* and *KRT7* (Fig. 4C). However, in contrast to CG-5, glucose deprivation diminished the mRNA expression of *GPX3*, *GSTP1*, and *THBS1*, and increased that of *TACSTD2*.

Role of DNMT1 downregulation in CG-5-facilitated activation of epigenetically silenced genes

As evidenced by the greater suppressive effect of 5 μM CG-5 on the expression of DNMT1 versus that of DNMT3A (81% and 26%, respectively; Fig. 1B, upper panel), we rationalized that DNMT1 downregulation played a major role in the CG-5-mediated activation of these methylation-silenced genes. We obtained two lines of evidence to corroborate this premise. First,

qRT-PCR analysis indicated that siRNA-mediated knockdown of DNMT1 in LNCaP cells mimicked the effects of CG-5 by activating, by at least 2-fold, many of the same epigenetically silenced genes, including *IGFBP3* (7.5-fold), *BASP1* (3.8-fold), *LAMB3* (2.9-fold), and *GSTP1* (2.3-fold), as well as to sharply reduce the expression of *PDLIM4* (Fig. 5A). Second, ectopic DNMT1 expression attenuated the effect of CG-5 on the expression of many of the 13 epigenetically silenced genes examined (Fig. 5B). With the exception of *IGFBP3*, overexpression of DNMT1 diminished the extent of CG-5-mediated gene activation, returning the expression levels of many of these genes, such as *BASP1*, *GADD45b*, *GPX3*, and *GSTP1*, to the basal level or lower. Moreover, the suppressive effect of CG-5 on the mRNA expression of *PDLIM4* and *TACSTD2* was abrogated by the overexpression of DNMT1. However, ectopic DNMT1 expression had no significant effect on *S100A4* mRNA levels.

CG-5 alters CpG methylation in the promoter region of the 13 hypermethylated genes in LNCaP cells

To correlate the aforementioned changes in gene expression with the effects of 5-aza-dC, CG-5, and glucose deprivation on DNA methylation, we used pyrosequencing to analyze DNA methylation at CpG islands in the promoter regions of the aforementioned 13 genes in response to individual treatments (Fig. 6A - M). Pyrosequencing has emerged as the leading method for quantitative DNA methylation analysis, in part, due to its ability to identify differentially methylated positions in close proximity, thereby allowing concurrent quantification of multiple CpG sites in the promoter region (39). As neighboring CpG sites within a single promoter showed different degrees of methylation (Fig. 6A – M, right panels; each color-coded circle represents a single CpG site and each designated row represents one of the aforementioned treatments), the average of all sites was used to represent the level of methylation for each gene in this study (left panels).

LNCaP cells were treated with DMSO (Fig. 6, control; a and b for 48 and 72 h, respectively), 5 μM 5-aza-dC (c and d for 48 and 72 h, respectively), 5 μM CG-5 (e and f for 48 and 72 h, respectively), or glucose-depleted medium (g

and h for 48 and 72 h, respectively), after which genomic DNA was then collected for pyrosequencing analysis of DNA methylation patterns. As noted, the promoter and/or the first exon of each of these 13 genes contain multiple CpG sites, ranging from 3 to 19 sites. Not only did the methylation level among these sites vary within a single promoter/exon region (Fig. 6 A-M, right panels, a and b), but also the total methylation levels of the promoters/exons varied greatly among the 13 genes (left panels, a and b). For example, while many of these genes were highly methylated, *BASP1* and *THBS1* showed only 10% and 20% CpG methylation, respectively, in control cells (Fig. 6A and M, respectively). Consistent with the qRT-PCR findings, 5-aza-dC, CG-5, and glucose-depleted medium exhibited differential effects on the DNA methylation patterns of these 13 genes. 5-Aza-dC facilitated decreases in DNA methylation in all of the 13 genes examined (all panels, c and d). These epigenetic changes correlated with activation of these genes in 5-aza-dC-treated LNCaP cells (Fig. 4A) with the exception of *GADD45b* (panel D), of which the mRNA levels remained unaltered after drug treatment. It is noteworthy that, while CG-5 mediated the hypomethylation and the resulting activation of many tumor suppressor genes, it enhanced the DNA methylation of *PDLIM4* (panel J) and the tumor-promoting genes *S100A4* and *TACSTD2* (panels K and L, respectively), resulting in the downregulated expression of these genes (Fig. 4B). The effects of glucose-depleted medium on DNA methylation of many of these 13 genes paralleled those of CG-5, however, to a lesser extent. Nevertheless, glucose starvation contrasted with CG-5-induced energy restriction in its opposite effects on the DNA methylation pattern of *GPX3*, *GSTP1*, *TACSTD2*, and *THBS1* (panels E, F, L, and M, respectively), which underlies the observed differences in the effects of these two treatments on the activation of these DNA methylation-silenced genes (Fig. 4C).

DISCUSSION

Aberrant promoter hypermethylation of critical pathway genes plays an important role in prostate carcinogenesis and tumor progression (40,41), thereby representing a therapeutically relevant target for cancer treatment (42). In this study, we demonstrate the high potency of the novel ERMA CG-5 relative to 2-DG in suppressing the expression of DNMT1 and, to a lesser extent, DNMT3A, which led to the reactivation of a series of DNA methylation-silenced tumor suppressor genes, including *GADD45a*, *GADD45b*, *IGFBP3*, *LAMB3*, *BASP1*, *GPX3*, and *GSTP1*, in prostate cancer cells through promoter hypomethylation.

The effect of CG-5 on DNA methylation profiles is largely associated with the reduction in the expression of DNMT1 as siRNA-mediated knockdown and ectopic expression of DNMT1 mimicked and diminished, respectively, the ability of CG-5 to modulate the expression of these silenced genes. Although CG-5 and 5-aza-dC share the ability to downregulate DNMT1 expression, the underlying mechanisms are distinctly different. Evidence suggests that CG-5 facilitated the downregulation of DNMT1 expression through transcriptional repression, which our data suggest is associated with the reduced expression of Sp1 and E2F1. Our previous study demonstrated that β-transducin repeat-containing protein (β-TrCP)-dependent proteasomal degradation of Sp1 represents one of the energy restriction-associated cellular responses elicited by CG-12 (8), and likely represents the mechanism by which Sp1 is suppressed in CG-5-treated cells. In contrast, CG-5-mediated suppression of E2F1 expression was at the transcriptional level.

The specificity with which CG-5 activates DNA methylation-silenced genes is noteworthy, and contrasts with the nonspecific reactivation of nearly of all the silenced genes examined by 5-aza-dC. For example, our data indicate that CG-5 reduced the basal expression levels of *PDLIM4* and the three tumor/invasion-promoting genes, namely *CD44*, *S100A4*, and *TACSTD2*, while 5-aza-dC increased the expression of these genes by 8- to 26-fold. This target specificity was further confirmed by pyrosequencing analysis, which showed the differential effect of CG-5 versus 5-aza-dC on DNA methylation in

the promoter regions of the 13 genes examined. While 5-aza-dC caused universal hypomethylation of all of these 13 genes, CG-5 enhanced the DNA methylation of *PDLIM4* and the tumor-promoting genes *S100A4* and *TACSTD2*. However, the suppressive effect of CG-5 on CD44 promoter methylation relative to the control (65.9% versus 67.42%; P = 0.033) represents an anomaly since CG-5 reduced *CD44* expression.

From a mechanistic perspective, this differential regulation of DNA methylation-silenced genes is attributed not just to CG-5's effect on DNA hypomethylation alone, but also reflects its ability to affect the expression of transcription factors, such as Sp1 and E2F1, and histone-modifying enzymes (9). Together, these concerted actions underlines a more complicated mode of epigenetic gene regulation than that by the inhibitory effect of 5-aza-dC on DNMT activity alone.

CONCLUSIONS

It is well recognized that cancer cells undergo a metabolic shift to anaerobic glycolysis that provides growth advantages within the tumor microenvironment. Consequently, there is intense interest in targeting tumor metabolism as a therapeutic strategy, including small-molecule approaches. In this study, we demonstrate that epigenetic activation of DNA methylation-silenced tumor suppressor genes represents an important antitumor response to energy restriction. Moreover, our novel small-molecule ERMA, CG-5, regulates the expression of these genes through modulation of DNA methylation and, perhaps by virtue of its concomitant effects on histone modifications, exhibits target gene specificity and a broader spectrum of antitumor gene activation that might offer therapeutic advantages over DNMT inhibitors.

REFERENCES

1. Kroemer G, Pouyssegur J. Tumor cell metabolism: cancer's Achilles' heel. Cancer Cell 2008;13:472-82.
2. Vander Heiden MG. Targeting cancer metabolism: a therapeutic window opens. Nat Rev Drug Discov 2011;10:671-84.
3. Denko NC. Hypoxia, HIF1 and glucose metabolism in the solid tumour. Nat Rev Cancer 2008;8:705-13.
4. Elstrom RL, Bauer DE, Buzzai M, Karnauskas R, Harris MH, Plas DR, et al. Akt stimulates aerobic glycolysis in cancer cells. Cancer Res 2004;64:3892-9.
5. Osthus RC, Shim H, Kim S, Li Q, Reddy R, Mukherjee M, et al. Deregulation of glucose transporter 1 and glycolytic gene expression by c-Myc. J Biol Chem 2000;275:21797-800.
6. Matoba S, Kang JG, Patino WD, Wragg A, Boehm M, Gavrilova O, et al. p53 regulates mitochondrial respiration. Science 2006;312:1650-3.
7. Kelloff GJ, Hoffman JM, Johnson B, Scher HI, Siegel BA, Cheng EY, et al. Progress and promise of FDG-PET imaging for cancer patient management and oncologic drug development. Clin Cancer Res 2005;11:2785-808.
8. Wei S, Kulp SK, Chen CS. Energy restriction as an antitumor target of thiazolidinediones. J Biol Chem 2010;285:9780-91.
9. Chen CH, Huang PH, Chu PC, Chen MC, Chou CC, Wang D, et al. Energy restriction-mimetic agents induce apoptosis in prostate cancer cells in part through epigenetic activation of KLF6 tumor suppressor gene expression. J Biol Chem 2011;286:9968-76.
10. Sharma S, Kelly TK, Jones PA. Epigenetics in cancer. Carcinogenesis 2010;31:27-36.
11. Yang J, Wei S, Wang DS, Wang YC, Kulp SK, Chen CS. Pharmacological exploitation of the peroxisome proliferator-activated receptor gamma agonist ciglitazone to develop a novel class of androgen receptor-ablative agents. J Med Chem 2008;51:2100-7.
12. Livak KJ, Schmittgen TD. Analysis of relative gene expression data using real-time quantitative PCR and the 2(-Delta Delta C(T)) Method. Methods 2001;25:402-8.

13. Tost J, Gut IG. DNA methylation analysis by pyrosequencing. Nat Protoc 2007;2:2265-75.
14. Ibragimova I, Ibanez de Caceres I, Hoffman AM, Potapova A, Dulaimi E, Al-Saleem T, et al. Global reactivation of epigenetically silenced genes in prostate cancer. Cancer Prev Res (Phila) 2010;3:1084-92.
15. Goldstein AS, Lawson DA, Cheng D, Sun W, Garraway IP, Witte ON. Trop2 identifies a subpopulation of murine and human prostate basal cells with stem cell characteristics. Proc Natl Acad Sci U S A 2008;105:20882-7.
16. Herrlich P, Morrison H, Sleeman J, Orian-Rousseau V, Konig H, Weg-Remers S, et al. CD44 acts both as a growth- and invasiveness-promoting molecule and as a tumor-suppressing cofactor. Ann N Y Acad Sci 2000;910:106-18; discussion 118-20.
17. Li F, Tiede B, Massague J, Kang Y. Beyond tumorigenesis: cancer stem cells in metastasis. Cell Res 2007;17:3-14.
18. Hartl M, Nist A, Khan MI, Valovka T, Bister K. Inhibition of Myc-induced cell transformation by brain acid-soluble protein 1 (BASP1). Proc Natl Acad Sci U S A 2009;106:5604-9.
19. Zerbini LF, Libermann TA. GADD45 deregulation in cancer: frequently methylated tumor suppressors and potential therapeutic targets. Clin Cancer Res 2005;11:6409-13.
20. Qiu W, David D, Zhou B, Chu PG, Zhang B, Wu M, et al. Down-regulation of growth arrest DNA damage-inducible gene 45beta expression is associated with human hepatocellular carcinoma. Am J Pathol 2003;162:1961-74.
21. Yu YP, Yu G, Tseng G, Cieply K, Nelson J, Defrances M, et al. Glutathione peroxidase 3, deleted or methylated in prostate cancer, suppresses prostate cancer growth and metastasis. Cancer Res 2007;67:8043-50.
22. Cairns P, Esteller M, Herman JG, Schoenberg M, Jeronimo C, Sanchez-Cespedes M, et al. Molecular detection of prostate cancer in urine by GSTP1 hypermethylation. Clin Cancer Res 2001;7:2727-30.
23. Massoner P, Colleselli D, Matscheski A, Pircher H, Geley S, Jansen Durr P, et al. Novel mechanism of IGF-binding protein-3 action on prostate cancer cells:

inhibition of proliferation, adhesion, and motility. Endocr Relat Cancer 2009;16:795-808.
24. Mehta H, Gao Q, Galet C, Paharkova V, Wan J, Said JW, et al. IGFBP-3 is a Metastasis Suppression Gene in Prostate Cancer. Cancer Res 2011; 71:5154-63.
25. Sathyanarayana UG, Padar A, Suzuki M, Maruyama R, Shigematsu H, Hsieh JT, et al. Aberrant promoter methylation of laminin-5-encoding genes in prostate cancers and its relationship to clinicopathological features. Clin Cancer Res 2003;9:6395-400.
26. Vanaja DK, Grossmann ME, Cheville JC, Gazi MH, Gong A, Zhang JS, et al. PDLIM4, an actin binding protein, suppresses prostate cancer cell growth. Cancer Invest 2009;27:264-72.
27. Boye K, Maelandsmo GM. S100A4 and metastasis: a small actor playing many roles. Am J Pathol 2010;176:528-35.
28. Li Q, Ahuja N, Burger PC, Issa JP. Methylation and silencing of the Thrombospondin-1 promoter in human cancer. Oncogene 1999;18:3284-9.
29. Ghoshal K, Datta J, Majumder S, Bai S, Kutay H, Motiwala T, et al. 5-Aza-deoxycytidine induces selective degradation of DNA methyltransferase 1 by a proteasomal pathway that requires the KEN box, bromo-adjacent homology domain, and nuclear localization signal. Mol Cell Biol 2005;25:4727-41.
30. Patel K, Dickson J, Din S, Macleod K, Jodrell D, Ramsahoye B. Targeting of 5-aza-2'-deoxycytidine residues by chromatin-associated DNMT1 induces proteasomal degradation of the free enzyme. Nucleic Acids Res 2010;38:4313-24.
31. Palii SS, Van Emburgh BO, Sankpal UT, Brown KD, Robertson KD. DNA methylation inhibitor 5-Aza-2'-deoxycytidine induces reversible genome-wide DNA damage that is distinctly influenced by DNA methyltransferases 1 and 3B. Mol Cell Biol 2008;28:752-71.
32. Fang Y, Brass A, Hoyle DC, Hayes A, Bashein A, Oliver SG, et al. A model-based analysis of microarray experimental error and normalisation. Nucleic Acids Res 2003;31:e96.

33. Liu S, Liu Z, Xie Z, Pang J, Yu J, Lehmann E, et al. Bortezomib induces DNA hypomethylation and silenced gene transcription by interfering with Sp1/NF-kappaB-dependent DNA methyltransferase activity in acute myeloid leukemia. Blood 2008;111:2364-73.
34. Kimura H, Nakamura T, Ogawa T, Tanaka S, Shiota K. Transcription of mouse DNA methyltransferase 1 (Dnmt1) is regulated by both E2F-Rb-HDAC-dependent and -independent pathways. Nucleic Acids Res 2003;31:3101-13.
35. Yang CC, Wang YC, Wei S, Lin LF, Chen CS, Lee CC, et al. Peroxisome proliferator-activated receptor gamma-independent suppression of androgen receptor expression by troglitazone mechanism and pharmacologic exploitation. Cancer Res 2007;67:3229-38.
36. Ohtani K, DeGregori J, Nevins JR. Regulation of the cyclin E gene by transcription factor E2F1. Proc Natl Acad Sci U S A 1995;92:12146-50.
37. Ma Y, Yuan J, Huang M, Jove R, Cress WD. Regulation of the cyclin D3 promoter by E2F1. J Biol Chem 2003;278:16770-6.
38. Palapattu GS, Wu C, Silvers CR, Martin HB, Williams K, Salamone L, et al. Selective expression of CD44, a putative prostate cancer stem cell marker, in neuroendocrine tumor cells of human prostate cancer. Prostate 2009;69:787-98.
39. Dejeux E, El abdalaoui H, Gut IG, Tost J. Identification and quantification of differentially methylated loci by the pyrosequencing technology. Methods Mol Biol 2009;507:189-205.
40. Li LC, Carroll PR, Dahiya R. Epigenetic changes in prostate cancer: implication for diagnosis and treatment. J Natl Cancer Inst 2005;97:103-15.
41. Park JY. Promoter hypermethylation in prostate cancer. Cancer Control 2010;17:245-55.
42. Issa JP, Kantarjian HM. Targeting DNA methylation. Clin Cancer Res 2009;15:3938-46.

FIGURES AND TABLES

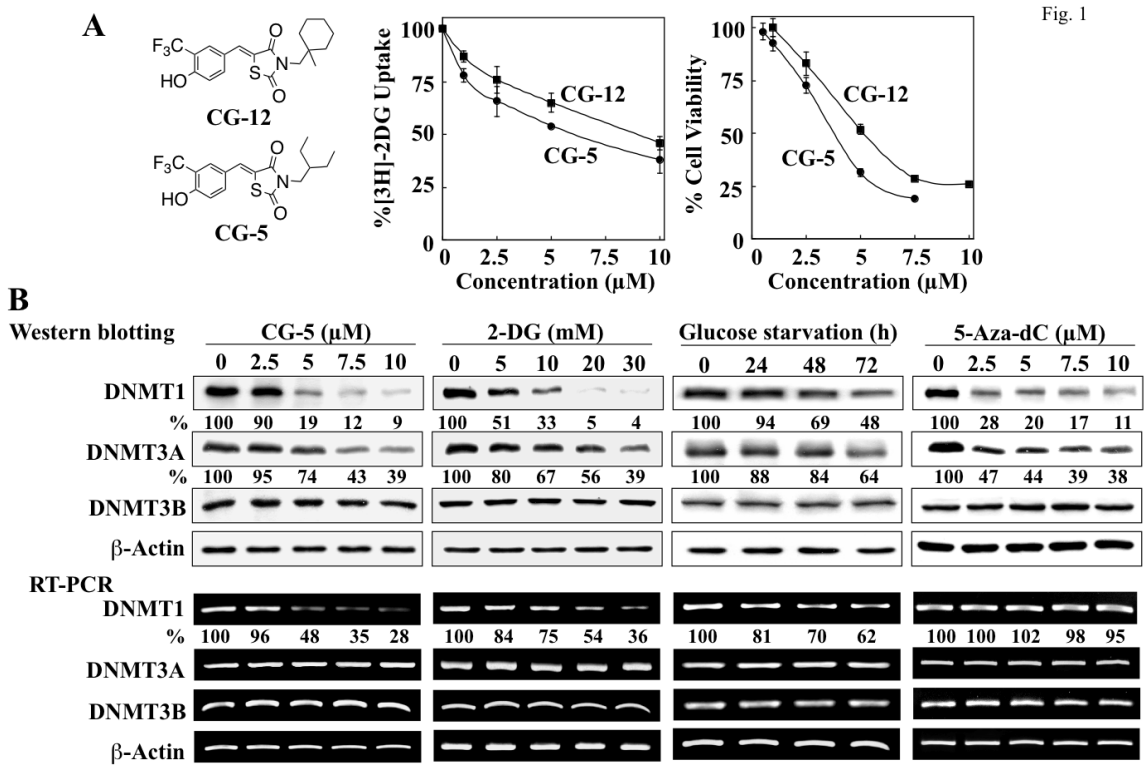

Fig. 1

Fig. 1. CG-5, 2-DG, glucose starvation and 5-aza-dC differentially affect the expression levels of DNMT isoforms. (A) Left panel, structures of CG-12 and CG-5. Central panel, dose-dependent inhibitory effects of CG-5 versus CG-12 on the uptake of [3H]-2DG into LNCaP cells in Krebs-Ringer phosphate buffer at 37 °C after 30 min of drug treatment. Point, mean; bars, SD (*N* = 3). Right panel, the corresponding effects on the viability of LNCaP cells by MTT assays in 10% FBS-containing RPMI 1640 medium after 72 h of drug treatment. Point, mean; bars, SD (*N* = 6). (B) LNCaP cells were treated with CG-5, 2-DG and 5-aza-dC at the indicated concentrations in 10% FBS-supplemented RPMI 1640 medium for 48 h or glucose-free medium for various time intervals. The expression levels of DNMT1, DNMT3A and DNMT3B were determined by Western blotting (upper panel) and RT-PCR (lower panel). All treatments suppressed, to varying degrees, the protein levels of DNMT1 and, to a lesser extent, DNMT3A. Parallel reductions in mRNA expression levels were observed only for DNMT1 in cells treated with CG-5, 2-DG and glucose deprivation, but

not with 5-aza-dC. The percentages denote the relative intensities of mRNA and protein bands of treated samples to those of the respective DMSO vehicle-treated controls after normalization to the respective internal reference β-actin. Each value represents the average of three independent experiments.

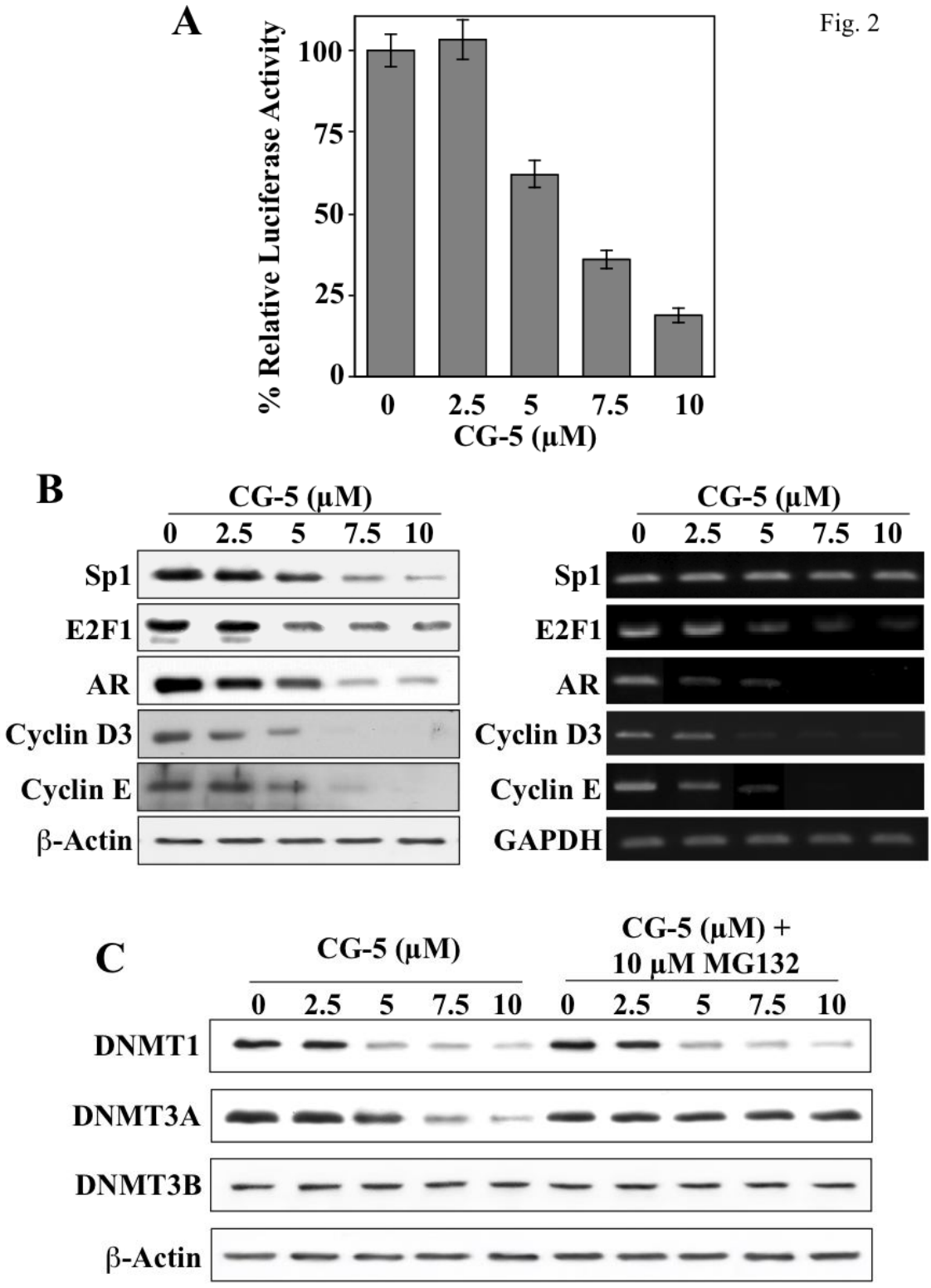

Fig. 2. CG-5 suppresses the expression of DNMT1 and DNMT3A through transcriptional repression and proteasomal degradation, respectively. (A) Dose-dependent, suppressive effect of CG-5 on DNMT1 promoter activity.

LNCaP cells were transiently transfected with the DNMT1 promoter-luciferase reporter plasmid pGL3-DNMT1-Luc, and exposed to CG-5 at the indicated concentrations or DMSO vehicle control in 10% FBS-containing medium for 48 h. Column, mean (n = 3); error bars, SD. (B) Parallel Western blot and RT-PCR analyses of the dose-dependent suppressive effect of CG-5 on the expression levels of Sp1 and E2F1. (C) The proteasome inhibitor MG132 protected cells from CG-5-induced ablation of DNMT3A, but not DNMT1. LNCaP cells were treated with CG-5 at the indicated concentrations for 36 h, followed by co-treatment with 10 μM MG132 for an additional 12 h. Cell lysates were analyzed by immunoblotting for DNMT1 and -3A.

Fig. 3

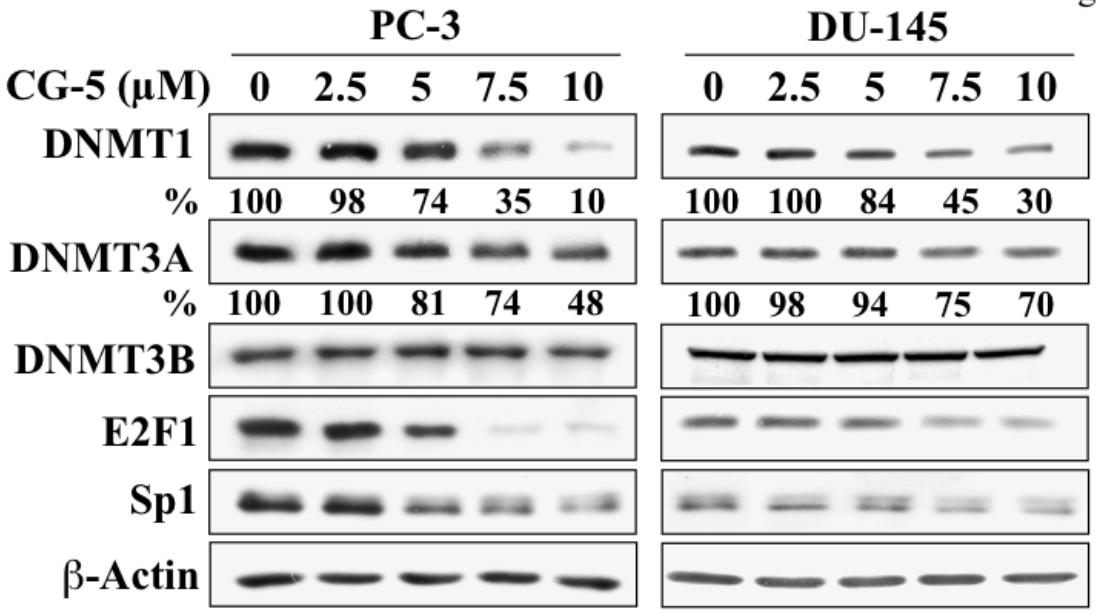

Fig. 3. Western blot analysis of the dose-dependent effects of CG-5 on the expression of DNMT1, DNMT3A, DNMT3B, E2F1, and Sp1 in PC-3 and DU-145 cells. Cells were treated with CG-5 at the indicated concentrations in 10% FBS-supplemented RPMI 1640 medium for 48 h. The percentages denote the relative intensities of protein bands of treated samples to those of the respective DMSO vehicle-treated controls after normalization to the respective internal reference β-actin. Each value represents the average of three independent experiments.

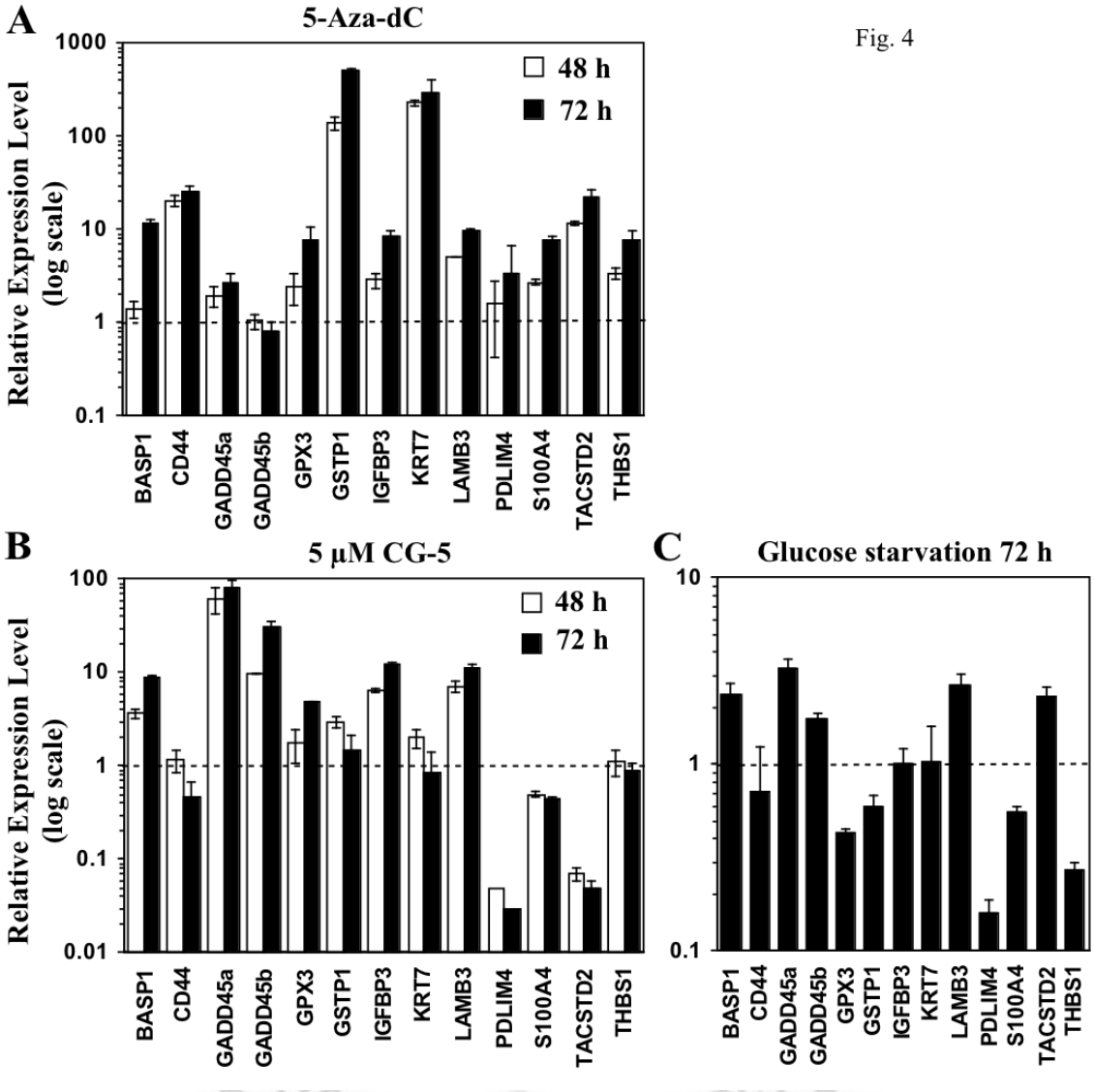

Fig. 4. Effects of 5-aza-dC, CG-5, and glucose deprivation on the expression levels of methylation-silenced cancer-related genes. LNCaP cells were treated with (A) 5 μM CG-5 or (B) 5 μM 5-aza-dC in 10% FBS-supplemented medium for 48 or 72 h, or with (C) glucose-depleted medium for 72 h. Total RNA was isolated and reversed transcribed to cDNA and the sequences of thirteen target genes reported to be silenced by DNA hypermethylation in prostate cancer cells were amplified and quantitated by qRT-PCR. Column, mean (n = 3); error bars, SD.

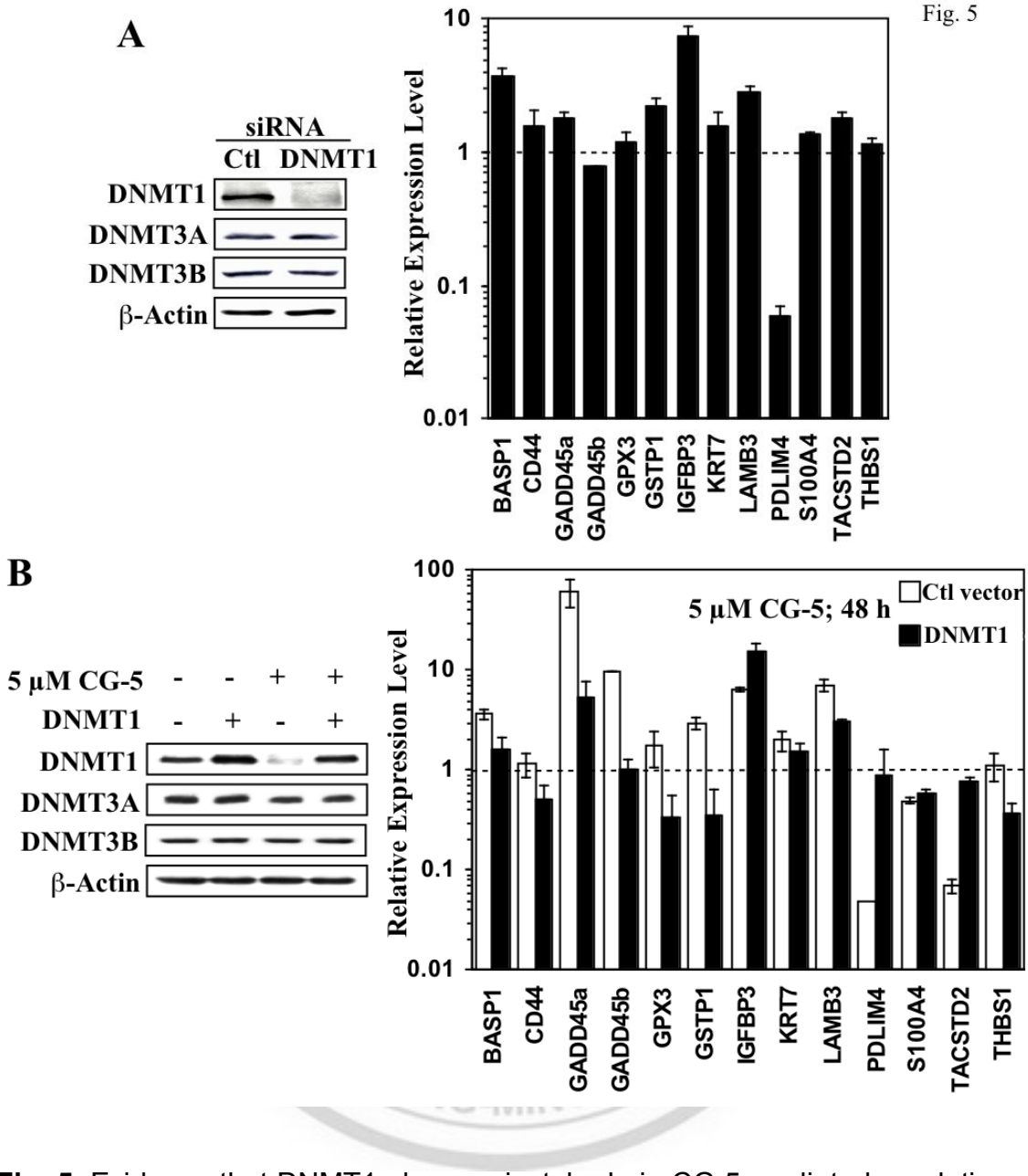

Fig. 5. Evidence that DNMT1 plays a pivotal role in CG-5-mediated regulation of methylation-silenced cancer-related gene expression. (A) siRNA-mediated knockdown of DNMT1 mimics CG-5 in modulating the expression of the selected thirteen genes reported to be silenced by DNA hypermethylation in prostate cancer cells, as determined by qRT-PCR (right panel). LNCaP cells were transiently transfected with DNMT1 or control (Ctl) siRNA, and then treated with 5 μM CG-5 for 72 h. The expression levels of DNMT1, DNMT3A, and DNMT3B in the transient transfectants were analyzed by Western blotting to confirm the specificity of the knockdown (left panel). Column, mean (n = 3);

error bars, SD. (B) Ectopic expression of DNMT1 protects cells from CG-5-mediated effects on the expression of the selected thirteen methylation-silenced genes, as determined by qRT-PCR (right panel). LNCaP cells were transiently transfected with the Flag-tagged DNMT1 or control (Ctl) vector, and then treated with 5 μM CG-5 for 48 h. The expression levels of DNMT1, DNMT3A, and DNMT3B in the transient transfectants following treatment with CG-5 or DMSO control were analyzed by Western blotting (left panel). Column, mean (n = 3); error bars, SD.

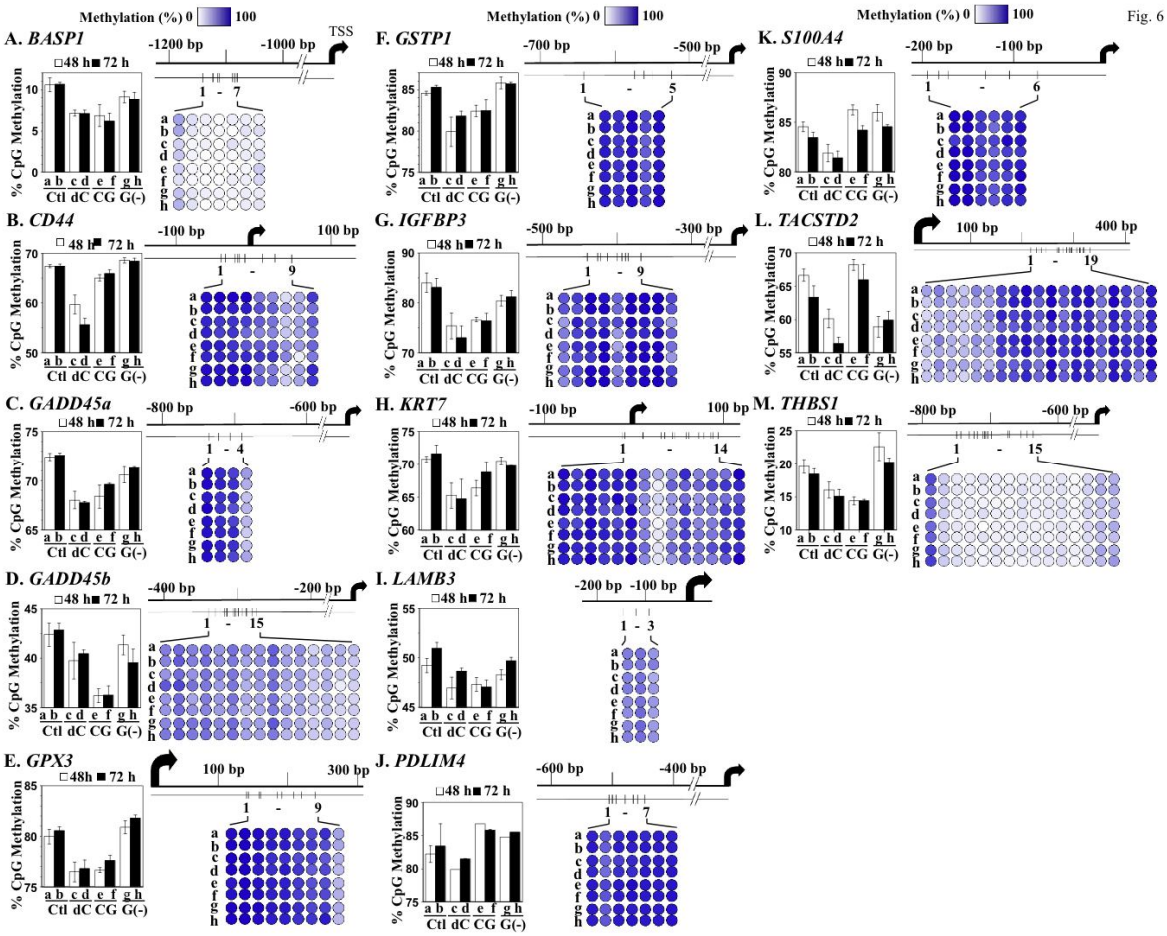

Fig. 6. Effects of CG-5, glucose deprivation, and 5-aza-dC on CpG island methylation in methylation-silenced cancer-related genes. LNCaP cells were treated with DMSO control (Ctl), 5 μM 5-aza-dC (dC), 5 μM CG-5 (CG) or glucose-depleted medium [G(-)] for 48 and 72 h. Pyrosequencing analysis of CpG island methylation in the promoter/first exon regions of the selected thirteen methylation-silenced genes was performed as described in Materials and Methods. A, *BASP1*; B, *CD44*; C, *GADD45a*; D, *GADD45b*; E, *GPX3*; F, *GSTP1*; G, *IGFBP3*; H, *KRT7*; I, *LAMB3*; J, *PDLIM4*; K, *S100A4*; L, *TACSTD2*; M, *THBS1*. Average methylation levels of individual CpG sites in the promoter/first exon of each of the genes examined under each condition were represented by the color-coded circles (right panels), with dark blue being 100% and white being 0% (scale at top of each column). As neighboring CpG sites within the promoter/first exon of each gene showed different degrees of methylation, the average of all sites was used to represent the level of

methylation for each of the thirteen genes under each treatment condition (left panel; column, mean (n = 3 - 19); error bars, SD). **a** and **b**: DMSO control for 48 and 72 h, respectively; **c** and **d**: 5 μM 5-aza-dC for 48 and 72 h, respectively; **e** and **f**: 5 μM CG-5 for 48 and 72 h, respectively; **g** and **h**: glucose-depleted medium for 48 and 72 h, respectively.

Table 1. Microarray analyses of the effects of 10 μM CG-12 versus glucose depletion on the expression of DNMTs in LNCaP cells after 48 h of treatment

Gene Name	10 μM CG-12		Glucose Depletion	
	Fold Change	***P* value**	**Fold Change**	***P* value**
DNMT1	-2.208398	5.32E-06	-2.1143294	6.45E-07
DNMT3A	-1.023485	0.690570233	-1.0391039	0.404186671
DNMT3B	-1.468048	0.001498209	-1.3947437	2.82E-04

Table 2. Microarray analyses of the effects of 10 μM CG-12 versus glucose depletion on the expression of thirteen DNA methylation-silenced genes in LNCaP cells after 48 h of treatment

Gene Name	Gene Description	Molecular Function	CG-12	Glucose Depletion
			Fold change (*P* value)	
BASP1 (NM_006317_1)	Brain acid soluble protein 1	Inhibition of Myc-induced cell transformation; a potential tumor suppressor (18)	1.182303151 (0.027893026)	0.920825697 (0.307789115)
CD44 (NM_000610_1)	Receptor for hyaluronic acid	Cell adhesion; markers for breast and prostate cancer stem cells (17)	n/a	n/a
GADD45a (NM_001924-1)	Growth arrest and DNA-damage-inducible protein 45a	Apoptosis, cell cycle arrest, and DNA repair; tumor suppressive (19)	5.838104359 (3.73E-10)	3.11320375 (1.21E-08)
GADD45b (AL050044_1)	Growth arrest and DNA-damage-inducible protein 45b	Apoptosis, cell cycle arrest, and DNA repair; reported tumor suppressor in hepatocellular carcinoma (20)	5.333934097 (2.01E-08)	4.483731849 (5.37E-09)
GPX3 (NM_002084)	Glutathione peroxidase 3	Maintaining genomic integrity via the detoxification of reactive oxygen species; tumor suppressive (21)	1.089147993 (0.370942845)	0.946090435 (0.352881698)
GSTP1 (NM_000852_1)	Glutathione *S*-transferase pi	Conjunction and detoxification of carcinogens; tumor suppressive (22)	1.192508872 (0.028969162)	0.952208888 (0.362806007)

IGFBP3 (NM_000598_1)	Insulin-like growth factor binding protein 3	Inhibiting cancer cell proliferation, adhesion, motility, and metastasis; tumor suppressive (23,24)	5.195274579 (4.89E-08)	2.137167525 (4.50E-07)
KRT7 (NM_005556_1)	Keratin 7	Cytoskeletal organization and biogenesis (14)	1.241685666 (0.018831416)	1.04298615 (0.622715314)
LAMB3 (NM_000228_1)	Laminin, b3	A component of the extracellular matrix involved in cell adhesion, growth, migration, proliferation, and differentiation; tumor suppressive (25)	n/a	1.22357285 (0.031432552)
PDLIM4 (NM_003687_1)	PDZ and LIM domain 3	An actin-binding protein; tumor suppressive (26)	0.993684661 (0.94564817)	0.981663174 (0.801008691)
S100A4 (NM_019554_1)	S100 calcium-binding protein A4	A Ca^{2+}-binding protein; promoting metastasis (27)	0.900563555 (0.217905821)	0.933789972 (0.206088795)
TACSTD2 (NM_002353_1)	Tumor-associated calcium signal transducer 2	A marker of human prostate basal cells with stem cell characteristics; promoting tumorigenesis and invasion (15)	n/a	0.907644973 (0.10922003)
THBS1 (NM_003246_1)	Thrombo-spondin-1	Cell adhesion and motility; a p53 and Rb regulated angiogenesis inhibitor; tumor suppressive (28)	2.609367236 (8.89E-08)	0.986198525 (0.755628795)

Supplementary Table 1. Primer Sequences

A. DNMT promotor/luciferase reporter plasmid construct

Construct	Forward (5'→3')	Reverse (5'→3')
pGL3-DNMT1-Luc	CAGGTACCTGGGTATAGAAGTGGCATGGGCCT'	TAAGATCTCCTACCGCCTGCGGACATCG

B. Semi-quantitative RT-PCR primers

Gene	Forward (5'→3')	Reverse (5'→3')
DNMT1	ACCGCTTCTACTTCCTCGAGGCCTA'	GTTGCAGTCCTCTGTGAACACTGTGG
DNMT3A	ACCACAGAGGCGGAAATACC	GTCTCCCTGCTGCTAACTGG
DNMT3B	CAGGAGACCTACCCTCCACA	TTACGTCGTGGCTCCAGTTA
Sp1	GGCGAGAGGCCATTTATGTGT	TGCATGACGTTGATGCCACT
E2F1	GGACCTGGAAACTGACCATCAG	GCTTTGATCACCATAACCATCT
AR	AGATGGGCTTGACTTTCCCAGAAAG	ATGGCTGTCATTCAGTACTCCTGGA
Cyclin D3	TGATTTCCTGGCCTTCATTC	AGCTTGACTAGCCACCGAAA
Cyclin E	TGATAATGTGGAGAGGGCAG	GAGGCGTGCGTTTGCTTTTA
β-actin	CACGAAACTACCTTCAACTCCA	GAAGCATTTGCGGTGGACGAT

C. qRT-PCR primers

Gene	Forward (5'→3')	Reverse (5'→3')
LAMB3	CCAAGCCTGAGACCTACTGC	GCCACATTCTCTACTCGGTGA
IGFBP3	CTCTGCGTCAACGCTAGTGC	CGGTCTTCCTCCGACTCAC

TACSTD2	AATGTATCCCCTTTCGGTCC	TCCCGGGTTGTCATACAGAT
GSTP1	ACCTCCGCTGCAAATACATC	CTCAAAAGGCTTCAGTTGCC
S100A4	AACTAAAGGAGCTGCTGACCC'	TGTTGCTGTCCAAGTTGCTC
GADD45a	CTCTTGGAGACCGACGCTG	GCAGGATCCTTCCATTGAGA
KRT7	CTGCCTACATGAGCAAGGTG	GGGACTGCAGCTCTGTCAAC
THBS1	CAATGCCACAGTTCCTGATG	CACAGCTCGTAGAACAGGAGG
CD44	GACAAGTTTTGGTGGCACG	CACGTGGAATACACCTGCAA
PDLIM4	CCCTCACCATCTCACGG	GCTCTGTGCTCTCACCATTG
GPX3	GCCGGGGACAAGAGAAGT	GGATGTACTCCTCCCCATCA
BASP1	GCTAACTCAGGGGCTGCATA	GGCTTTCTCGTCGTTCACAT
GADD45b	ACAGTGGGGGTGTACGAGTC	GATGTCATCCTCCTCCTCCTC
DNMT1	TTCTGTTAAGCTGTCTCTTTCCA	TGCTGAAGCCTCCGAGAT
18S rRNA	ACCCGTTGAACCCCATTCGTGA	GCCTCACTAAACCATCCAATCGG

Supplementary Table 1. Primer Sequences (continued)

D. Primer sequences used for pyrosequencing analysis		
Gene	**PCR primer for bisulfite-converted DNA**	**Sequencing primer**
LAMB3 (forward)	AATTTAAAGTGGTTTTGAATGGTATTG	AATGGTATTGGAGGTTA
LAMB3 (reverse)	Biotin-ACTCCAACTTCCTCCTCTA	
IGFBP3 (forward)	GTGGGTTTTTGGGGATATAAATAG	GTTAAAGGAATTAAATTTTAGAAAG
IGFBP3 (reverse)	Biotin-ATCACCCCAATCACTCCT	
TACSTD2 (forward)	GGGTAGGTAGGGTAGAGTATAAGAG	GGTAGGGTAGAGTATAAGAGT
TACSTD2 (reverse)	Biotin-AAACTACACACCATCATCTTATTAAT	
GSTP1 (forward)	Biotin-AATATTTGGGTGATGGGATGAT	CACATCTAACTAATTTTTATATTTT
GSTP1 (reverse)	CTCCAATTCAAACAATTCTACTTCAACC	
S100A4 (forward)	AGTTATGTATATTGGGTGGTGTTT	ATTTTATTTAGTTTTTTGTTAGTA
S100A4 (reverse)	Biotin-AACCTCTAACACCCCTTACA	
GADD45a (forward)	GAGAATTTGGGTTGTTAGGGATTTTTATA	GGGATTTTTATATGTGGTTAT
GADD45a (reverse)	Biotin-CCAAACCTCCCAAACAAAATTTACCTC	
KRT7 (forward)	GGGGTTTGGTAGTAGAGAAAGG	AGTAGAGAAAGGTGG
KRT7 (reverse)	Biotin-ACCAACAAACTCTAATTAATAATAACCT	
THBS1 (forward)	GTTGTTTTTTTAGGGTTTTTTGATGAGAAT	TTTTTAGGGTTTTTTGATGAGAATA
THBS1 (reverse)	Biotin-AAAAACCATTCCTTAAAATACCTACCCC	
CD44 (forward)	AGGAGAGGTTAAAGGTTGAATTTAATG	AGGTTGAATTTAATGGTG

CD44 (reverse)	Biotin-ACACCCAAACAAAAAAAACTATAACTA	
PDLIM4 (forward)	AGGTGGTTTGAGAGGAGTTTGTAAG	GAGGATTTTTTTGTGTTTATT
PDLIM4 (reverse)	Biotin-TACCCCAACTCAAATACCTCCTCAT	
GPX3 (forward)	GTGGGGAGTTGAGGGTAA	GTTATATTAGAGGGTTTGAAAGG
GPX3 (reverse)	Biotin-ACCCCAAAACTCACTCACCTT	
BASP1 (forward)	GGTTTTTGAGGGAAGGTAAAATTGG	TTTGTGTTTAGGTGTTAAAT
BASP1 (reverse)	Biotin-TTTAATATCTATACTTTAATAAAAACCACC	
GADD45b (forward)	TTTATTTTTAGTAGAATTTGGGAAAGG	AGGGGATTTTAGGTTT
GADD45b (reverse)	Biotin-AATAAAATCATTCCCCCCTCCTATTAAT	

PUBLICATIONS

1. **Lin HY**, Chong KW, Hsu JH, Yu HC, Shih CC, MD, Huang CH, Lin SJ, Chen CH, Chiang CC, Ho HJ, Lee PC, Kao CH, Cheng KH, Hsueh C, Niu DM. High Incidence of the Cardiac Variant of Fabry Disease Revealed by Newborn Screening in the Taiwan Chinese Population. Circ Cardiovasc Genet. 2009; 2: 450-6.

2. **Lin HY**, Huang CH, Yu HC, Chong KW, Hsu JH, Lee PC, Cheng KH, Chiang CC, Ho HJ, Lin SP, Chen SJ, Lin PK, Niu DM. Enzyme assay and clinical assessment in subjects with a Chinese hotspot late-onset Fabry mutation (IVS4+919G>A). J Inherit Metab Dis. 2010; 33: 619-24.

3. **Lin HY**, Kuo YC, Weng YI, Lai IL, Huang TH, Lin SP, Niu DM, Chen CS. Activation of silenced tumor suppressor genes in prostate cancer cells by a novel energy restriction-mimetic agent. Prostate. 2012 Apr 26. doi: 10.1002/pros.22530. [Epub ahead of print]

Circulation
Cardiovascular Genetics
JOURNAL OF THE AMERICAN HEART ASSOCIATION

High Incidence of the Cardiac Variant of Fabry Disease Revealed by Newborn Screening in the Taiwan Chinese Population

Hsiang-Yu Lin, Kah-Wai Chong, Ju-Hui Hsu, Hsiao-Chi Yu, Chun-Che Shih, Cheng-Hung Huang, Shing-Jong Lin, Chen-Huan Chen, Chuan-Chi Chiang, Huey-Jane Ho, Pi-Chang Lee, Chuan-Hong Kao, Kang-Hsiang Cheng, Chuen Hsueh and Dau-Ming Niu

Circ Cardiovasc Genet 2009;2;450-456; originally published online Jul 24, 2009;
DOI: 10.1161/CIRCGENETICS.109.862920
Circulation: Cardiovascular Genetics is published by the American Heart Association. 7272 Greenville Avenue, Dallas, TX 72514
 Print ISSN: 1942-325X. Online ISSN: 1942-3268

High Incidence of the Cardiac Variant of Fabry Disease Revealed by Newborn Screening in the Taiwan Chinese Population

Hsiang-Yu Lin, MD; Kah-Wai Chong, BS; Ju-Hui Hsu, MS; Hsiao-Chi Yu, MS; Chun-Che Shih, MD, PhD; Cheng-Hung Huang, MD, MS; Shing-Jong Lin, MD, PhD; Chen-Huan Chen, MD; Chuan-Chi Chiang, PhD; Huey-Jane Ho, MS; Pi-Chang Lee, MD; Chuan-Hong Kao, MD, MS; Kang-Hsiang Cheng, MD; Chuen Hsueh, MD; Dau-Ming Niu, MD, PhD

Background—Fabry disease is a treatable lysosomal storage disorder, which is often misdiagnosed or belatedly diagnosed.

Methods and Results—To determine the disease incidence in the Taiwan Chinese population, a Fabry disease newborn screening study was initiated. A total of 110 027 newborns were screened by assaying the α-galactosidase A (α-Gal A) activity using dry blood spots. Low plasma α-Gal A activity and presence of a Fabry mutation was demonstrated in 45 neonates (3 females). Eight different mutations were identified, including 3 known missense mutations (R112H, A143T, and R356W), 4 novel missense mutations (G104V, M296L, G360C, and K391T), and one known intronic mutation (IVS4+919G→A). The IVS4+919G→A mutation was most common (82% of patients). A total of 20 maternal grandparents of infants harboring this intronic mutation were evaluated by echocardiography, mutation analysis and α-Gal A activity assay. The intronic mutation was found in 9 grandfathers and 11 grandmothers. Of these grandparents, 3 grandfathers (33%) but none of the grandmothers had hypertrophic cardiomyopathy. Additionally, 16 males who had been diagnosed with idiopathic hypertrophic cardiomyopathy were screened by mutation analysis and α-Gal A activity; 4 (25%) showed deficient plasma α-Gal A activity in combination with the intronic mutation.

Conclusion—We found an unexpected high prevalence of the cardiac variant Fabry mutation IVS4+919G→A among both newborns (≈1 in 1600 males) and patients with idiopathic hypertrophic cardiomyopathy in the Taiwan Chinese population. The early identification of undiagnosed patients allows timely therapeutic intervention providing a better clinical outcome. **(*Circ Cardiovasc Genet*. 2009;2:450-456.)**

Key Words: hypertrophy ■ Fabry disease ■ hypertrophic cardiomyopathy ■ newborn screening ■ Taiwan Chinese population

Fabry disease (MIM 301500) is an X-linked recessive lysosomal storage disorder resulting from deficient α-galactosidase A (α-Gal A) activity. It has been estimated that this disease affects 1 in ≈50 000 males in the general population.[1,2] α-Gal A is an enzyme involved in the metabolic breakdown of globotriaosylceramide (GL-3) and deficient activity of this enzyme results in GL-3 accumulation in the walls of small blood vessels, nerves, dorsal root ganglia, renal glomerular and tubular epithelial cells, and cardiomyocytes. It is a complex multisystemic disorder characterized clinically by peripheral neuropathic pains (chronic burning and acute episodes of severe pain), gastrointestinal disturbances, characteristic skin lesions (angiokeratomata), progressive renal impairment, cardiomyopathy, and early stroke.[1]

Clinical Perspective on p 456

In the past decades, 2 variant types of Fabry disease with manifestations primarily involving the heart[3–8] or kidneys[9,10] have been reported, and several studies found that the Fabry cardiac variants usually mimic idiopathic hypertrophic car-

Received March 5, 2009; accepted July 21, 2009.

From the Institute of Clinical Medicine (H.Y.L., K.W.C., C.C.S., S.J.L., D.M.N.), National Yang-Ming University, Taipei; Department of Pediatrics (H.Y.L.), Mackay Memorial Hospital and Mackay Medicine, Nursing and Management College, Taipei; Department of Pediatrics (J.H.H., H.C.Y., C.H.H., P.C.L., C.H.K., K.H.C., D.M.N.), Taipei Veterans General Hospital, Taipei; Division of Cardiovascular Surgery (C.C.S.), Taipei Veterans General Hospital, Taipei; Division of Cardiology (S.J.L., C.H.C.), Department of Internal Medicine, Taipei Veterans General Hospital, Taipei; Cardiovascular Research Center (S.J.L., C.H.C.), National Yang-Ming University, Taipei; Department of Public Health (C.H.C.), National Yang-Ming University, Taipei; Neonatal Screening Center (C.C.C.), Chinese Foundation of Health, Taipei; Section of Newborn Screening (H.J.H.), Taipei Institute of Pathology, Taipei; and Department of Pathology (C.H.), Chang Gung Memorial Hospital, Linko, Chang Gung University, College of Medicine, Taoyuan, Taiwan.

Correspondence to Dau-Ming Niu, MD, PhD, Taipei Veterans General Hospital, No. 201, Sec. 2, Shih-Pai Road, Taipei 112, Taiwan. E-mail dmniu@vghtpe.gov.tw

Circ Cardiovasc Genet **is available at http://circgenetics.ahajournals.org** **DOI: 10.1161/CIRCGENETICS.109.862920**

diomyopathy (HCM). Patients with the cardiac variant lack the classical symptoms of Fabry disease and present in the 5th to 8th decades of life with left ventricular hypertrophy, arrhythmias, and/or cardiomyopathy.[3–8] Previous studies have shown that 1% to 4% of male patients with left ventricular hypertrophy or HCM had undiagnosed Fabry disease.[6–8]

Enzyme replacement therapies (ERT) are available, and experiences to date indicate that early therapeutic intervention results in a better outcome.[11–15] Therefore, early detection of Fabry disease, especially of the variant types, is important. In the past decade, a new fluorimetric α-Gal A activity assay using dried blood spots (DBS) has been successfully developed and is a useful tool for Fabry disease screening initiatives.[16–19] Spada et al[20] were the first to report the use of this assay in their Italian newborn screening program. This group found a higher than expected incidence of α-Gal A deficiency (1 in ≈3100 newborns) with a late-onset to classic type ratio of 11:1.

Our newborn screening study aimed at assessing the incidence of Fabry disease in the Taiwan Chinese population and is the largest Fabry screening study performed to date. In addition, our study aimed at identifying unrecognized Fabry patients among family members of diagnosed newborns and among individuals with idiopathic HCM.

Patients and Methods

Participants

The large-scale newborn screening program for Fabry disease was based on assessment of the α-Gal A enzyme activity using DBS on filter paper and was conducted at 2 newborn screening centers, the Chinese Foundation of Health and the Taipei Institute of Pathology, Taipei, Taiwan. The centers screen ≈55% of all newborns in Taiwan. Routine newborn screening DBS samples collected by the age of 3 days in 110 027 newborns between January 2008 and January 2009 were analyzed. Parental informed written consent was obtained for each sample collected. The study was approved by the ethics committee of the Taipei Veterans General Hospital, Taipei, Taiwan.

DBS Test

Alpha-Gal A activity in DBS on filter paper was determined using a fluorescence-based high-throughput method with modifications of a reported procedure.[16] To establish a normal population mean, α-Gal A activity was measured in 10,000 anonymous newborn samples. The normal mean of α-Gal A activity was 7.54±3.69 nmol/h/mL plasma. The activity of α-Gal A was rechecked if the newborns' α-Gal A activity was <3 μmol/h/L (i.e. <40% of the normal mean). If the re-tested activity of α-Gal A was still <40%, "screen positive" was considered. For these individuals a second blood spot was requested and assayed. In the second blood spot, newborns with blood spot α-Gal A activities <2 μmol/h/L (i.e. <25% of the normal mean) were considered "double DBS screen positive", and were recalled to Taipei Veterans General Hospital for confirmatory testing, including genetic analysis of the α-Gal A gene (Figure 1).

Plasma α-Gal A Enzyme Activity Assay

Plasma α-Gal A activity was determined using the substrate 4-methylumbelliferyl α-D-galactopyranoside (5 mmol/L) freshly prepared in 117 mmol/L *N*-acetyl-D-galactosamine/50 mmol/L citric-phosphate buffer, pH 4.6, before every assay. In brief, 50 μL of plasma was mixed with 300 μL of the substrate solution, incubated at 37°C for 2 hours, and 0.2 N glycine-NaOH was added to stop the reaction. Fluorescence intensity was measured with the excitation and emission wavelengths of 365 and 450 μm, respectively.[21,22]

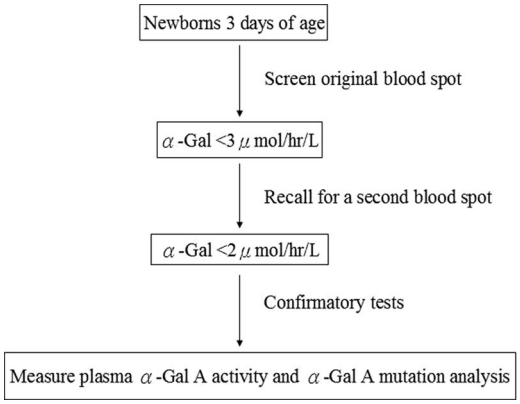

Figure 1. Algorithm used in the newborn screening program for Fabry disease in Taiwan.

α-Gal A Gene Mutation Analysis

Patients with low α-Gal A enzyme activities (normal range: 7.9 to 16.9 nmol/h/mL plasma[21,22]) were subject to genetic analysis. Blood samples were obtained from these patients in blood collecting tubes containing ethylene diamine tetraacetic acid, and samples were stored at 4°C. DNA was isolated from whole blood using the GFX genomic Blood DNA Purification Kit (Amersham Biosciences, UK) following the manufacturer's instructions. The human α-Gal A gene consists of 7 exons. Each exon of α-Gal A gene was amplified by polymerase chain reaction using appropriate primers.[23] The polymerase chain reaction products were analyzed by 1.5% agarose I (Amresco) gel electrophoresis and then eluted in the polymerase chain reaction Advanced PCR Clean Up System (Viogene, USA.). Direct sequencing of the α-Gal A gene was processed using the BigDye Terminator v3.1 Cycle Sequencing Kit (Applied Biosystems) and ABI Prism 3730 Sequencer.

Pedigree Studies

For each patient, a complete pedigree was drawn and genetic counseling and pedigree analysis were provided to family members. Parents and grandparents of these patients were offered the combination of α-Gal A activity assay, mutation analysis, and related medical evaluations.

Screening of Patients With Idiopathic HCM in Cardiac Clinics

Twenty-three patients (16 men, 7 women; mean age 50.6±14.3 years; age range 18 to 67 years), who had been diagnosed with idiopathic HCM, were subject to analyses of plasma α-Gal A activity and the IVS4+919G→A mutation.

Results

Fabry Screening in Newborns

Of the 110 027 newborns screened, 57 451 (52.2%) were males and 52 576 (47.8%) females. There were 67 "double DBS screen positive" newborns (9 females) recalled to our hospital for confirmatory testing, of whom 45 newborns (3 females) were identified to have low plasma α-Gal A activity and a α-Gal A mutation (Table 1). Eight mutations were detected, including 3 known missense mutations (R112H,[24,25] A143T,[26,27] and R356W[24,28]), 4 novel missense mutations (G104V, M296L, G360C, and K391T), and one known intronic splicing mutation (IVS4+919G→A[29]; Table 2). None of these mutations were found in 50 unrelated healthy females. The IVS4+919G→A mutation was noted to be the most common mutation among these newborns (82% of patients). Although this splicing mutation has been found in

Table 1. Results of the Newborn Screening Program for Fabry Disease in Taiwan (January 2008–January 2009)

Newborns ≤3 d of Age Tested With DBS, n	Males, 57 451	Incidence (%) 95% CI*	Females, 52 576	Incidence (%) 95% CI*	Total, 110 027	Incidence (%) 95% CI*
First DBS test positive,† n	1094	1.90±0.11	515	0.98±0.08	1609	1.46±0.07
Second DBS test positive,‡ n	58	0.10±0.03	9	0.02±0.01	67	0.06±0.01
Newborns with Fabry mutations,§ n	42	0.07±0.02	3	0.006±0.007	45	0.04±0.01
Intronic splicing mutation:						
IVS4+919G→A (male) or IVS4+919G/A (female), n	35	0.06±0.02	2	0.004±0.005	37	0.034±0.01

*Calculated using a normal approximation to the binomial distribution. Some incidences are small and lower confidence intervals have negative values.
†α-Gal activity <3 μmol/hr/L.
‡α-Gal <2 μmol/hr/L.
§Deficient plasma α-Gal A activity and identification of α-Gal A mutation.

Japanese Fabry patients with a cardiac variant,[29] its incidence in Japan is still unknown. In our study, the incidence of Fabry mutations was 1 in 1368 for males. If the 4 novel missense mutations were excluded, the incidence of the known disease-causing mutations would be 1 in 1512 males.

Pedigree Studies

Data on enzyme activity levels and genetic analyses from the maternal grandparents was limited due to the unavailability of data, personal concerns or death. Among the 35 male neonates with the IVS4+919G→A mutation, 20 maternal grandparents were ascertained to have the same mutation, including 9 grandfathers and 11 grandmothers (Table 3). Because of the high prevalence of the Fabry cardiac variant mutation IVS4+919G→A among the Taiwan Chinese population, we paid attention to the cardiac conditions of family members with the IVS4+919G→A mutation. Among 9 maternal grandfathers with the IVS4+919G→A mutation, 3 (33%) had HCM, compared with none of the 11 grandmothers with this disease (Table 3). The plasma α-Gal A activities of the 9 grandfathers ranged from 0.56 to 2.40 nmol/h/mL, whereas those of the 11 grandmothers ranged from 3.87 to 10.72 nmol/h/mL (Table 3).

Screening of Patients With Idiopathic HCM in Cardiac Clinics

To explore the occurrence of the cardiac variant mutation IVS4+919G→A in Taiwan Chinese idiopathic HCM patients, we analyzed the plasma α-Gal A activities and presence of this mutation in 23 patients diagnosed with HCM in the outpatient clinics. Four of 16 male patients (25%) had both deficient plasma α-Gal A activities (ranging from 0.65 to 0.98 nmol/h/mL) and the IVS4+919G→A mutation (Table 4). In contrast, the plasma α-Gal A activities in male patients without the IVS4+919G→A mutation ranged from 9.39 to 14.53 nmol/h/mL. It is noteworthy that none of the female patients was detected to have the IVS4+919G/A mutation and that their plasma α-Gal A activities ranged from 6.59 to 16.12 nmol/h/mL.

Histologic examination of endomyocardial tissue of Patient 4 in Table 4, a 67-year-old male patient with HCM, showed disorderly arranged myocytes with marked hypertrophy and

Table 2. Results of *α-Gal A* Gene Mutation Analysis and α-Gal A Enzyme Activity Screening in 110 027 Newborns

Patient No.	Gender	Location	α-Gal A Mutation	DBS α-Gal A Activity, μmol/hr/L	Plasma α-Gal A Activity,* nmol/hr/mL	Potential Phenotype
Missense mutation						
1	M	Exon 2	c.311 G→T, p.G104V	0.50	0.60	Unknown
2	M	Exon 2	c.334 G→A, p.R112H	0.35	1.70	Renal/cardiac variant[24,25]
3	M	Exon 3	c.427 G→A, p.A143T	0.94	3.42	Renal/cardiac variant[26,27]
4	M	Exon 6	c.886 A→T, p.M296L	0.01	1.04	Unknown
5	M	Exon 7	c.1066 C→T, p.R356W	0.01	3.13	Mild classic[24,28]
6	F	Exon 7	c.1078 G→T, p.G360C	0.97	7.40	Unknown
7	M	Exon 7	c.1078 G→T, p.G360C	0.37	3.60	Unknown
8	M	Exon 7	c.1172 A→C, p.K391T	1.37	1.70	Unknown
Total No. of Patients	**Gender**	**Location**	**α-Gal A Mutation**	**DBS α-Gal A Activity, μmol/hr/L**	**Plasma α-Gal A Activity,* nmol/hr/mL**	**Potential Phenotype**
Intronic splicing mutation						
35	M	Intron 4	IVS4+919G→A	1.00±0.42	2.80±0.71	Cardiac variant[29]
2	F	Intron 4	IVS4+919G/A	1.08±0.21	4.61±2.27	Cardiac variant[29]

*Normal reference range, 7.9 to 16.9 nmol/hr/mL.

Table 3. Plasma α-Gal A Activity and Echocardiographic Features in Maternal Grandparents With α-Gal A Mutations IVS4+919G→A (Grandfather) or IVS4+919G/A (Grandmother)

Family	Maternal Grandparents	Age, y	Plasma α-Gal A Activity,* nmol/hr/mL	α-Gal A Mutation	Echocardiography
14	Grandfather	67	0.72	IVS4+919G→A	HCM, mild MR, TR
17	Grandfather	57	1.12	IVS4+919G→A	Minimal PR, MR
18	Grandfather	53	1.26	IVS4+919G→A	Mild TR
22	Grandfather	52	1.16	IVS4+919G→A	Minimal PR, mild TR
23	Grandfather	54	0.84	IVS4+919G→A	Minimal MR, mild TR
26	Grandfather	62	2.40	IVS4+919G→A	HCM, mild AR, MR, TR
33	Grandfather	57	0.64	IVS4+919G→A	HCM, mild TR
34	Grandfather	56	0.56	IVS4+919G→A	Minimal PR, mild TR
35	Grandfather	54	0.63	IVS4+919G→A	Minimal TR
10	Grandmother	56	6.51	IVS4+919G/A	Mild TR
12	Grandmother	45	5.53	IVS4+919G/A	Minimal TR
19	Grandmother	51	5.81	IVS4+919G/A	Moderate MR, mild to moderate TR, mild AR
30	Grandmother	49	3.87	IVS4+919G/A	Mild TR
32	Grandmother	62	5.96	IVS4+919G/A	Moderate TR, mild MR, MVP
36	Grandmother	56	10.72	IVS4+919G/A	Minimal TR
37	Grandmother	57	8.13	IVS4+919G/A	Minimal MR, TR
40	Grandmother	51	5.97	IVS4+919G/A	Mild TR
41	Grandmother	54	9.33	IVS4+919G/A	Mild TR
43	Grandmother	55	5.98	IVS4+919G/A	Mild TR
45	Grandmother	54	5.36	IVS4+919G/A	Minimal TR

*Normal reference range, 7.9 to 16.9 nmol/hr/mL.

MR indicates mitral regurgitation; TR, tricuspid regurgitation; PR, pulmonary regurgitation; AR, aortic regurgitation; MVP, mitral valve prolapse.

large perinuclear and sarcoplasmic vacuoles, accompanied by focal interstitial fibrosis, which is consistent with the diagnosis of Fabry disease (Figure 2).

Discussion

One of the important findings of our large-scale newborn screening study in the Taiwan Chinese population is the high incidence of Fabry mutations. The incidence of Fabry mutations was 1 in 1368 for males. This incidence is ≈30 times higher than previous estimates[1,2] and 2 times higher compared with the incidence found in an Italian newborn screening study.[20]

Eight different mutations were identified, including 3 known missense mutations (R112H,[24,25] A143T,[26,27] and R356W[24,28]), 4 novel missense mutations (G104V, M296L, G360C, and K391T), and one known intronic mutation (IVS4+919G→A[29]). The IVS4+919G→A mutation was most common (82% of patients). The 3 known mutations

Table 4. Clinical Profiles, Plasma α-Gal A Activity, and Echocardiographic Features in 4 Patients With Both the Intronic Splicing Mutation (IVS4+919G→A) and HCM From the Outpatient Clinics

Patient No.	Age, y	Gender	Plasma α-Gal A Activity,* nmol/hr/mL	α-Gal A Mutation	Echocardiography
1	42	M	0.65	IVS4+919G→A	HCM, mild TR
2	67	M	0.69	IVS4+919G→A	HCM, minimal AR, mild PR, MR
3	53	M	0.88	IVS4+919G→A	HCM
4	67	M	0.98	IVS4+919G→A	HCM, mild AS, MR, TR

*Normal reference range, 7.9 to 16.9 nmol/hr/mL.

TR indicates tricuspid regurgitation; AR, aortic regurgitation; PR, pulmonary regurgitation; MR, mitral regurgitation; AS, aortic stenosis.

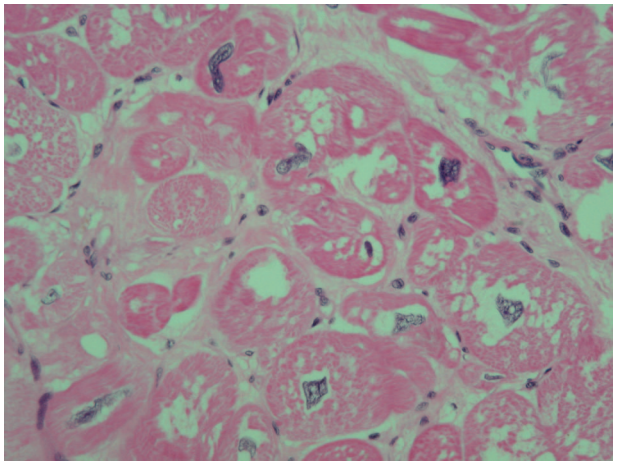

Figure 2. Histologic examination of endomyocardial tissue (patient 4 in Table 4) showed markedly hypertrophic and disarrayed myocytes with large perinuclear and sarcoplasmic vacuoles (hematoxylin and eosin; ×400).

have been reported to be associated with mild classic (R356W[24,28]) or late-onset renal or cardiac (R112H,[24,25] A143T[26,27]) forms. The intronic mutation (IVS4+919G→A) was reported to be a cardiac variant Fabry mutation.[29]

None of the 4 novel mutations were found in 50 unrelated healthy females, which makes the possibility of polymorphisms unlikely. However, whether these mutations will eventually cause Fabry disease remains unknown. Further comprehensive family studies and long-term follow-up for identified individuals with these mutations are warranted. If the 4 novel missense mutations are excluded, the incidence of the known disease-causing mutations would be 1 in 1512 males.

In our study, only 1 newborn was noted to have a previously reported mutation (R356W) causing a classic phenotype. Therefore, the calculated incidence of classic Fabry disease in the Taiwan Chinese population is ≈1 in 57 000 males, which is equivalent to previous estimates.[1,2]

There was a surprisingly high incidence of the IVS4+919G→A mutation among newborns with α-Gal A deficiency. This intronic mutation was detected in 83.3% of the 42 male newborns found with Fabry mutations, which translates in an incidence of ≈1 in 1600 male newborns. This IVS4+919G→A mutation has been reported to be associated with cardiac variant Fabry disease by Ishii et al[29] It can activate an alternative splicing in intron 4 causing insertion of a 57-nucleotide sequence between exons 4 and 5 of the α-Gal A cDNA and subsequent premature termination after 7 altered amino acid residues downstream from exon 4. In general, the alternatively spliced transcript was present in a small amount (<5% of normal transcript) in most normal human tissues. However, in Fabry patients with the IVS4+919G→A mutation, the alternatively spliced transcript will be largely increased (>70% in lymphoblasts) and the enzyme activity will be decreased to <10% of normal activity (lymphoblast).

Another interesting finding of our study is that the mild-form pathogenic mutation IVS4+919G→A apparently does not consistently cause Fabry-related HCM in all affected individuals. Of the 9 maternal grandfathers with the IVS4+919G→A mutation, only 3 had HCM. It remains to be elucidated why some patients with this mutation suffer from cardiomyopathy as early as in their 40s, whereas others with this same mutation do not have any symptoms or signs of cardiomyopathy even in their 70s. In this study, no correlation between the plasma α-Gal A activity and the existence of HCM was found. However, the sample size is too small to make definite conclusions regarding the likelihood of the IVS4+919G→A mutation leading to the cardiac variant of Fabry disease. Because the newborn screening is still ongoing, we hope that we will be able to eventually expand the database and get a clearer picture of this. Further investigations are required to identify genes or other factors involved in the modification of clinical expression of Fabry disease and to elucidate if there are other pathogenic mutations related to mild phenotypes.

Fabry disease has historically been described as an X-linked recessive disease, however, a substantial proportion of heterozygous females will develop disease manifestations. In some, the disease presentation may be as severe as seen in young males and others may remain relatively asymptomatic until late adulthood.[30,31] This phenomenon is, in part, caused by skewed X chromosome inactivation. If most of the mutation-harboring X chromosomes are inactive in females, then the clinical presentation will be rather mild. On the other hand, the clinical presentation can be severe when most of the normal X chromosomes are inactive. With regard to cardiac involvement in female Fabry patients, Fabry disease may account for up to 12% of females with late-onset HCM.[32] Kampmann et al[33] evaluated 55 affected females and reported echocardiographic evidence of cardiac involvement in 56% of women younger than 38 years, in 86% of women older than 38 years, and in all female patients older than 45 years of age. Schiffmann et al[34] reported natural history data on 168 ERT-naive female Fabry patients of whom 35% had developed a cardiac event (eg, arrhythmia, angina, myocardial infarction, and cardiac surgery) by a mean age of ≈44 years. X-inactivation patterns vary widely between female Fabry patients and different tissues, and the enzyme activity measured in lymphocytes can be very different from other tissues, such as heart or kidney. Therefore, in females, the result of the lymphocyte enzyme activity assay is not predictive of disease severity in a particular organ, and the result may fall within the normal range although the female can be clinically affected.[35] Thus, the lymphocyte enzyme activity assay is not suitable as a screening tool in female populations, and it is not surprising that only a very few females were detected via the enzyme activity screening in this study. Screening for hot spot mutations may be an alternative method to detect unidentified female Fabry patients in high-risk populations.

Although only ⅓ of the grandfathers with the IVS4+919G→A mutation had significant HCM, the high prevalence of this mutation in the Taiwan Chinese population points at an important presence of the cardiac variant of Fabry disease among patients with HCM in this particular population. Although the studied sample size of HCM is small and the Fabry screening in patients with HCM is still ongoing, we strongly recommend

that Fabry disease must be ruled out before the diagnosis of idiopathic HCM is made in the Taiwan Chinese population, both in males and females.

There are few debates that early detection, genetic counseling, regular follow-up, and timely early therapeutic intervention for the classic Fabry disease is beneficial. However, for the individuals who have atypical Fabry mutations, particularly, for those whose residual enzyme activities are >10% to 20% of normal, the strategy for regular follow-up and therapeutic intervention should be different from those with the classic type, because our study showed that a significant proportion of the individuals older than 50 years of age with IVS4+919G→A mutation still have not developed any symptoms or signs of this disease. Therefore, the early detection of babies with atypical Fabry mutations results in several clinical impacts: When is the best time to start evaluating the cardiac conditions of these individuals with IVS4+919G→A mutation? When is the best time to start ERT? Do we need to start ERT early, when there are only controversial or minimal manifestations of heart problems? Or do we need to wait until the cardiac manifestations become marked? Several reports indicate that ERT for the advanced form of Fabry cardiomyopathy is not very effective.[12] Therefore, further investigations are needed to find out the best way for early detection of meaningful cardiac manifestations in patients with atypical Fabry mutations, and to identify the most appropriate time for them to start ERT.

In summary, this study in the Taiwan Chinese population demonstrates the feasibility of a large-scale neonatal screening program for Fabry disease. The incidence of Fabry mutations among newborns was unexpectedly high (≈1 in 1400 male newborns), as was the prevalence of the cardiac variant mutation IVS4+919G→A. The diagnosis of Fabry disease should be considered in all patients with idiopathic HCM. The early identification of undiagnosed patients allows timely medical intervention providing a better clinical outcome.

Disclosures

None.

References

1. Desnick RJ, Ioannou YA, Eng CM. α-galactosidase A deficiency: Fabry disease. In: Scriver CR, Beaudet AL, Sly WS, Valle D, eds. *The Metabolic and Molecular Bases of Inherited Disease.* New York: McGraw-Hill; 2001:3733–3774.
2. Meikle PJ, Hopwood JJ, Clague AE, Carey WF. Prevalence of lysosomal storage disorders. *JAMA*. 1999;281:249–254.
3. von Scheidt W, Eng CM, Fitzmaurice TF, Erdmann E, Hubner G, Olsen EG, Christomanou H, Kandolf R, Bishop DF, Desnick RJ. An atypical variant of Fabry's disease with manifestations confined to the myocardium. *N Engl J Med*. 1991;324:395–399.
4. Chimenti C, Ricci R, Pieroni M, Natale L, Russo MA, Frustaci A. Cardiac variant of Fabry's disease mimicking hypertrophic cardiomyopathy. *Cardiologia*. 1999;44:469–473.
5. Ommen SR, Nishimura RA, Edwards WD. Fabry disease: a mimic for obstructive hypertrophic cardiomyopathy? *Heart*. 2003;89:929–930.
6. Nakao S, Takenaka T, Maeda M, Kodama C, Tanaka A, Tahara M, Yoshida A, Kuriyama M, Hayashibe H, Sakuraba H, Tanaka H. An atypical variant of Fabry's disease in men with left ventricular hypertrophy. *N Engl J Med*. 1995;333:288–293.
7. Sachdev B, Takenaka T, Teraguchi H, Tei C, Lee P, McKenna WJ, Elliott PM. Prevalence of Anderson-Fabry disease in male patients with late onset hypertrophic cardiomyopathy. *Circulation*. 2002;105:1407–1411.
8. Monserrat L, Gimeno-Blanes JR, Marín F, Hermida-Prieto M, García-Honrubia A, Pérez I, Fernández X, de Nicolas R, de la Morena G, Payá E, Yagüe J, Egido J. Prevalence of Fabry disease in a cohort of 508 unrelated patients with hypertrophic cardiomyopathy. *J Am Coll Cardiol*. 2007;50:2399–2403.
9. Nakao S, Kodama C, Takenaka T, Tanaka A, Yasumoto Y, Yoshida A, Kanzaki T, Enriquez ALD, Eng CE, Tanaka H, Tei C, Desnick RJ. Fabry disease: detection of undiagnosed hemodialysis patients and identification of a "renal variant" phenotype. *Kidney Int*. 2003;64:801–807.
10. Kotanko P, Kramar R, Devrnja D, Paschke E, Voigtlander T, Auinger M, Demmelbauer K, Lorenz M, Hauser AC, Kofler HJ, Lhotta K, Neyer U, Pronai W, Wallner M, Wieser C, Wiesholzer M, Zodl H, Fodinger M, Sunder-Plassmann G. Results of a nationwide screening for Anderson-Fabry disease among dialysis patients. *J Am Soc Nephrol*. 2004;15:1323–1329.
11. Germain DP, Waldek S, Banikazemi M, Bushinsky DA, Charrow J, Desnick RJ, Lee P, Loew T, Vedder AC, Abichandani R, Wilcox WR, Guffon N. Sustained, long-term renal stabilization after 54 months of agalsidase beta therapy in patients with Fabry disease. *J Am Soc Nephrol*. 2007;18:1547–1557.
12. Weidemann F, Niemann M, Breunig F, Herrmann S, Beer M, Störk S, Voelker W, Ertl G, Wanner C, Strotmann J. Long-term effects of enzyme replacement therapy on Fabry cardiomyopathy: evidence for a better outcome with early treatment. *Circulation*. 2009;119:524–529.
13. Schiffmann R, Ries M, Timmons M, Flaherty JT, Brady RO. Long-term therapy with agalsidase alfa for Fabry disease: safety and effects on renal function in a home infusion setting. *Nephrol Dial Transplant*. 2006;21:345–354.
14. Banikazemi M, Bultas J, Waldek S, Wilcox WR, Whitley CB, McDonald M, Finkel R, Packman S, Bichet DG, Warnock DG, Desnick RJ. Agalsidase-beta therapy for advanced Fabry disease: a randomized trial. *Ann Intern Med*. 2007;146:77–86.
15. Pierre-Louis B, Kumar A, Frishman WH. Fabry disease: cardiac manifestations and therapeutic options. *Cardiol Rev*. 2009;17:31–35.
16. Chamoles NA, Blanco M, Gaggioli D. Fabry disease: enzymatic diagnosis in dried blood spots on filter paper. *Clin Chim Acta*. 2001;308:195–196.
17. Meikle PJ, Ranieri E, Simonsen H, Rozaklis T, Ramsay SL, Whitfield PD, Fuller M, Christensen E, Skovby F, Hopwood JJ. Newborn screening for lysosomal storage disorders: clinical evaluation of a two-tier strategy. *Pediatrics*. 2004;114:909–916.
18. Li Y, Scott CR, Chamoles NA, Ghavami A, Pinto BM, Turecek F, Gelb MH. Direct multiplex assay of lysosomal enzymes in dried blood spots for newborn screening. *Clin Chem*. 2004;50:1785–1796.
19. Pagliardini S, Spada M. A simple and rapid approach for screening lysosomal storage disorders. *J Inherit Metab Dis*. 2003;26:S1.
20. Spada M, Pagliardini S, Yasuda M, Tukel T, Thiagarajan G, Sakuraba H, Ponzone A, Desnick RJ. High incidence of later-onset Fabry disease revealed by newborn screening. *Am J Hum Genet*. 2006;79:31–40.
21. Sheu SS, Chan LP, Liao SC, Hsiao KJ, Shu KH, Lu YS, Cheng CH, Lian JD. Fabry's disease: clinical, pathologic and biochemical manifestations in two Chinese males. *Zhonghua Yi Xue Za Zhi*. 1994;54:368–372.
22. Desnick RJ, Allen KY, Desnick SJ, Raman MK, Bernlohr RW, Krivit W. Fabry's disease: enzymatic diagnosis of hemizygotes and heterozygotes. Alpha-galactosidase activities in plasma, serum, urine, and leukocytes. *J Lab Clin Med*. 1973;81:157–171.
23. Chen CH, Shyu PW, Wu SJ, Sheu SS, Desnick RJ, Hsiao KJ. Identification of a novel point mutation (S65T) in alpha-galactosidase A gene in Chinese patients with Fabry disease. Mutations in brief no 169. *Hum Mutat*. 1998;11:328–330.
24. Ishii S, Chang HH, Kawasaki K, Yasuda K, Wu HL, Garman SC, Fan JQ. Mutant alpha-galactosidase A enzymes identified in Fabry disease patients with residual enzyme activity: biochemical characterization and restoration of normal intracellular processing by 1-deoxygalactonojirimycin. *Biochem J*. 2007;406:285–295.
25. Eng CM, Niehaus DJ, Enriquez AL, Burgert TS, Ludman MD, Desnick RJ. Fabry disease: twenty-three mutations including sense and antisense CpG alterations and identification of a deletional

hot-spot in the alpha-galactosidase A gene. *Hum Mol Genet*. 1994;3:1795–1799.
26. Spada M, Marongiu A, Voglino G, Merlino S, Alluto A, La Dolcetta M, Pagliardini S. Molecular study in 20 unrelated male patients with Fabry disease: the A143T genotype correlates with the late-onset end-stage nephropathy. *J Inherit Metab Dis*. 2003;26:171.
27. Eng CM, Ashley GA, Burgert TS, Enriquez AL, D'Souza M, Desnick RJ. Fabry disease: thirty-five mutations in the alpha-galactosidase A gene in patients with classic and variant phenotypes. *Mol Med*. 1997;3:174–182.
28. Bernstein HS, Bishop DF, Astrin KH, Kornreich R, Eng CM, Sakuraba H, Desnick RJ. Fabry disease: six gene rearrangements and an exonic point mutation in the alpha-galactosidase gene. *J Clin Invest*. 1989;83:1390–1399.
29. Ishii S, Nakao S, Minamikawa-Tachino R, Desnick RJ, Fan JQ. Alternative splicing in the alpha-galactosidase A gene: increased exon inclusion results in the Fabry cardiac phenotype. *Am J Hum Genet*. 2002;70:994–1002.
30. Wilcox WR, Oliveira JP, Hopkin RJ, Ortiz A, Banikazemi M, Feldt-Rasmussen U, Sims K, Waldek S, Pastores GM, Lee P, Eng CM, Marodi L, Stanford KE, Breunig F, Wanner C, Warnock DG, Lemay RM, Germain DP. Females with Fabry disease frequently have major organ involvement: lessons from the Fabry Registry. *Mol Genet Metab*. 2008;93:112–128.
31. Wang RY, Lelis A, Mirocha J, Wilcox WR. Heterozygous Fabry women are not just carriers, but have a significant burden of disease and impaired quality of life. *Genet Med*. 2007;9:34–45.
32. Chimenti C, Pieroni M, Morgante E, Antuzzi D, Russo A, Russo MA, Maseri A, Frustaci A. Prevalence of Fabry disease in female patients with late-onset hypertrophic cardiomyopathy. *Circulation*. 2004;110:1047–1053.
33. Kampmann C, Baehner F, Whybra C, Martin C, Wiethoff CM, Ries M, Gal A, Beck M. Cardiac manifestations of Anderson-Fabry disease in heterozygous females. *J Am Coll Cardiol*. 2002;40:1668–1674.
34. Schiffmann R, Warnock DG, Banikazemi M, Bultas J, Linthorst GE, Packman S, Sorensen SA, Wilcox WR, Desnick RJ. Fabry disease: progression of nephropathy, and prevalence of cardiac and cerebrovascular events before enzyme replacement therapy. *Nephrol Dial Transplant.* 2009;24:2102–2111 [Epub ahead of print].
35. Linthorst GE, Vedder AC, Aerts JM, Hollak CE. Screening for Fabry disease using whole blood spots fails to identify one-third of female carriers. *Clin Chim Acta*. 2005;353:201–203.

CLINICAL PERSPECTIVE

This study in the Taiwan Chinese population demonstrates the feasibility of a large-scale neonatal screening program for Fabry disease. The incidence of Fabry mutations among newborns was unexpectedly high (≈1 in 1400 male newborns), as was the prevalence of the cardiac variant mutation IVS4+919G→A. Awareness of this information may be important for physicians evaluating Chinese patients with hypertrophic cardiomyopathy because some patients could represent cardiac Fabry disease. The early identification of Fabry disease may allow timely therapeutic intervention with enzyme replacement therapy, possibly resulting in better clinical outcome.

J Inherit Metab Dis (2010) 33:619–624
DOI 10.1007/s10545-010-9166-7

ORIGINAL ARTICLE

Enzyme assay and clinical assessment in subjects with a Chinese hotspot late-onset Fabry mutation (IVS4+919G→A)

Hsiang-Yu Lin · Cheng-Hung Huang · Hsiao-Chi Yu · Kah-Wai Chong · Ju-Hui Hsu · Pi-Chang Lee · Kang-Hsiang Cheng · Chuan-Chi Chiang · Huey-Jane Ho · Shuan-Pei Lin · Shih-Jen Chen · Po-Kang Lin · Dau-Ming Niu

Received: 1 March 2010 / Revised: 17 June 2010 / Accepted: 29 June 2010 / Published online: 7 September 2010

Abstract Newborn screening for Fabry disease in Taiwan Chinese has revealed a high incidence of the late-onset GLA mutation IVS4+919G→A (~1 in 1,500–1,600 males). We studied 94 adults with this mutation [22 men, 72 women; mean age: men 57.8±6.0 (range 42–68), women 39.1±14.1 years (range 19–82)]. Plasma α-galactosidase A activity assay was 10.4±11.2% of normal in the men and 48.6±19.5% of normal in the women. Echocardiography in 90 of the adults revealed left ventricular hypertrophy (LVH) in 19 (21%), including 14 of 21 men (67%) and 5 of 69 women (7%). Microalbuminuria, based on the urine albumin-to-creatinine ratio measured on at least two occasions, was present in 17 of 86 subjects (20%) (men: 5/20, 25%; women 12/66, 18%). At least one ocular manifestation consistent with Fabry disease was present in 41 of 52 subjects (79%) who underwent ophthalmologic examination, including 8 (15%) with conjunctival vessel tortuosity, 15 (29%) with cornea verticillata, 10 (19%) with Fabry cataract, and 34 (65%) with retinal vessel tortuosity. Among subjects over 40 years of age, men were more likely than women to have LVH [14/21 (67%) vs 5/25 (20%), $p<0.001$]. Cardiovascular, renal and ocular abnormalities are highly prevalent in adult Taiwan Chinese subjects with the Fabry mutation IVS4+919G→A. Our findings contribute to the limited understanding of the course of this late-onset disease variant and underscore the need for close follow up in such patients.

Introduction

Fabry disease (MIM 301500) is an X-linked lysosomal storage disorder characterized by deficient α-galactosidase A

Communicated by: Olaf Bodamer

Competing interest: None declared.

H.-Y. Lin · C.-H. Huang · K.-W. Chong · D.-M. Niu (✉)
Institute of Clinical Medicine, National Yang-Ming University,
No.155, Sec. 2, Linong Street,
Taipei 112, Taiwan
e-mail: dmniu1111@yahoo.com.tw

H.-Y. Lin · S.-P. Lin
Department of Pediatrics, Mackay Memorial Hospital
and Mackay Medicine, Nursing and Management College,
Taipei, Taiwan

C.-H. Huang · H.-C. Yu · J.-H. Hsu · P.-C. Lee · K.-H. Cheng · D.-M. Niu
Department of Pediatrics, Taipei Veterans General Hospital,
No. 201, Section 2, Shih-Pai Road,
Taipei 112, Taiwan

C.-C. Chiang
Neonatal Screening Center, Chinese Foundation of Health,
Taipei, Taiwan

H.-J. Ho
Section of Newborn Screening, Taipei Institute of Pathology,
Taipei, Taiwan

S.-J. Chen · P.-K. Lin (✉)
Department of Ophthalmology, Taipei Veterans General Hospital,
No. 201, Section 2, Shih-Pai Road,
Taipei 112, Taiwan
e-mail: pklin123@hotmail.com

S.-J. Chen · P.-K. Lin
School of Medicine, National Yang-Ming University,
No. 155, Sec. 2, Linong Street,
Taipei 112, Taiwan

P.-K. Lin
Graduate Institute of Biomedical Electronic and Bioinformatics,
National Taiwan University,
Taipei, Taiwan

(α-Gal A) activity, leading to progressive accumulation of globotriaosylceramide (GL-3) in the vascular endothelium of the skin, kidney, heart, and brain. It is a complex, multisystemic disorder characterized clinically by angiokeratomas, acroparesthesias, hypohydrosis, corneal opacities, gastrointestinal disturbances, progressive renal impairment, cardiomyopathy, and early stroke (Desnick et al. 2001). The estimated incidence of classic Fabry disease is 1 in 40,000–60,000 males in the general population (Desnick et al. 2001; Meikle et al. 1999). There is increasing recognition that manifestations in heterozygous females can range from no symptoms at all to abnormalities as severe as those in affected males (Deegan et al. 2006; Wang et al. 2007; Wilcox et al. 2008).

During the past decade, there have been reports of late-onset phenotypes of Fabry disease primarily involving the heart (Monserrat et al. 2007; Nakao et al. 1995; Sachdev et al. 2002), kidneys (Kotanko et al. 2004; Nakao et al. 2003; Tanaka et al. 2005) or cerebrovascular system (Rolfs et al. 2005). Patients with the cardiac variant lack the classic symptoms of Fabry disease and present with left ventricular hypertrophy (LVH), arrhythmias, or hypertrophic cardiomyopathy in the fifth to eighth decades of life. It has been suggested that 1–4% of men with LVH or hypertrophic cardiomyopathy have undiagnosed Fabry disease (Monserrat et al. 2007; Nakao et al. 1995; Sachdev et al. 2002). Patients with the renal variant develop proteinuria and may progress to end-stage renal disease, typically after 50 years of age. Screening by plasma α-Gal A activity has shown that 0.25–1% of men undergoing hemodialysis were identified with previously undiagnosed Fabry disease (Kotanko et al. 2004; Nakao et al. 2003; Tanaka et al. 2005). Ocular findings may suggest the diagnosis in some individuals, where progressive deposition of GL-3 in ocular structures may result in abnormalities at the level of the conjunctival vessels, cornea, lens, or retinal vessels (Nguyen et al. 2005; Orssaud et al. 2003; Sher et al. 1979; Sodi et al. 2007).

In Japan, an IVS4+919G→A splicing mutation has been reported in patients with the late-onset cardiac phenotype (Ishii et al. 2002). Lin et al. (2009) screened ~57,000 newborn boys and found various Fabry mutations in ~1 in 1,400, 83% of whom had the cardiac variant mutation IVS4+919G→A, for an incidence of ~1 in 1,600. Hwu et al. (2009) screened ~90,000 baby boys and found Fabry mutations in ~1 in 1,250, 86% with IVS4+919G→A, an incidence of 1 in 1,500. This suggests a substantial incidence of the mutation in the Taiwanese population as a whole, but little is known about its phenotype in adult men and women. We previously looked for LVH in 20 maternal grandparents of babies carrying this mutation (Lin et al. 2009). The aim of the present study was to perform enzyme assays and assess clinical manifestations in a larger group of Taiwanese adults who carry the IVS4+919G→A mutation in order to help to delineate the natural history of late-onset Fabry disease associated with this genotype.

Materials and methods

Study design and subjects

Pedigree analysis was offered to the parents of the newborns with the IVS4+919G→A mutation who had been identified via the Fabry disease newborn screening program in Taiwan (Lin et al. 2009). Once families had consented to participate, parents, grandparents and other blood relatives underwent mutation analysis. Ninety-four adult subjects who were found to have the IVS4+919G→A mutation were enrolled in the current study. Informed written consent was obtained from each of the subjects. The study was approved by the ethics committee of Taipei Veterans General Hospital, Taipei, Taiwan.

Molecular, biochemical and clinical assessments

The α-Gal A exons and adjacent intronic and promoter regions were sequenced using standard techniques as described elsewhere (Shabbeer et al. 2005; Shabbeer et al. 2006). Plasma α-Gal A enzyme activity was measured according to the method described by Desnick et al. (1973) and expressed as numerical value and as the percentage of the mean in normals (i.e. 12.4 nmol/h/mL plasma; Desnick et al. 1973; Sheu et al. 1994).

A total of 94 subjects carried the mutation and were asked to undergo screening for cardiac, renal, and ocular abnormalities. However, it was up to the subjects to follow through with all instructions. All had at least one of the examinations.

Spot urine samples for measurement of albumin and creatinine levels were collected on at least two occasions to

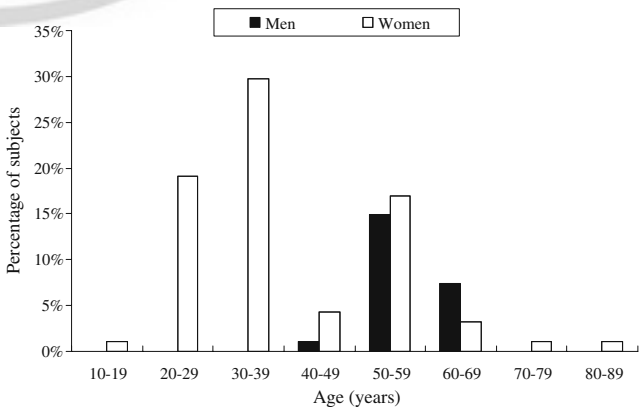

Fig. 1 Age distribution of adult subjects with late-onset Fabry mutation IVS4+919G→A (n=94; 72 women, 22 men)

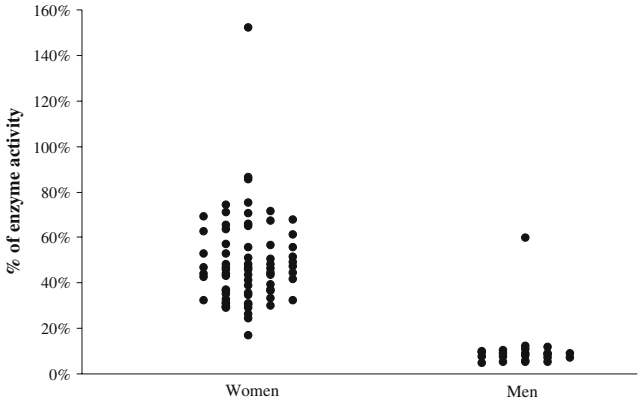

Fig. 2 Residual α-galactosidase activity in women (n=72) and men (n=22) with late-onset Fabry mutation IVS4+919G→A. Activity is expressed as percentage of the normal mean (12.4±2.25 nmol/h/mL plasma)

rule out confounding factors unrelated to Fabry disease. The ratio of concentrations of urinary albumin and creatinine expressed as mg/mmol was used to estimate the total daily albumin excretion. Microalbuminuria was defined as urinary albumin-to-creatinine ratio ≥2.0 mg/mmol for men and ≥2.8 mg/mmol for women on at least two occasions, based on the National Kidney Foundation's Kidney Disease Outcome Quality Initiative working group definition (National Kidney Foundation 2002).

Cardiac evaluation included electrocardiography and standard echocardiography. LVH was defined as left ventricular mass >259 g in men and >166 g in women (Levy et al. 1987).

Ophthalmological evaluation included slit lamp examination of the bulbar conjunctiva, cornea, lens and fundus.

Statistical analysis

The Statistical Package for Social Sciences (SPSS®) version 11.5 (SPSS, Chicago, IL) was used to analyze the plasma α-Gal A activity, as well as clinical manifestations and gender differences. Relationships between clinical findings and age, as well as clinical findings and plasma α-Gal A activity, were tested using Pearson correlation, and significance was tested using Fisher r–z transformations. Differences were considered to be statistically significant if the p value was less than 0.05.

Results

Among the 94 adult subjects with the IVS4+919G→A mutation, there were 22 men and 72 women. Their mean age (±SD, range) was 57.8 (6.0, 42-68) and 39.1 (14.1, 19-82) years, respectively (Fig. 1). Half the subjects were women under 40 years of age, and 22 men (23% of all subjects) and 25 women (27%) were older than 40.

The plasma α-Gal A activity was analyzed in all subjects; the mean (±SD, % of normal) values were 1.29 (1.39, 10.4±11.2) nmol/h/mL plasma for men and 6.03 (2.42, 48.6±19.5) nmol/h/mL plasma for women (Fig. 2). There were no correlations (p>0.05) between clinical findings and plasma α-Gal A activity in both men and women.

Echocardiographic examinations (n=90) revealed LVH in 67% of 21 men assessed and in 7% of 69 women (Table 1). Men over 40 years were more likely to have LVH than women over 40 (67 and 20%, respectively; p<0.001). LVH was more likely to occur in women over 40 than in

Table 1 Clinical findings in subjects with Fabry mutation IVS4+919G→A

Examinations	Echocardiography	Urinary analysis	Slit lamp examination				
	(n=90)	(n=86)	(n=52)				
Findings[a]	Left ventricular hypertrophy	Microalbuminuria	Conjunctival vessel tortuosity	Cornea verticillata	Fabry cataract	Retinal vessel tortuosity	At least one Fabry ocular finding
Men any age	14/21 (67)	5/20 (25)	1/7 (14)	1/7 (14)	0/7 (0)	2/7 (29)	3/7 (43)
Women any age	5/69 (7)	12/66 (18)	7/45 (16)	14/45 (31)	10/45 (22)	32/45 (71)	38/45 (84)
Men aged ≥40 years	14/21 (67)	5/20 (25)	1/7 (14)	1/7 (14)	0/7 (0)	2/7 (29)	3/7 (43)
Women aged ≥40 years	5/25 (20)	7/23 (30)	1/11 (9)	2/11 (18)	2/11 (18)	6/11 (55)	8/11 (73)
p value	<0.001	0.700	0.751	0.841	0.257	0.310	0.229
Women aged <40 years	0/44 (0)	5/43 (12)	6/34 (18)	12/34 (35)	8/34 (24)	26/34 (76)	30/34 (88)
p value difference women aged ≥ and <40 years	<0.005	0.060	0.507	0.297	0.718	0.171	0.227

[a] n/subjects examined (%)

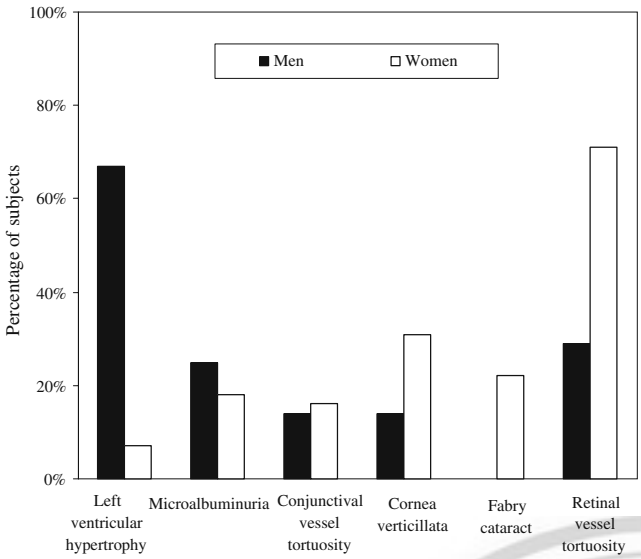

Fig. 3 Prevalence of individual abnormalities in men (n=22) and women (n=72) with late-onset Fabry mutation IVS4+919G→A

women under 40 years of age (p<0.005) and developed progressively (r=0.588, p<0.01).Microalbuminuria or higher levels of proteinuria were found in 17 subjects (20% of 86), including 5 men (25%) and 12 women (18%; Table 1). There was no significant difference between its presence in men (25%) and women (30%) older than 40 (p=0.700), and between women older and younger than 40 (p=0.06). However, (micro)albuminuria or proteinuria developed progressively in women (r=0.281, p<0.05).

At least one Fabry-related ocular manifestation was present in 41 subjects (79% of subjects examined); in 43% of men and 84% of women. Ocular abnormalities included retinal vessel tortuosity (29%, 71%, respectively), cornea verticillata (14%, 31%), Fabry cataract (0%, 22%) and conjunctival vessel tortuosity (14%, 16%) (Table 1, Fig. 3). There were no statistically significant differences between genders or age categories. The examinations were mostly performed by PKL (79%), whereas 21% of the subjects were examined by other ophthalmologists at the ophthalmology outpatient clinic.

Discussion

The natural history of early-onset "classic" Fabry disease is well documented in the literature (Desnick et al. 2001; Zarate and Hopkin 2008). Cases of late-onset forms of Fabry disease have been reported but, to date, there are no reports of clinical findings in sizeable cohorts of patients. This is the first report describing the clinical features in both male and female patients carrying the IVS4+919G→A mutation in the GLA gene. We confirm a high prevalence of cardiovascular, renal, and ocular manifestations associated with Fabry disease in these Taiwan Chinese adult subjects, including women. Similar to the findings of Ishii et al. (2002) of ~10% residual α-Gal A activity in lymphocytes from patients hemizygous for the IVS4+919G→A mutation, the mean enzyme activity in the 22 men in our study was 10.4% of normal. Our study is the first to report α-Gal A activities in heterozygous women with the IVS4+919G/A mutation, i.e. 48.6% of the normal mean (n=72), and 14 women (19.4%) had normal α-Gal A enzyme activity (normal range: 7.9–16.9 nmol/h/mL plasma; Desnick et al. 1973; Sheu et al. 1994).

Among subjects over 40 years of age, 67% (14/21) of men and 20% (5/25) of women had LVH. The high

Table 2 Prevalence of ocular manifestations of classic Fabry disease in various populations compared with Taiwan Chinese with a late-onset Fabry disease gene

References	Area	Gender	Ocular manifestations			
			Conjunctival vessel tortuosity (%)	Cornea verticillata (%)	Fabry cataract (%)	Retinal vessel tortuosity (%)
Sher et al. 1979	USA	37 males	78	94.5	37	70
		25 females	46	88	14	25
Orssaud et al. 2003	France	32 males	68.7	43.7	37.5	56.2
Nguyen et al. 2005	Australia	34 males	97.1	94.1	11.8	76.5
		32 females	78.1	71.9	0	18.8
Sodi et al. 2007	10 European countries[a]	91 males	NR	73.1	23.1	NR
		82 females	NR	76.9	9.8	NR
Present study	Taiwan	7 males	14	14	0	29
		45 females	16	31	22	71

NR Not reported

[a] The majority of the patients originated from Italy (n=33), the UK (n=28), Spain (n=26) and Norway (n=23)

incidence in men is consistent both with the study from Japan and our earlier investigation (Ishii et al. 2002; Lin et al. 2009). However, the present study also revealed a substantial number of women over 40 with the mutation who also had LVH. Our study was not designed to rule out other causes of LVH, so we cannot conclusively state that these individuals in fact had late-onset Fabry disease as a cause of their cardiac abnormality. However, we have previously found some cases of hypertrophic cardiomyopathy in which the patients carried this mutation (Lin et al. 2009). In a population with a relatively high incidence of this genotype, perhaps gene testing should be considered in patients who appear to have idiopathic hypertrophic cardiomyopathy.

Microalbuminuria was also relatively common in our subjects who were tested, one quarter of the men and nearly a third of the women over 40 years of age. As with LVH, it is possible that they may have had latent renal disease from other causes. But our study suggests that late-onset Fabry disease belongs in the differential diagnosis for these individuals.

Ocular findings are also among the early hallmarks of Fabry disease (Nguyen et al. 2005; Orssaud et al. 2003; Sher et al. 1979; Sodi et al. 2007) and readily detectable by slit lamp examination. Progressive deposition of GL-3 in ocular structures often leads to cornea verticillata (vortex keratopathy), changes of conjunctival and retinal vessels (dilatation, tortuosity, aneurysms) or lenticular changes (a "spoke-like" pattern at the level of the posterior capsule, usually referred to as "Fabry cataract"). Most women (84%) and less than half (43%) of men had at least one of these ocular manifestations. The prevalences of Fabry cataract (22%) and retinal vessel tortuosity (71%) among females were surprisingly high as compared to previous reports (Table 2). It remains to be elucidated if there is an ethnic predilection for these types of ocular abnormalities in the Taiwan Chinese Fabry patient population, or specifically in subjects with the IVS4+919G→A mutation. The prevalence of cornea verticillata was considerably lower (14% of men, 31% of women) as compared with the overall gender-specific prevalences of ~75% reported by other groups (Table 2). This may support the belief that the IVS4+919G→A mutation is a rather mild pathogenic mutation.

Our findings demonstrate that the phenotype associated with this mutation cannot be accurately predicted from the genotype alone. As expected, men who were hemizygous for IVS4+919G→A had lower enzyme activity than did women who were heterozygous. Further investigations are needed to identify genes or other factors that modify the clinical expression of late-onset Fabry disease related to this mutation.

Enzyme replacement therapy has been used to treat Fabry disease and experience reveals that early medical intervention provides a better clinical outcome (Banikazemi et al. 2007; Weidemann et al. 2009; Wraith et al. 2008). This leaves little doubt that early detection and timely therapy are important for patients with classic Fabry disease. These paradigms are also applicable for patients with the late-onset mutation IVS4+919G→A as cardiovascular, renal and ocular manifestations are highly prevalent among these individuals. Our data contribute to the understanding of the clinical course of this late-onset variant and provide a rational for modification of current follow up and therapeutic intervention strategies.

Limitations

Fabry disease is an X-linked lysosomal storage disorder, but we had relatively few men in our sample. As subjects were selected based on the family pedigree of neonates found to have the IVS4+919G→A mutation, most were young mothers or maternal grandparents. Half were women younger than 40. It would be good to study larger groups of men, especially those younger than 40. Another limitation is the lack of complete data for all of our subjects, as they were not uniformly able to follow through on all the examinations.

Conclusion

This study documents a high prevalence of cardiovascular, renal, and ocular manifestations in Taiwan-Chinese adult subjects with Fabry mutation IVS4+919G→A. This hot-spot mutation has been described as a "cardiac variant" mutation, but our data demonstrate that the clinical manifestations are not confined only to the heart. Although more detailed data on the longitudinal progression of the disease will be required, our findings will be helpful in determining the necessity and timing of therapeutic intervention with enzyme replacement therapy.

Acknowledgements We would like to express our sincere thanks to Dr. Hans Ebels for his critical review and valuable comments and Ms. Tsai-Feng Ho for her professional assistance in biostatistics. This work was supported by Taipei Veterans General Hospital (V99C1-147).

References

Banikazemi M, Bultas J, Waldek S et al (2007) Agalsidase-beta therapy for advanced Fabry disease: a randomized trial. Ann Intern Med 146:77–86

Deegan P, Bähner AF, Barba-Romero MA, Hughes D, Kampmann C, Beck M (2006) Natural history of Fabry disease in females in the Fabry Outcome Survey. J Med Genet 43:347–352

Desnick RJ, Allen KY, Desnick SJ, Raman MK, Bernlohr RW, Krivit W (1973) Fabry's disease: enzymatic diagnosis of hemizygotes and heterozygotes. Alpha-galactosidase activities in plasma, serum, urine, and leukocytes. J Lab Clin Med 81:157–171

Desnick RJ, Ioannou YA, Eng CM (2001) Alpha-Galactosidase a deficiency: fabry disease. In: Scriver CR, Beaudet AL, Sly WS, Valle D (eds); Childs B, Kinzler KW, Vogelstein B (assoc eds). The metabolic and molecular bases of inherited disease, 8th edn. McGraw-Hill, New York, pp 3733–3774

Hwu WL, Chien YH, Lee NC et al (2009) Newborn screening for Fabry disease in Taiwan reveals a high incidence of the later-onset GLA mutation c.936+919G>A (IVS4+919G>A). Hum Mutat 30:1397–1405

Ishii S, Nakao S, Minamikawa-Tachino R, Desnick RJ, Fan JQ (2002) Alternative splicing in the alpha-galactosidase A gene: increased exon inclusion results in the Fabry cardiac phenotype. Am J Hum Genet 70:994–1002

Kotanko P, Kramar R, Devrnja D et al (2004) Results of a nationwide screening for Anderson-Fabry disease among dialysis patients. J Am Soc Nephrol 15:1323–1329

Levy D, Savage DD, Garrison RJ, Anderson KM, Kannel WB, Castelli WP (1987) Echocardiographic criteria for left ventricular hypertrophy: the Framingham Heart Study. Am J Cardiol 59:956–960

Lin HY, Chong KW, Hsu JH et al (2009) High incidence of the cardiac variant of Fabry disease revealed by newborn screening in the Taiwan Chinese population. Circ Cardiovasc Genet 2:450–456

Meikle PJ, Hopwood JJ, Clague AE, Carey WF (1999) Prevalence of lysosomal storage disorders. JAMA 281:249–254

Monserrat L, Gimeno-Blanes JR, Marín F et al (2007) Prevalence of Fabry disease in a cohort of 508 unrelated patients with hypertrophic cardiomyopathy. J Am Coll Cardiol 50:2399–2403

Nakao S, Takenaka T, Maeda M et al (1995) An atypical variant of Fabry's disease in men with left ventricular hypertrophy. N Engl J Med 333:288–293

Nakao S, Kodama C, Takenaka T et al (2003) Fabry disease: detection of undiagnosed hemodialysis patients and identification of a "renal variant" phenotype. Kidney Int 64:801–807

National Kidney Foundation (2002) K/DOQI clinical practice guidelines for chronic kidney disease: evaluation, classification, and stratification. Am J Kidney Dis 39:S1–S266

Nguyen TT, Gin T, Nicholls K, Low M, Galanos J, Crawford A (2005) Ophthalmological manifestations of Fabry disease: a survey of patients at the Royal Melbourne Fabry Disease Treatment Centre. Clin Experiment Ophthalmol 33:164–168

Orssaud C, Dufier J, Germain D (2003) Ocular manifestations in Fabry disease: a survey of 32 hemizygous male patients. Ophthalmic Genet 24:129–139

Rolfs A, Böttcher T, Zschiesche M et al (2005) Prevalence of Fabry disease in patients with cryptogenic stroke: a prospective study. Lancet 366:1794–1796

Sachdev B, Takenaka T, Teraguchi H et al (2002) Prevalence of Anderson-Fabry disease in male patients with late onset hypertrophic cardiomyopathy. Circulation 105:1407–1411

Shabbeer J, Robinson M, Desnick RJ (2005) Detection of alpha-galactosidase a mutations causing Fabry disease by denaturing high performance liquid chromatography. Hum Mutat 25:299–305

Shabbeer J, Yasuda M, Benson SD, Desnick RJ (2006) Fabry disease: identification of 50 novel alpha-galactosidase A mutations causing the classic phenotype and three-dimensional structural analysis of 29 missense mutations. Hum Genomics 2:297–309

Sher NA, Letson RD, Desnick RJ (1979) The ocular manifestations in Fabry's disease. Arch Ophthalmol 97:671–676

Sheu SS, Chan LP, Liao SC et al (1994) Fabry's disease: clinical, pathologic and biochemical manifestations in two Chinese males. Zhonghua Yi Xue Za Zhi 54:368–372

Sodi A, Ioannidis AS, Mehta A, Davey C, Beck M, Pitz S (2007) Ocular manifestations of Fabry's disease: data from the Fabry Outcome Survey. Br J Ophthalmol 91:210–214

Tanaka M, Ohashi T, Kobayashi M et al (2005) Identification of Fabry's disease by the screening of alpha-galactosidase a activity in male and female hemodialysis patients. Clin Nephrol 64:281–287

Wang RY, Lelis A, Mirocha J, Wilcox WR (2007) Heterozygous Fabry women are not just carriers, but have a significant burden of disease and impaired quality of life. Genet Med 9:34–45

Weidemann F, Niemann M, Breunig F et al (2009) Long-term effects of enzyme replacement therapy on Fabry cardiomyopathy: evidence for a better outcome with early treatment. Circulation 119:524–529

Wilcox WR, Oliveira JP, Hopkin RJ et al (2008) Females with Fabry disease frequently have major organ involvement: lessons from the Fabry Registry. Mol Genet Metab 93:112–128

Wraith JE, Tylki-Szymanska A, Guffon N et al (2008) Safety and efficacy of enzyme replacement therapy with agalsidase beta: an international, open-label study in pediatric patients with Fabry disease. J Pediatr 152:563–570

Zarate YA, Hopkin RJ (2008) Fabry's disease. Lancet 372:1427–1435

Activation of Silenced Tumor Suppressor Genes in Prostate Cancer Cells by a Novel Energy Restriction-Mimetic Agent

Hsiang-Yu Lin,[1,2,3] Yi-Chiu Kuo,[1] Yu-I Weng,[4] I-Lu Lai,[1] Tim H.-M. Huang,[4] Shuan-Pei Lin,[3] Dau-Ming Niu,[2,5]** and Ching-Shih Chen[1]*

[1]*Division of Medicinal Chemistry, College of Pharmacy, The Ohio State University, Columbus, Ohio*
[2]*Institute of Clinical Medicine, National Yang-Ming University, Taipei, Taiwan*
[3]*Department of Pediatrics, Mackay Memorial Hospital and Mackay Medicine, Nursing and Management College, Taipei, Taiwan*
[4]*Human Cancer Genetics Program, The Ohio State University, Columbus, Ohio*
[5]*Department of Pediatrics, Taipei Veterans General Hospital, Taipei, Taiwan*

BACKGROUND. Targeting tumor metabolism by energy restriction-mimetic agents (ERMAs) has emerged as a strategy for cancer therapy/prevention. Evidence suggests a mechanistic link between ERMA-mediated antitumor effects and epigenetic gene regulation.
METHODS. Microarray analysis showed that a novel thiazolidinedione-derived ERMA, CG-12, and glucose deprivation could suppress DNA methyltransferase (DNMT)1 expression and reactivate DNA methylation-silenced tumor suppressor genes in LNCaP prostate cancer cells. Thus, we investigated the effects of a potent CG-12 derivative, CG-5, vis-à-vis 2-deoxyglucose, glucose deprivation and/or 5-aza-deoxycytidine, on DNMT isoform expression (Western blotting, RT-PCR), DNMT1 transcriptional activation (luciferase reporter assay), and expression of genes frequently hypermethylated in prostate cancer (quantitative real-time PCR). Promoter methylation was assessed by pyrosequencing analysis. SiRNA-mediated knockdown and ectopic expression of DNMT1 were used to validate DNMT1 as a target of CG-5.
RESULTS. CG-5 and glucose deprivation upregulated the expression of DNA methylation-silenced tumor suppressor genes, including *GADD45a*, *GADD45b*, *IGFBP3*, *LAMB3*, *BASP1*, *GPX3*, and *GSTP1*, but also downregulated methylated tumor/invasion-promoting genes, including *CD44*, *S100A4*, and *TACSTD2*. In contrast, 5-aza-deoxycytidine induced global reactivation of these genes. CG-5 mediated these epigenetic effects by transcriptional repression of DNMT1, which was associated with reduced expression of Sp1 and E2F1. SiRNA-mediated knockdown and ectopic expression of DNMT1 corroborated DNMT1's role in the modulation of gene expression by CG-5. Pyrosequencing revealed differential effects of CG-5 versus 5-aza-deoxycytidine on promoter methylation in these genes.

Additional supporting information may be found in the online version of this article.

Grant sponsor: National Institutes of Health; Grant number: CA112250; Grant sponsor: Department of Defense Prostate Cancer Research Program; Grant number: W81XWH-09-0198; Grant sponsor: National Science Council, Taiwan.

The authors declare no conflicts of interest.

*Correspondence to: Dr. Ching-Shih Chen, College of Pharmacy, The Ohio State University, 500 West 12th Avenue, Columbus, OH 43210. E-mail: chen.844@osu.edu

**Correspondence to: Dau-Ming Niu, Department of Pediatrics, Taipei Veterans General Hospital, No. 201, Section 2, Shih-Pai Road, Taipei 112, Taiwan. E-mail: dmniu1111@yahoo.com.tw

Received 2 December 2011; Accepted 30 March 2012
DOI 10.1002/pros.22530
Published online in Wiley Online Library (wileyonlinelibrary.com).

CONCLUSIONS. These findings reveal a previously uncharacterized epigenetic effect of ERMAs on DNA methylation-silenced tumor suppressor genes, which may foster novel strategies for prostate cancer therapy. *Prostate* © 2012 Wiley Periodicals, Inc.

KEY WORDS: **energy restriction-mimetic agent; prostate cancer; energy restriction; DNA methyltransferases; epigenetics**

INTRODUCTION

Cells undergoing malignant transformation often exhibit a shift in cellular metabolism from oxidative phosphorylation to glycolysis, known as the Warburg effect, to gain growth advantage in the microenvironment [1,2]. This enhanced glycolysis appears to be attributable to the dysregulation of multiple oncogenic signaling pathways [1], including those mediated by hypoxia-inducible factor 1 [3], Akt [4], c-Myc [5], and p53 [6], and enables cancer cells to adapt to low-oxygen environments, to produce biosynthetic building blocks needed for cell proliferation, to acidify the local environment to facilitate tumor invasion, and to generate NADPH and glutathione through the pentose phosphate shunt to increase resistance to oxidative stress [1,2]. The Warburg effect is considered to be a fundamental property of neoplasia, and constitutes the basis for tumor imaging by [^{18}F]2-fluoro-2-deoxyglucose positron emission tomography [7]. From a therapeutic perspective, targeting glycolysis represents a relevant strategy for cancer prevention and treatment [2], of which the proof-of-concept is provided by the effective suppression of carcinogenesis in various animal models by dietary caloric restriction and natural product-based energy restriction-mimetic agents (ERMAs), such as 2-deoxyglucose (2-DG) and resveratrol.

Previously, based on the scaffold of thiazolidinediones, we developed a novel class of ERMAs, as represented by CG-12, that mimic the ability of 2-DG and glucose deprivation to elicit starvation-like cellular responses with high potency in cancer cells through the inhibition of glucose uptake [8]. The suppression of energy metabolism by CG-12 leads to an intricate signaling network mediated by silent information regulator 1, AMP-activated protein kinase, and oxidative stress, the interplay among which culminates in autophagy and apoptosis in cancer cells. More recently, we demonstrated an epigenetic effect of CG-12 in cancer cells involving histone acetylation and H3 lysine 4 methylation, leading to the transcriptional activation of Kruppel-like factor 6 (*KLF6*) and a series of proapoptotic genes [9]. In this study, we report the unique ability of CG-5, a structurally optimized CG-12 derivative (Fig. 1A) to suppress the expression of DNA methyltransferase (DNMT)1 and DNMT3A in prostate cancer cells, resulting in the reactivation of a series of DNA methylation-silenced tumor suppressor genes. Pyrosequencing analysis indicates that this effect was attributable to hypomethylation in the promoter regions of these tumor suppressor genes. In light of the important role of aberrant DNA methylation in carcinogenesis [10], our findings underscore the translational potential of this novel class of glucose uptake inhibitors in prostate cancer prevention and therapy.

MATERIALS AND METHODS

Detailed information on materials, reagents, their commercial sources, and experimental procedures are available in Supplementary Information.

Microarray Analysis

Total RNA isolated from LNCaP cells exposed to 10 μM CG-12 or glucose-depleted medium for 48 hr was submitted to the Microarray Shared Resource at The Ohio State University Comprehensive Cancer Center for microarray analysis of gene expression.

Glucose Uptake Assay

This assay was performed as we described previously [8] with modifications. Specifically, LNCaP cells were treated with test agents for 1.5 hr, followed by exposure to [^{3}H]2-DG in the presence of excess non-radioactive 2-DG for 30 min.

Cell Viability Assay

Cell viability was determined using the 3-(4,5-dimethylthiazol-2-yl)-2,5-diphenyltetrazolium bromide (MTT) assay as we described previously [8].

RNA Interference and Luciferase Reporter Assay

For siRNA experiments, cells were transfected with scrambled or DNMT1-specific siRNA. Knockdown of DNMT1 was confirmed by immunoblotting. For the DNMT1 promoter-luciferase reporter assay, luciferase activities were determined with the dual-luciferase system, which uses co-transfected herpes simplex virus thymidine kinase promoter-driven *Renilla reniformis* luciferase as an internal control.

Western Blotting

Western blotting was performed as described previously [8]. Relative differences in protein levels

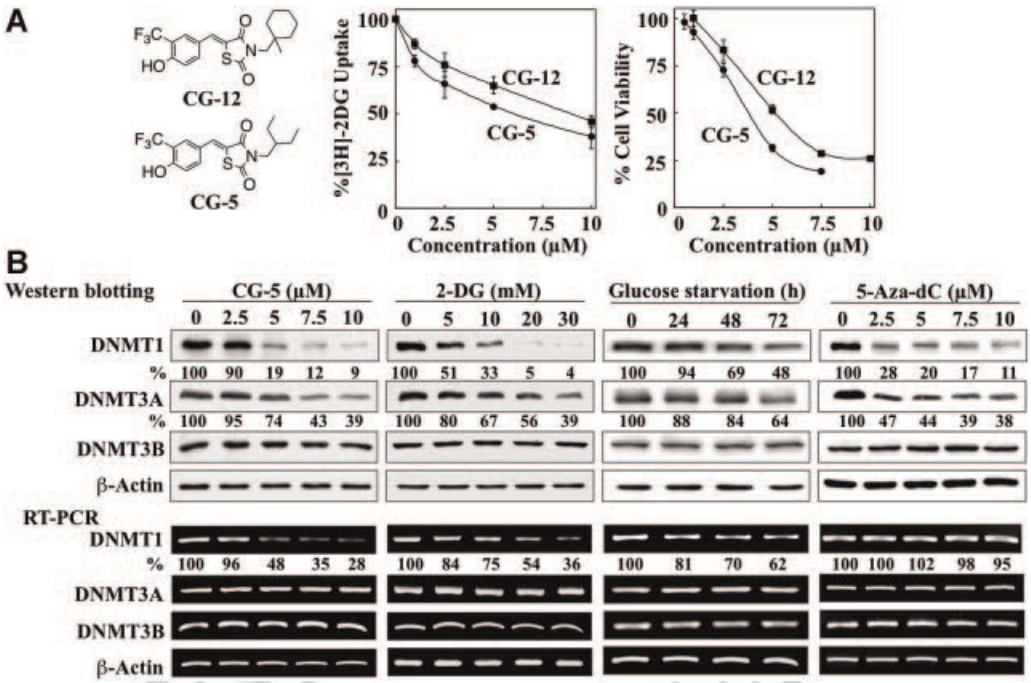

Fig. 1. CG-5, 2-DG, glucose starvation and 5-aza-dC differentially affect the expression levels of DNMT isoforms. **A**: **Left**, structures of CG-12 and CG-5. Center, dose-dependent inhibitory effects of CG-5 versus CG-12 on the uptake of [^{3}H]-2DG into LNCaP cells after 30 min of treatment. Point, mean; bars, SD (n = 3). **Right**, dose-dependent inhibitory effects of CG-5 versus CG-12 on the viability of LNCaP cells by MTT assays after 72 hr of treatment. Point, mean; bars, SD (n = 6). **B**: LNCaP cells were treated with CG-5, 2-DG, and 5-aza-dC at the indicated concentrations in 10% FBS-supplemented medium for 48 hr or glucose-free medium for various time intervals. The expression levels of DNMT1, DNMT3A and DNMT3B were determined by Western blotting (**upper**) and RT-PCR (**lower**). The percentages denote the relative intensities of mRNA and protein bands of treated samples to those of the respective DMSO vehicle-treated controls after normalization to the respective internal reference β-actin. Each value represents the average of three independent experiments.

among experimental groups were determined by densitometry.

DNA Methylation Analysis by Pyrosequencing

To determine methylation levels of candidate genes in response to drug treatment or glucose deprivation, the Pyrosequencing System (Qiagen) was used to detect methylated CpG sites in sequencing reactions [11].

Statistical Analysis

Data from quantitative real time (qRT)-PCR, luciferase reporter assays and pyrosequencing were analyzed using Student's *t*-test. Differences between group means were considered significant at $P < 0.05$.

RESULTS

Microarray Analysis Reveals the Suppression of *DNMT1* and *DNMT3A* Expression and the Upregulation of Methylation-Silenced Genes by Energy Restriction in Prostate Cancer Cells

Pursuant to our hypothesis that energy restriction mediates antitumor effects, in part, through epigenetic gene regulation, we examined the effect of 10 μM CG-12 versus glucose depletion on global gene expression in LNCaP cells via cDNA microarray analysis after 48 hr of treatment. This microarray analysis showed that both treatments significantly reduced the gene expression of *DNMT1*, accompanied by a modest, but statistically significant, decrease in *DNMT3B* expression and no change in *DNMT3A* levels (Table I).

The ability of CG-12 and glucose starvation to downregulate DNMT expression suggests a mechanistic link between energy restriction and epigenetic regulation of gene expression through changes in DNA methylation. Previously, a global survey of DNA methylation patterns in prostate cancer cell lines identified a number of cancer-related genes that were transcriptionally silenced due to aberrant promoter hypermethylation [12]. Based on this report, we examined the microarray data for the effect of CG-12 versus glucose depletion on the expression of 13 genes reported to be silenced by DNA methylation (Table II). Among these, *BASP1*, *GADD45a*, *GADD45b*, *GPX3*, *GSTP1*, *IGFBP3*, *KRT7*, *LAMB3*, *PDLIM4*, and *THBS1* are tumor-suppressive genes, whereas *CD44*, *S100A4*, and *TACSTD2* have been

TABLE I. Microarray Analyses of the Effects of 10 μM CG-12 Versus Glucose Depletion on the Expression of DNMTs in LNCaP Cells After 48 hr of Treatment

	10 μM CG-12		Glucose depletion	
Gene name	Fold change	*P*-value	Fold change	*P*-value
DNMT1	−2.208398	5.32E−06	−2.1143294	6.45E−07
DNMT3A	−1.023485	0.690570233	−1.0391039	0.404186671
DNMT3B	−1.468048	0.001498209	−1.3947437	2.82E−04

associated with tumorigenesis or aggressive phenotype of prostate cancer [13–15]. It is noteworthy that CG-12 mimicked the ability of glucose starvation to activate the expression of *GADD45a*, *GADD45b*, and *IGFBP3*, while many other genes examined were not affected by either treatment, with the exception of *THBS1*, which was upregulated by CG-12.

Energy Restriction Suppresses the Expression of DNMT1 and DNMT3A Through Transcriptional Repression and Proteasomal Degradation, Respectively

Our efforts to structurally optimize CG-12 led to the identification of CG-5, an active derivative in which the terminal methylcyclohexyl ring was replaced by a 3-pentyl moiety. This simple modification improved the potency of CG-5 relative to CG-12 in suppressing [^{3}H]-2DG uptake (IC_{50}, 6 μM vs. 9 μM) and cell viability (IC_{50}, 4.5 μM vs. 6 μM) in LNCaP cells (Fig. 1A). Consequently, we used CG-5 to validate our microarray data by examining the dose-dependent suppressive effects of CG-5 and 2-DG vis-à-vis glucose starvation on the expression of DNMT1, DNMT3A, and DNMT3B, at both protein and mRNA levels, in LNCaP cells. In addition, the DNMT inhibitor 5-aza-dC was used as a control in light of its reported activity in suppressing DNMT1 expression via proteasomal degradation [27,28], and, to a lesser extent, DNMT3A through a yet unidentified mechanism [29].

Western blot analysis indicated that CG-5, 2-DG, and glucose depletion shared with 5-aza-dC the ability to decrease the expression levels of DNMT1 and, to a lesser extent, DNMT3A in a dose- or time-dependent manner (Fig. 1B, upper panel). Nevertheless, the mechanism underlying energy restriction-facilitated downregulation of DNMT1 was different from that of 5-aza-dC as CG-5, 2-DG, and glucose starvation decreased DNMT1 mRNA levels, while no significant changes were noted in response to 5-aza-dC (Fig. 1B, lower panel). In addition, consistent with the microarray findings, no changes in the mRNA level of DNMT3A were noted in response to any of these treatments, suggestive of a posttranslational effect on protein levels. As for DNMT3B, neither the protein nor mRNA expression level was affected by any of the treatments, which contrasted with the microarray data that showed a modest decrease in DNMT3B gene expression in response to energy restriction (Table I). This discrepancy might have arisen from inherent systematic errors associated with microarrays [30].

To examine the mechanism by which CG-5 suppressed the mRNA expression of DNMT1, we assessed its effect on the promoter activity of DNMT1 by using a DNMT1 promoter-luciferase reporter construct. As shown, CG-5 diminished the luciferase activity in a dose-dependent manner (Fig. 2A), suggesting that CG-5 suppressed DNMT1 expression through transcriptional repression. As the core promoter region of *DNMT1* contains three Sp1 [31] and four E2F [32] binding sites, we examined the effect of CG-5 on the expression of these transcription factors and their target genes, androgen receptor (AR) for Sp1 [33], and cyclins E and D3 for E2F1 [34,35].

In line with our previous findings with CG-12 [8,9], CG-5 facilitated a dose-dependent decrease in Sp1 protein level without affecting mRNA expression, suggestive of proteasomal degradation (Fig. 2B). It is noteworthy that the expression of E2F1, at both protein and mRNA levels, was also reduced suggesting a different mode of regulation from that of Sp1. Moreover, decreases in the expression of Sp1 and E2F1 were accompanied by parallel decreases in the expression of their respective targets, namely AR and cyclins D3 and E (Fig. 2B).

As for the CG-5-mediated inhibition of DNMT3A protein expression, a role for proteasomal degradation was supported by the ability of the proteasome inhibitor MG-132 to rescue DNMT3A protein expression from drug-induced suppression in LNCaP cells (Fig. 2C).

Similar findings regarding the ability of CG-5 to suppress the expression of DNMT1 and DNMT3A without disturbing that of DNMT3B was also noted

TABLE II. Microarray Analyses of the Effects of 10 μM CG-12 Versus Glucose Depletion on the Expression of 13 DNA Methylation-Silenced Genes in LNCaP Cells After 48 hr of Treatment

Gene name	Gene description	Molecular function	CG-12	Glucose depletion
			Fold change (*P*-value)	
BASP1 (NM_006317_1)	Brain acid soluble protein 1	Inhibition of Myc-induced cell transformation; a potential tumor suppressor [16]	1.182303151 (0.027893026)	0.920825697 (0.307789115)
CD44 (NM_000610_1)	Receptor for hyaluronic acid	Cell adhesion; markers for breast and prostate cancer stem cells [15]	n/a	n/a
GADD45a (NM_001924-1)	Growth arrest and DNA-damage-inducible protein 45a	Apoptosis, cell cycle arrest, and DNA repair; tumor suppressive [17]	5.838104359 (3.73E−10)	3.11320375 (1.21E−08)
GADD45b (AL050044_1)	Growth arrest and DNA-damage-inducible protein 45b	Apoptosis, cell cycle arrest, and DNA repair; reported tumor suppressor in hepatocellular carcinoma [18]	5.333934097 (2.01E−08)	4.483731849 (5.37E−09)
GPX3 (NM_002084)	Glutathione peroxidase 3	Maintaining genomic integrity via the detoxification of reactive oxygen species; tumor suppressive [19]	1.089147993 (0.370942845)	0.946090435 (0.352881698)
GSTP1 (NM_000852_1)	Glutathione *S*-transferase pi	Conjunction and detoxification of carcinogens; tumor suppressive [20]	1.192508872 (0.028969162)	0.952208888 (0.362806007)
IGFBP3 (NM_000598_1)	Insulin-like growth factor binding protein 3	Inhibiting cancer cell proliferation, adhesion, motility, and metastasis; tumor suppressive [21,22]	5.195274579 (4.89E−08)	2.137167525 (4.50E−07)
KRT7 (NM_005556_1)	Keratin 7	Cytoskeletal organization and biogenesis [12]	1.241685666 (0.018831416)	1.04298615 (0.622715314)
LAMB3 (NM_000228_1)	Laminin, b3	A component of the extracellular matrix involved in cell adhesion, growth, migration, proliferation, and differentiation; tumor suppressive [23]	n/a	1.22357285 (0.031432552)
PDLIM4 (NM_003687_1)	PDZ and LIM domain 3	An actin-binding protein; tumor suppressive [24]	0.993684661 (0.94564817)	0.981663174 (0.801008691)
S100A4 (NM_019554_1)	S100 calcium-binding protein A4	A Ca^{2+}-binding protein; promoting metastasis [25]	0.900563555 (0.217905821)	0.933789972 (0.206088795)
TACSTD2 (NM_002353_1)	Tumor-associated calcium signal transducer 2	A marker of human prostate basal cells with stem cell characteristics; promoting tumorigenesis and invasion [13]	n/a	0.907644973 (0.10922003)
THBS1 (NM_003246_1)	Thrombo-spondin-1	Cell adhesion and motility; a p53 and Rb regulated angiogenesis inhibitor; tumor suppressive [26]	2.609367236 (8.89E−08)	0.986198525 (0.755628795)

n/a: Gene was not listed in the array results.

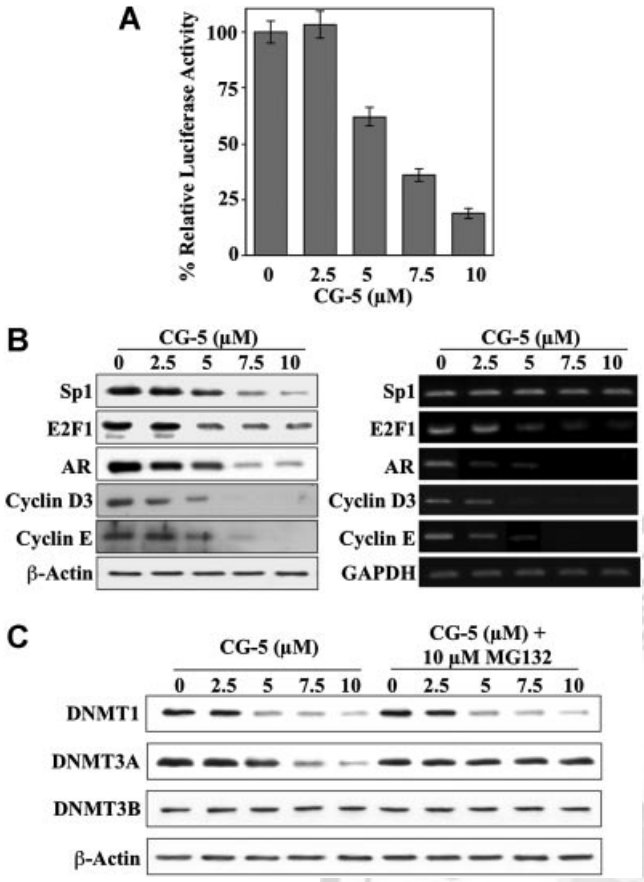

Fig. 2. CG-5 suppresses the expression of DNMT1 and DNMT3A through transcriptional repression and proteasomal degradation, respectively. **A**: Dose-dependent, suppressive effect of CG-5 on DNMT1 promoter activity. LNCaP cells were transiently transfected with the DNMT1 promoter-luciferase reporter plasmid pGL3-DNMT1-Luc, and exposed to CG-5 at the indicated concentrations or DMSO vehicle control in 10% FBS-containing medium for 48 hr. Column, mean (n = 3); error bars, SD. **B**: Parallel Western blot and RT-PCR analyses of the dose-dependent suppressive effect of CG-5 on the expression levels of Sp1, E2F1, AR, and cyclins D3 and E. **C**: The proteasome inhibitor MG132 protected cells from CG-5-induced ablation of DNMT3A, but not DNMT1. LNCaP cells were treated with CG-5 at the indicated concentrations for 36 hr, followed by co-treatment with 10 μM MG132 for an additional 12 hr. Cell lysates were analyzed by immunoblotting for DNMT1 and -3A.

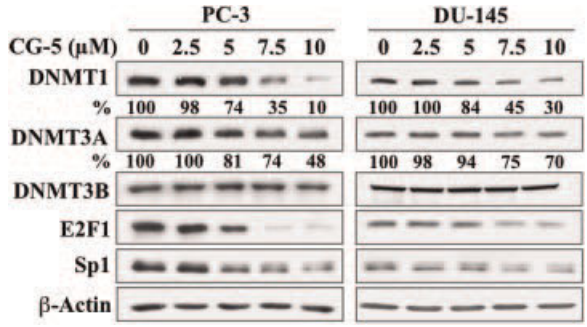

Fig. 3. Western blot analysis of the dose-dependent effects of CG-5 on the expression of DNMT1, DNMT3A, DNMT3B, E2F1, and Sp1 in PC-3 and DU-145 cells. Cells were treated with CG-5 at the indicated concentrations for 48 hr. The percentages denote the relative intensities of protein bands of treated samples to those of the respective DMSO vehicle-treated controls after normalization to the respective internal reference β-actin. Each value represents the average of three independent experiments.

in PC-3 and DU-145 cells (Fig. 3), indicating that this was not a cell line-specific effect. Moreover, the drug's effect on DNMT1 expression correlated with that on E2F1 and Sp1 expression in a dose-dependent manner, suggestive of a causal relationship.

Differential Effects of Energy Restriction on the Activation of DNA Methylation-Silenced Genes

The 13 DNA methylation-silenced genes previously evaluated by microarray analysis (Table II) were assessed by qRT-PCR for changes in expression in response to energy restriction. LNCaP cells were exposed to 5 μM CG-5 or 5 μM 5-aza-dC in 10% FBS-supplemented RPMI 1640 medium for 48 or 72 hr, or to 10% FBS-supplemented glucose-free medium for 72 hr. qRT-PCR analysis indicates that these treatments led to distinct patterns of activation of these epigenetically silenced genes (Fig. 4). 5-Aza-dC mediated varying degrees of activation of 12 of the 13 genes examined relative to the DMSO control (at 72 hr: *GSTP1*, 510-fold; *KRT7*, 295-fold; *CD44*, 26-fold; *TACSTD2*, 23-fold; *BASP1*, 12-fold; *LAMB3*, 10-fold; *IGFBP3*, 9-fold; *GPX3*, *S100A4*, and *THBS1*, 8-fold; *PDLIM4* and *GADD45a*, 3-fold), while no significant change in *GADD45b* mRNA expression was noted (Fig. 4A). In contrast, CG-5 activated 7 of the 13 genes with a distinct preference for the two DNA damage response genes *GADD45a* and *GADD45b* (81- and 31-fold, respectively), followed by *IGFBP3* (12-fold), *LAMB3* (11-fold), *BASP1* (9-fold), *GPX3* (5-fold), and *GSTP1* (2-fold) at 72 hr, while only modest increases (<2-fold) in the expression of *KRT7* and *THBS1* were noted (Fig. 4B). Moreover, CG-5 downregulated the mRNA levels of *PDLIM4*, *S100A4*, and *TACSTD2* by 97%, 56%, and 95%, respectively. Although CG-5 caused a modest, but statistically insignificant, increase in *CD44* mRNA expression at 48 hr (1.16-fold), the treatment led to a 54% decrease ($P < 0.05$) at 72 hr. It is noteworthy that two of these downregulated genes, *S100A4* and *TACSTD2*, are associated with the promotion of tumorigenesis, tumor invasion, and metastasis [13,25], and that CD44 represents a putative marker for prostate cancer stem cells [36].

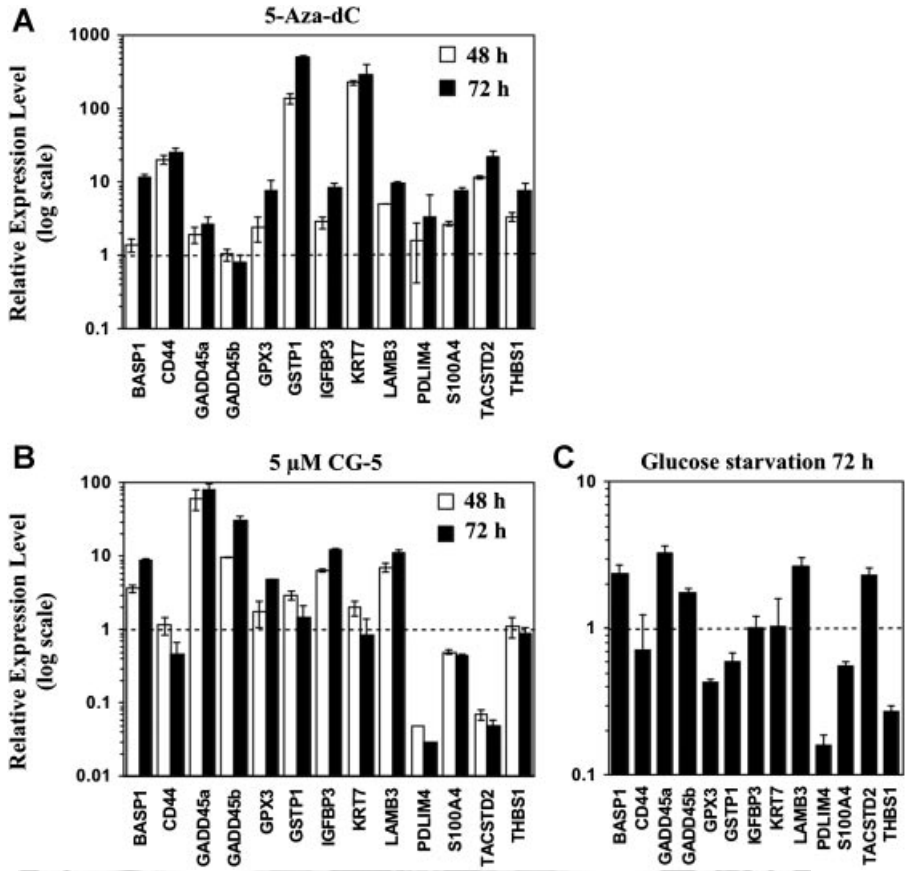

Fig. 4. Effects of 5-aza-dC, CG-5, and glucose deprivation on the expression levels of methylation-silenced cancer-related genes. LNCaP cells were treated with (**A**) 5 μM CG-5 or (**B**) 5 μM 5-aza-dC in 10% FBS-supplemented medium for 48 or 72 hr, or with (**C**) glucose-depleted medium for 72 hr. The expression levels of 13 target genes reported to be silenced by DNA hypermethylation in prostate cancer cells were quantitated by qRT-PCR. Column, mean (n = 3); error bars, SD.

As compared to CG-5-induced energy restriction, glucose deprivation showed a qualitatively similar, but muted effect on gene activation, which, in part, may be reflective of smaller decreases in the expression levels of DNMT1 and DNMT3A. Glucose-depleted medium shared the ability of CG-5 to activate *GADD45a* (3.3-fold), *LAMB3* (2.7-fold), *BASP1* (2.4-fold), and *GADD45b* (1.8-fold), as well as to downregulate the expression of *PDLIM4* and *S100A4*, while having no significant impact on the mRNA expression of *CD44* and *KRT7* (Fig. 4C). However, in contrast to CG-5, glucose deprivation diminished the mRNA expression of *GPX3*, *GSTP1*, and *THBS1*, and increased that of *TACSTD2*.

Role of DNMT1 Downregulation in CG-5-Facilitated Activation of Epigenetically Silenced Genes

Given the greater suppressive effect of CG-5 on DNMT1 expression than on that of DNMT3A (81% and 26%, respectively; Fig. 1B, upper panel), we rationalized that DNMT1 downregulation played a major role in the CG-5-mediated activation of these methylation-silenced genes. This premise was corroborated by two lines of evidence. First, qRT-PCR analysis indicated that siRNA-mediated knockdown of DNMT1 in LNCaP cells mimicked the effects of CG-5 by activating, by at least 2-fold, many of the same genes, including *IGFBP3* (7.5-fold), *BASP1* (3.8-fold), *LAMB3* (2.9-fold), and *GSTP1* (2.3-fold), as well as sharply reducing the expression of *PDLIM4* (Fig. 5A). Second, ectopic DNMT1 expression attenuated the effect of CG-5 on the expression of many of the 13 genes examined (Fig. 5B). With the exception of *IGFBP3*, DNMT1 overexpression diminished the extent of CG-5-mediated gene activation, returning the expression levels of many of these genes, such as *BASP1*, *GADD45b*, *GPX3*, and *GSTP1*, to the basal level or lower. DNMT1 overexpression also abrogated the suppressive effect of CG-5 on the expression of *PDLIM4* and *TACSTD2*. However, ectopic DNMT1 expression had no significant effect on *S100A4* expression.

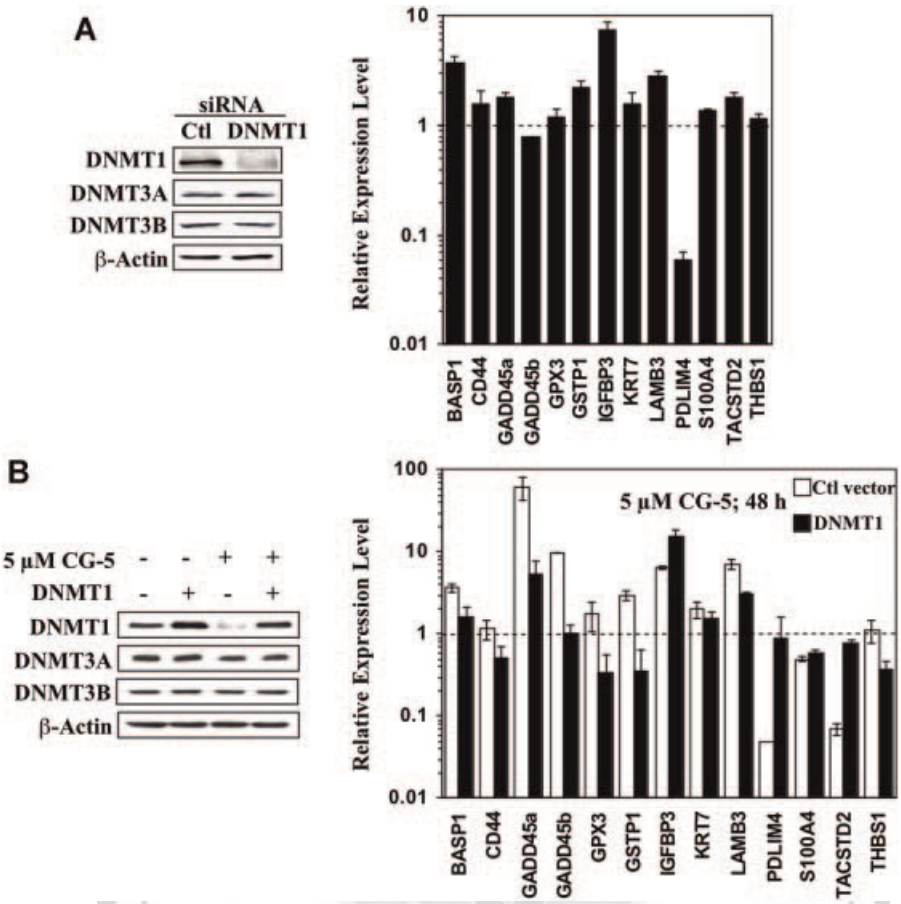

Fig. 5. Evidence that DNMTI plays a pivotal role in CG-5-mediated regulation of methylation-silenced cancer-related gene expression. **A**: siRNA-mediated knockdown of DNMTI mimics the effect of CG-5 on the expression of the selected I3 genes reported to be silenced by DNA hypermethylation in prostate cancer cells, as determined by qRT-PCR (**right**). LNCaP cells were transiently transfected with DNMTI or control (Ctl) siRNA, and then treated with 5 μM CG-5 for 72 hr. The expression levels of DNMT isoforms were analyzed by Western blotting to confirm the specificity of the knockdown (**left**). Column, mean (n = 3); error bars, SD. **B**: Ectopic expression of DNMTI protects cells from CG-5-mediated effects on the expression of the selected I3 methylation-silenced genes, as determined by qRT-PCR (**right**). LNCaP cells were transiently transfected with the flag-tagged DNMTI or control (Ctl) vector, and then treated with 5 μM CG-5 for 48 hr. The expression levels of DNMT isoforms following treatment with CG-5 or DMSO control were analyzed by Western blotting (**left**). Column, mean (n = 3); error bars, SD.

CG-5 Alters CpG methylation in the Promoter Region of the I3 Hypermethylated Genes in LNCaP Cells

To correlate the aforementioned changes in gene expression with the effects of 5-aza-dC, CG-5, and glucose deprivation on DNA methylation, we used pyrosequencing to analyze DNA methylation at CpG islands in the promoter regions of the aforementioned 13 genes in response to individual treatments (Fig. 6A–M). Pyrosequencing is the leading method for quantitative DNA methylation analysis, in part, due to its ability to identify differentially methylated positions in close proximity, thereby allowing concurrent quantification of multiple CpG sites in the promoter region [37]. As neighboring CpG sites within a single promoter showed different degrees of methylation (Fig. 6A–M, right panels; each color-coded circle represents a single CpG site and each designated row represents a treatment condition), the average of all sites was used to represent the level of methylation for each gene (left panels).

LNCaP cells were treated with DMSO (Fig. 6, control; a and b for 48 and 72 hr, respectively), 5 μM 5-aza-dC (c and d), 5 μM CG-5 (e and f), or glucose-depleted medium (g and h), after which genomic DNA was collected for pyrosequencing analysis. As noted, the promoter and/or the first exon of each of these 13 genes contain multiple CpG sites, ranging from 3 to 19 sites. Not only did the methylation level among these sites vary within a single promoter/exon region (Fig. 6A–M, right panels, a and b), but also the total methylation levels of the promoters/

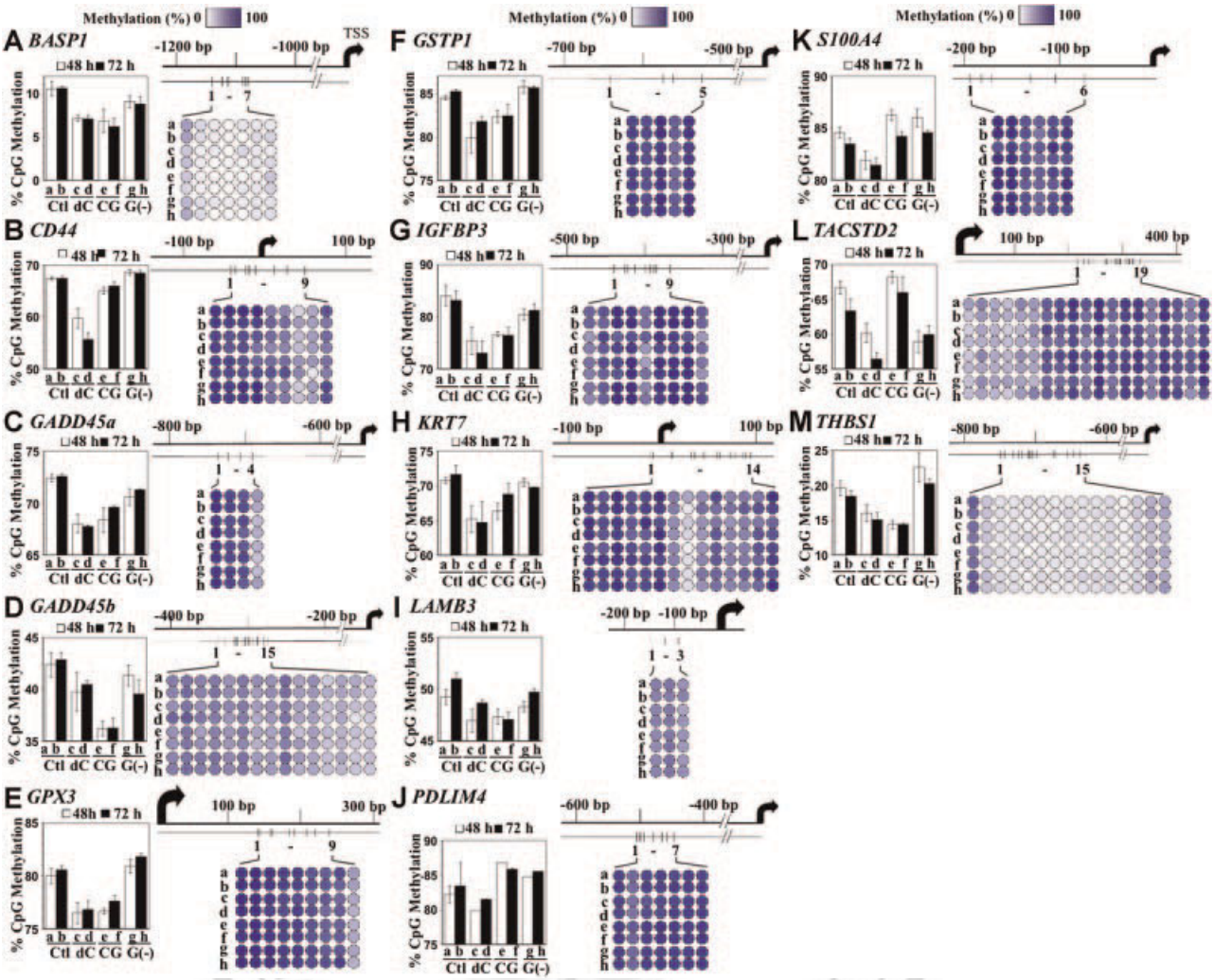

Fig. 6. Effects of CG-5, glucose deprivation, and 5-aza-dC on CpG island methylation in methylation-silenced cancer-related genes. LNCaP cells were treated with DMSO control (Ctl), 5 μM 5-aza-dC (dC), 5 μM CG-5 (CG), or glucose-depleted medium [G(−)] for 48 and 72 hr. Pyrosequencing analysis of CpG island methylation in the promoter/first exon regions of the selected 13 methylation-silenced genes was performed as described in Materials and Methods Section. **A**, *BASP1*; **B**, *CD44*; **C**, *GADD45a*; **D**, *GADD45b*; **E**, *GPX3*; **F**, *GSTP1*; **G**, *IGFBP3*; **H**, *KRT7*; **I**, *LAMB3*; **J**, *PDLIM4*; **K**, *S100A4*; **L**, *TACSTD2*; **M**, *THBS1*. Average methylation levels of individual CpG sites in the promoter/first exon of each of the genes examined under each condition are represented by the color-coded circles (**right panels**; dark blue, 100%; white, 0%; scale at top of each column). The average methylation level of all CpG sites within each of the promoters/first exons was used to represent the level of methylation for each of the 13 genes under each treatment condition (**left panel**; column, mean (n = 3–19); error bars, SD). **a** and **b**: DMSO control for 48 and 72 hr, respectively; **c** and **d**: 5 μM 5-aza-dC for 48 and 72 hr, respectively; **e** and **f**: 5 μM CG-5 for 48 and 72 hr, respectively; **g** and **h**: glucose-depleted medium for 48 and 72 hr, respectively.

exons varied greatly among these genes (left panels, a and b). For example, while many of these genes were highly methylated, *BASP1* and *THBS1* showed only 10% and 20% CpG methylation, respectively, in control cells (Fig. 6A and M, respectively). Consistent with the qRT-PCR findings, 5-aza-dC, CG-5, and glucose-depleted medium exhibited differential effects on the DNA methylation patterns of these genes. 5-Aza-dC facilitated decreases in DNA methylation in all of the genes examined (all panels, c and d). These epigenetic changes correlated with activation of these genes in 5-aza-dC-treated LNCaP cells (Fig. 4A) with the exception of *GADD45b* (panel D), of which the mRNA levels remained unaltered after drug treatment. It is noteworthy that, while CG-5 mediated the hypomethylation and resulting activation of many tumor suppressor genes, it enhanced the DNA methylation of *PDLIM4* (panel J) and the tumor-promoting genes *S100A4* and *TACSTD2* (panels K and L, respectively), resulting in the downregulated expression of these genes (Fig. 4B). The effects of glucose-depleted medium on DNA methylation of many of

these genes paralleled those of CG-5, however, to a lesser extent. Nevertheless, glucose starvation contrasted with CG-5-induced energy restriction in its opposite effects on the DNA methylation pattern of *GPX3*, *GSTP1*, *TACSTD2*, and *THBS1* (panels E, F, L, and M, respectively), which underlies the observed differences in the effects of these two treatments on the activation of these DNA methylation-silenced genes (Fig. 4C).

DISCUSSION

Aberrant promoter hypermethylation of critical pathway genes plays an important role in prostate carcinogenesis and tumor progression [38,39], thereby representing a therapeutically relevant target for cancer treatment [40]. In this study, we demonstrated the high potency of the novel ERMA CG-5 relative to 2-DG in suppressing the expression of DNMT1 and, to a lesser extent, DNMT3A, which led to the reactivation of a series of DNA methylation-silenced tumor suppressor genes, including *GADD45a*, *GADD45b*, *IGFBP3*, *LAMB3*, *BASP1*, *GPX3*, and *GSTP1*, in prostate cancer cells through promoter hypomethylation.

The effect of CG-5 on DNA methylation profiles is largely associated with the reduction in the expression of DNMT1 as siRNA-mediated knockdown and ectopic expression of DNMT1 mimicked and diminished, respectively, the ability of CG-5 to modulate the expression of these silenced genes. Although CG-5 and 5-aza-dC share the ability to downregulate DNMT1 expression, the underlying mechanisms are distinctly different. Evidence suggests that CG-5 facilitated the downregulation of DNMT1 expression through transcriptional repression, which our data suggest is be associated with the reduced expression of Sp1 and E2F1. Our previous study demonstrated that β-transducin repeat-containing protein (β-TrCP)-dependent proteasomal degradation of Sp1 represents one of the energy restriction-associated cellular responses elicited by CG-12 [8], and is likely the mechanism by which Sp1 is suppressed in CG-5-treated cells. In contrast, CG-5-mediated suppression of E2F1 expression occurred at the transcriptional level.

The specificity with which CG-5 activates DNA methylation-silenced genes is noteworthy, and contrasts with the nonspecific reactivation of nearly of all the silenced genes examined by 5-aza-dC. For example, our data indicate that CG-5 reduced the basal expression levels of *PDLIM4* and the three tumor/invasion-promoting genes, namely *CD44*, *S100A4*, and *TACSTD2*, while 5-aza-dC increased the expression of these genes by 8- to 26-fold. This target specificity was further confirmed by pyrosequencing analysis, which showed the differential effect of CG-5 versus 5-aza-dC on DNA methylation in the promoter regions of the 13 genes examined. While 5-aza-dC caused universal hypomethylation of all of these 13 genes, CG-5 enhanced the DNA methylation of *PDLIM4* and the tumor-promoting genes *S100A4* and *TACSTD2*. However, the suppressive effect of CG-5 on CD44 promoter methylation relative to the control (65.9% vs. 67.42%; $P = 0.033$) represents an anomaly since CG-5 reduced *CD44* expression.

Mechanistically, this differential regulation of DNA methylation-silenced genes is attributed not just to CG-5's effect on DNA hypomethylation alone, but also to its ability to affect the expression of transcription factors, such as Sp1 and E2F1, and histone-modifying enzymes [9]. Together, these concerted actions underline a more complicated mode of epigenetic gene regulation than that of 5-aza-dC's inhibitory effect on DNMT activity alone.

CONCLUSIONS

It is well recognized that cancer cells undergo a metabolic shift to anaerobic glycolysis that provides growth advantages within the tumor microenvironment. Consequently, there is intense interest in targeting tumor metabolism as a therapeutic strategy, including small-molecule approaches. In this study, we demonstrate that epigenetic activation of DNA methylation-silenced tumor suppressor genes represents an important antitumor response to energy restriction. Moreover, our novel small-molecule ERMA, GC5, regulates the expression of these genes through modulation of DNA methylation and, perhaps by virtue of its concomitant effects on histone modifications, exhibits target gene specificity and a broader spectrum of antitumor gene activation that might offer therapeutic advantages over DNMT inhibitors.

ACKNOWLEDGMENTS

This work was supported by National Institutes of Health grant CA112250 and Department of Defense. Prostate Cancer Research Program grant W81XWH-09-0198 to C.S.C.; Predoctoral fellowship NSC98-2917-I-010-103 to H.Y.L. from the Graduate Student Study Abroad Program of the National Science Council, Taiwan.

REFERENCES

1. Kroemer G, Pouyssegur J. Tumor cell metabolism: Cancer's Achilles' heel. Cancer Cell 2008;13(6):472–482.
2. Vander Heiden MG. Targeting cancer metabolism: A therapeutic window opens. Nat Rev Drug Discov 2011;10(9):671–684.

3. Denko NC. Hypoxia, HIF1 and glucose metabolism in the solid tumour. Nat Rev Cancer 2008;8(9):705–713.
4. Elstrom RL, Bauer DE, Buzzai M, Karnauskas R, Harris MH, Plas DR, Zhuang H, Cinalli RM, Alavi A, Rudin CM, Thompson CB. Akt stimulates aerobic glycolysis in cancer cells. Cancer Res 2004;64(11):3892–3899.
5. Osthus RC, Shim H, Kim S, Li Q, Reddy R, Mukherjee M, Xu Y, Wonsey D, Lee LA, Dang CV. Deregulation of glucose transporter 1 and glycolytic gene expression by c-Myc. J Biol Chem 2000;275(29):21797–21800.
6. Matoba S, Kang JG, Patino WD, Wragg A, Boehm M, Gavrilova O, Hurley PJ, Bunz F, Hwang PM. p53 regulates mitochondrial respiration. Science 2006;312(5780):1650–1653.
7. Kelloff GJ, Hoffman JM, Johnson B, Scher HI, Siegel BA, Cheng EY, Cheson BD, O'Shaughnessy J, Guyton KZ, Mankoff DA, Shankar L, Larson SM, Sigman CC, Schilsky RL, Sullivan DC. Progress and promise of FDG-PET imaging for cancer patient management and oncologic drug development. Clin Cancer Res 2005;11(8):2785–2808.
8. Wei S, Kulp SK, Chen CS. Energy restriction as an antitumor target of thiazolidinediones. J Biol Chem 2010;285(13):9780–9791.
9. Chen CH, Huang PH, Chu PC, Chen MC, Chou CC, Wang D, Kulp SK, Teng CM, Wang Q, Chen CS. Energy restriction-mimetic agents induce apoptosis in prostate cancer cells in part through epigenetic activation of KLF6 tumor suppressor gene expression. J Biol Chem 2011;286(12):9968–9976.
10. Sharma S, Kelly TK, Jones PA. Epigenetics in cancer. Carcinogenesis 2010;31(1):27–36.
11. Tost J, Gut IG. DNA methylation analysis by pyrosequencing. Nat Protoc 2007;2(9):2265–2275.
12. Ibragimova I, Ibanez de Caceres I, Hoffman AM, Potapova A, Dulaimi E, Al-Saleem T, Hudes GR, Ochs MF, Cairns P. Global reactivation of epigenetically silenced genes in prostate cancer. Cancer Prev Res (Phila) 2010;3(9):1084–1092.
13. Goldstein AS, Lawson DA, Cheng D, Sun W, Garraway IP, Witte ON. Trop2 identifies a subpopulation of murine and human prostate basal cells with stem cell characteristics. Proc Natl Acad Sci USA 2008;105(52):20882–20887.
14. Herrlich P, Morrison H, Sleeman J, Orian-Rousseau V, Konig H, Weg-Remers S, Ponta H. CD44 acts both as a growth- and invasiveness-promoting molecule and as a tumor-suppressing cofactor. Ann NY Acad Sci 2000;910:106–118; discussion 118–120.
15. Li F, Tiede B, Massague J, Kang Y. Beyond tumorigenesis: Cancer stem cells in metastasis. Cell Res 2007;17(1):3–14.
16. Hartl M, Nist A, Khan MI, Valovka T, Bister K. Inhibition of Myc-induced cell transformation by brain acid-soluble protein 1 (BASP1). Proc Natl Acad Sci USA 2009;106(14):5604–5609.
17. Zerbini LF, Libermann TA. GADD45 deregulation in cancer: Frequently methylated tumor suppressors and potential therapeutic targets. Clin Cancer Res 2005;11(18):6409–6413.
18. Qiu W, David D, Zhou B, Chu PG, Zhang B, Wu M, Xiao J, Han T, Zhu Z, Wang T, Liu X, Lopez R, Frankel P, Jong A, Yen Y. Down-regulation of growth arrest DNA damage-inducible gene 45beta expression is associated with human hepatocellular carcinoma. Am J Pathol 2003;162(6):1961–1974.
19. Yu YP, Yu G, Tseng G, Cieply K, Nelson J, Defrances M, Zarnegar R, Michalopoulos G, Luo JH. Glutathione peroxidase 3, deleted or methylated in prostate cancer, suppresses prostate cancer growth and metastasis. Cancer Res 2007;67(17):8043–8050.
20. Cairns P, Esteller M, Herman JG, Schoenberg M, Jeronimo C, Sanchez-Cespedes M, Chow NH, Grasso M, Wu L, Westra WB, Sidransky D. Molecular detection of prostate cancer in urine by GSTP1 hypermethylation. Clin Cancer Res 2001;7(9):2727–2730.
21. Massoner P, Colleselli D, Matscheski A, Pircher H, Geley S, Jansen Durr P, Klocker H. Novel mechanism of IGF-binding protein-3 action on prostate cancer cells: Inhibition of proliferation, adhesion, and motility. Endocr Relat Cancer 2009;16(3):795–808.
22. Mehta H, Gao Q, Galet C, Paharkova V, Wan J, Said JW, Sohn J, Lawson G, Cohen P, Cobb L, Lee KW. IGFBP-3 is a metastasis suppression gene in prostate cancer. Cancer Res 2011;71(15):5154–5163.
23. Sathyanarayana UG, Padar A, Suzuki M, Maruyama R, Shigematsu H, Hsieh JT, Frenkel EP, Gazdar AF. Aberrant promoter methylation of laminin-5-encoding genes in prostate cancers and its relationship to clinicopathological features. Clin Cancer Res 2003;9(17):6395–6400.
24. Vanaja DK, Grossmann ME, Cheville JC, Gazi MH, Gong A, Zhang JS, Ajtai K, Burghardt TP, Young CY. PDLIM4, an actin binding protein, suppresses prostate cancer cell growth. Cancer Invest 2009;27(3):264–272.
25. Boye K, Maelandsmo GM. S100A4 and metastasis: A small actor playing many roles. Am J Pathol 2010;176(2):528–535.
26. Li Q, Ahuja N, Burger PC, Issa JP. Methylation and silencing of the thrombospondin-1 promoter in human cancer. Oncogene 1999;18(21):3284–3289.
27. Ghoshal K, Datta J, Majumder S, Bai S, Kutay H, Motiwala T, Jacob ST. 5-Aza-deoxycytidine induces selective degradation of DNA methyltransferase 1 by a proteasomal pathway that requires the KEN box, bromo-adjacent homology domain, and nuclear localization signal. Mol Cell Biol 2005;25(11):4727–4741.
28. Patel K, Dickson J, Din S, Macleod K, Jodrell D, Ramsahoye B. Targeting of 5-aza-2′-deoxycytidine residues by chromatin-associated DNMT1 induces proteasomal degradation of the free enzyme. Nucleic Acids Res 2010;38(13):4313–4324.
29. Palii SS, Van Emburgh BO, Sankpal UT, Brown KD, Robertson KD. DNA methylation inhibitor 5-Aza-2′-deoxycytidine induces reversible genome-wide DNA damage that is distinctly influenced by DNA methyltransferases 1 and 3B. Mol Cell Biol 2008;28(2):752–771.
30. Fang Y, Brass A, Hoyle DC, Hayes A, Bashein A, Oliver SG, Waddington D, Rattray M. A model-based analysis of microarray experimental error and normalisation. Nucleic Acids Res 2003;31(16):e96. http://www.ncbi.nlm.nih.gov/pubmed/12907748
31. Liu S, Liu Z, Xie Z, Pang J, Yu J, Lehmann E, Huynh L, Vukosavljevic T, Takeki M, Klisovic RB, Baiocchi RA, Blum W, Porcu P, Garzon R, Byrd JC, Perrotti D, Caligiuri MA, Chan KK, Wu LC, Marcucci G. Bortezomib induces DNA hypomethylation and silenced gene transcription by interfering with Sp1/NF-kappaB-dependent DNA methyltransferase activity in acute myeloid leukemia. Blood 2008;111(4):2364–2373.
32. Kimura H, Nakamura T, Ogawa T, Tanaka S, Shiota K. Transcription of mouse DNA methyltransferase 1 (Dnmt1) is regulated by both E2F-Rb-HDAC-dependent and -independent pathways. Nucleic Acids Res 2003;31(12):3101–3113.
33. Yang CC, Wang YC, Wei S, Lin LF, Chen CS, Lee CC, Lin CC. Peroxisome proliferator-activated receptor gamma-independent suppression of androgen receptor expression by troglitazone mechanism and pharmacologic exploitation. Cancer Res 2007;67(7):3229–3238.

34. Ohtani K, DeGregori J, Nevins JR. Regulation of the cyclin E gene by transcription factor E2F1. Proc Natl Acad Sci USA 1995;92(26):12146–12150.

35. Ma Y, Yuan J, Huang M, Jove R, Cress WD. Regulation of the cyclin D3 promoter by E2F1. J Biol Chem 2003;278(19):16770–16776.

36. Palapattu GS, Wu C, Silvers CR, Martin HB, Williams K, Salamone L, Bushnell T, Huang LS, Yang Q, Huang J. Selective expression of CD44, a putative prostate cancer stem cell marker, in neuroendocrine tumor cells of human prostate cancer. Prostate 2009;69(7):787–798.

37. Dejeux E, El abdalaoui H, Gut IG, Tost J. Identification and quantification of differentially methylated loci by the pyrosequencing technology. Methods Mol Biol 2009;507:189–205.

38. Li LC, Carroll PR, Dahiya R. Epigenetic changes in prostate cancer: Implication for diagnosis and treatment. J Natl Cancer Inst 2005;97(2):103–115.

39. Park JY. Promoter hypermethylation in prostate cancer. Cancer Control 2010;17(4):245–255.

40. Issa JP, Kantarjian HM. Targeting DNA methylation. Clin Cancer Res 2009;15(12):3938–3946.